



Targeting the aryl hydrocarbon receptor with a novel set of triarylmethanes

Elizabeth Goya-Jorge, Celine Rampal, Nicolas Loones, Stephen J. Barigye, Laureano E. Carpio, Rafael Gozalbes, Clotilde Ferroud, Maité Sylla-Iyarreta, Rosa Maria Giner

► To cite this version:

Elizabeth Goya-Jorge, Celine Rampal, Nicolas Loones, Stephen J. Barigye, Laureano E. Carpio, et al.. Targeting the aryl hydrocarbon receptor with a novel set of triarylmethanes. *European Journal of Medicinal Chemistry*, 2020, 207, pp.112777 -. [10.1016/j.ejmech.2020.112777](https://doi.org/10.1016/j.ejmech.2020.112777). [hal-03491417](https://hal.science/hal-03491417)

HAL Id: hal-03491417

<https://hal.science/hal-03491417v1>

Submitted on 22 Sep 2022

HAL is a multi-disciplinary open access archive for the deposit and dissemination of scientific research documents, whether they are published or not. The documents may come from teaching and research institutions in France or abroad, or from public or private research centers.

L'archive ouverte pluridisciplinaire **HAL**, est destinée au dépôt et à la diffusion de documents scientifiques de niveau recherche, publiés ou non, émanant des établissements d'enseignement et de recherche français ou étrangers, des laboratoires publics ou privés.



Copyright - All rights reserved

Targeting the Aryl Hydrocarbon Receptor with a novel set of Triarylmethanes

Elizabeth Goya-Jorge ^{1,2}, Celine Rampal ³, Nicolas Loones ³, Stephen J. Barigye ², Laureano E. Carpio ², Rafael Gozalbes ², Clotilde Ferroud ³, Maité Sylla-Iyarreta Veitía^{3*}, Rosa M. Giner ^{1**}

¹ *Departament de Farmacologia, Facultat de Farmàcia, Universitat de València. Av. Vicente Andrés Estellés, s/n, 46100 Burjassot, Valencia, Spain.*

² *ProtoQSAR SL., CEEI (Centro Europeo de Empresas Innovadoras), Parque Tecnológico de Valencia. Av. Benjamin Franklin 12, 46980 Paterna, Valencia, Spain.*

³ *Equipe de Chimie Moléculaire du Laboratoire Génomique, Bioinformatique et Chimie Moléculaire (EA 7528), Conservatoire National des Arts et Métiers (Cnam), 2 rue Conté, 75003, HESAM Université, Paris, France.*

Corresponding authors.

*E-mail (M.S.-I. Veitía): maite.sylla@lecnam.net

**E-mail (RM. Giner): rosa.m.giner@uv.es

(M.S.-I. Veitía and RM. Giner equally contributed as the last authors)

Abbreviations

ADME: absorption, distribution, metabolism, and excretion; **AhR**: Aryl hydrocarbon Receptor; **AhR-HepG2**: AhR-Lucia™ human liver carcinoma HepG2; **ANOVA**: (one-way) analysis of variance; **bHLH**: basic helix–loop–helix; **BSD**: bisacodyl; **calcd**: calculated; **CH223191**: 2-methyl-2H-pyrazole-3-carboxylic acid; **Cy**: cyclohexane; **CYP1A1**: cytochrome P450 family 1 subfamily A polypeptide 1; **DCM**: dichloromethane; **DCE**: dichloroethane; **DMSO**: dimethyl sulfoxide; **EC₅₀**: half effective concentration; **ER**: estrogen receptor; **EtOAc**: ethyl acetate; **FBS**: fetal bovine serum; **FCC**: Flash Column Chromatography; **FICZ**: 5,11-dihydroindolo[3,2-b]carbazole-12-carbaldehyde; **GC-MS**: Gas Chromatography-Mass Spectrometry; **HPLC**: High Performance Liquid Chromatography; **HRMS**: High Resolution Mass Spectra; **IC₅₀**: half Inhibitory Concentration; **LRMS**: low-resolution mass spectra; **m-CPBA**: *m*-chloroperbenzoic acid; **MEM**: Minimum Essential Medium; **MTT**: 3-(4,5-dimethylthiazolyl-2)-2,5-diphenyltetrazolium bromide; **NEAA**: non-essential amino acids; **NMR**: Nuclear Magnetic Resonance; **OECD**: Organisation for Economic Co-operation and Development; **PAS**: PER, ARNT (AhR- nuclear translocator), Single-minded SIM; **PBS**: Phosphate Buffer Saline; **PC**: Positive Control; **PTSA**: *p*-toluenesulfonic acid; **TAM**: triarylmethane; **THF**: tetrahydrofuran; **TLC**: Thin Layer Chromatography; **RPC_{max}**: maximum response relative to the positive control; **rt**: room temperature; **SAR**: Structure-Activity Relationship; **SEM**: standard error of the mean; **SERM**: selective Estrogen Receptor modulators; **XRE**: xenobiotic response elements.

Abstract

The aryl hydrocarbon receptor (AhR) is a chemical sensor upregulating the transcription of responsive genes associated with endocrine homeostasis, oxidative balance, and diverse metabolic, immunological and inflammatory processes, which have raised the pharmacological interest on its modulation. Herein, a novel set of 32 unsymmetrical triarylmethane (TAM) class of structures has been synthesized, characterized and their AhR transcriptional activity was evaluated using a cell-based assay. Eight of the assayed TAM compounds (**14**, **15**, **18**, **19**, **21**, **22**, **25**, **28**) exhibited AhR agonism but none of them showed antagonist effects. TAMs bearing benzotrifluoride, naphthol or heteroaromatic (indole, quinoline or thiophene) rings seem to be prone to AhR activation unlike phenyl substituted or benzotriazole derivatives. A molecular docking analysis with the AhR ligand binding domain (LBD) showed similarities in the binding mode and in the interactions of the most potent TAM identified 4-(pyridin-2-yl(thiophen-2-yl)methyl)phenol (**22**) compared to the endogenous AhR agonist 5,11-dihydroindolo[3,2-b]carbazole-12-carbaldehyde (FICZ). Finally, *in silico* predictions of physicochemical and biopharmaceutical properties for the most potent agonistic compounds were performed and these exhibited acceptable druglikeness and good ADME profiles. To our knowledge, this is the first study assessing the AhR modulatory effects of unsymmetrical TAM class of compounds.

Keywords *(6): triarylmethane; Ah receptor; agonistic activity; CYP1A1; transcription factor.

1. Introduction

The widely expressed and multifunctional aryl hydrocarbon receptor (AhR) protein is a ligand-activated, evolutionarily conserved and pleiotropic transcription factor. It is classified as a member of the basic helix–loop–helix (bHLH) family of receptors. The cytosolic and resting state of AhR is found in association with the chaperones heat shock protein 90 (Hsp90), the immunophilin-like protein XAP2 (ARA9 or AIP) and p23 [1]. Although AhR is present in most tissues, its highest level of transcriptional activity is in cells with epithelial origin of liver, kidney, lung and spleen [2].

The ligand binding domain (LBD) of AhR is allocated in the PAS-B [(PER)/AhR nuclear translocator (ARNT)/single-minded (SIM)] domain of the receptor. Once ligands arrived at the cytosolic locations of the receptor, they induce or inhibit the conformational modifications needed to prompt its nuclear translocation. If AhR is activated, the chaperone proteins are dissociated and its HLH domain forms a heterodimer with the nuclear translocator ARNT. The differential recognition of specific sequences in the promoter of downstream genes is determined by the recruitment of coactivators and corepressors, modulating thereby AhR expression. Such sequences of recognition are known as xenobiotic response elements (XRE) and they are identified by the core sequence 5'-GCGTG-3' of the DNA [3]. Some XRE-independent mechanisms of AhR activation have been suggested on inflammatory and autoimmune conditions, particularly in selective hormone-sensitive cancer [4]. However, the main outcome of AhR expression is its canonical XRE-mediated signaling linked to the induction of xenobiotic metabolizing enzyme of the cytochrome P450 (CYP), in particular CYP1A1 from family 1, subfamily A, polypeptide 1 [5].

Several ligands have been identified as modulators of AhR including endogenous metabolites such 5,11-dihydroindolo[3,2-b]carbazole-12-carbaldehyde (FICZ) and indoxyl sulfate [6] as well as extensively used drugs such as omeprazole and leflunomide [7,8], and dietary phytochemicals as quercetin [9]. While exact interaction patterns of different ligands upon binding with AhR still lack of a completed crystallized structure of the receptor, important contributions are available for the LBD [10]. Moreover, vast studies of the toxic ligand/agonist of AhR known as 2,3,7,8-

tetrachlorodibenzo-p-dioxin (TCDD) has shed light on the activation mechanism as well as on the signaling patterns of the receptor [11,12]. The functional activity of AhR has proved to be determined by each specific ligand that binds to the LBD and that ultimately leads to dissimilar ligand- and AhR-dependent biological responses [13]. In general, aromatic or heteroaromatic hydrocarbon moieties are crucial structural determinants in all kind of AhR modulators suggested to date [14–18].

AhR ligands are associated with key physiological process such as proper development and metabolism, cell cycle regulation and immune defense [19]. Hence, while earlier perspectives focused on the function of AhR as xenobiotic sensor of toxicants like dioxins and polyaromatic hydrocarbons, recently suggestions placed AhR as an attractive pharmacological target [20–22]. Among the potential therapeutical uses of AhR modulation are included lung and vascular tissues health [23,24], treatment of liver and cystic fibrosis [25,26], control of the antioxidant response [27] and regulation of neural functions in both vertebrates and invertebrates [28]. Moreover, probably the most significant pharmacological applications of targeting AhR are in the treatment of several cancer types, in which the prodrug Phortress (NSC 710305) has been recommended as anticancerogenic and tumor suppressor chemotherapy for CYP1A1-positive tumors [4,29,30]. In addition, important inflammatory and immunological conditions could be modulated through AhR activation and particularly those affecting gut and intestinal tissues [31–33]. Hence, promising drug candidates such as NPD-0414-2 and NPD-0414-24 have been recently suggested in the pharmacotherapy of colitis [34]. AhR-mediated transcription converge with various nuclear receptor signaling pathway, mainly with the estrogen receptor (ER) [35]. Indeed, selective ER modulators (SERM) have been also identified as AhR ligands, which is probably contributing to their therapeutical effects in postmenopausal osteoporosis and breast cancers [36]. Some SERMs identified hold the triaryl methane (TAM) skeleton [37]. Moreover, the symmetric TAM compound tris-indolyl methane was evaluated in a recent publication as a dual modulator of AhR and Pregnane X receptor (PXR) [38]. However, to the best of our knowledge, unsymmetrical TAM compounds have never been addressed as potential modulators of AhR.

114 The TAMs are privileged structures in medicinal chemistry [39]. Numerous TAM
115 derivatives have found applicability in neurodegenerative diseases and vascular
116 disorders and as anti-inflammatory, antitumoral and anti-infective agents against
117 tuberculosis, human immunodeficiency virus and respiratory syncytial virus [40–42].
118 Notable examples are the TAM drug bisacodyl (BSD) and its analogs pointed out as
119 anti-inflammatory, antimicrobial and antiproliferative agents [43,44], and the well-known
120 antimycotic drug clotrimazole suggested in the antiproliferative and antiangiogenic
121 pharmacotherapy [44,45].

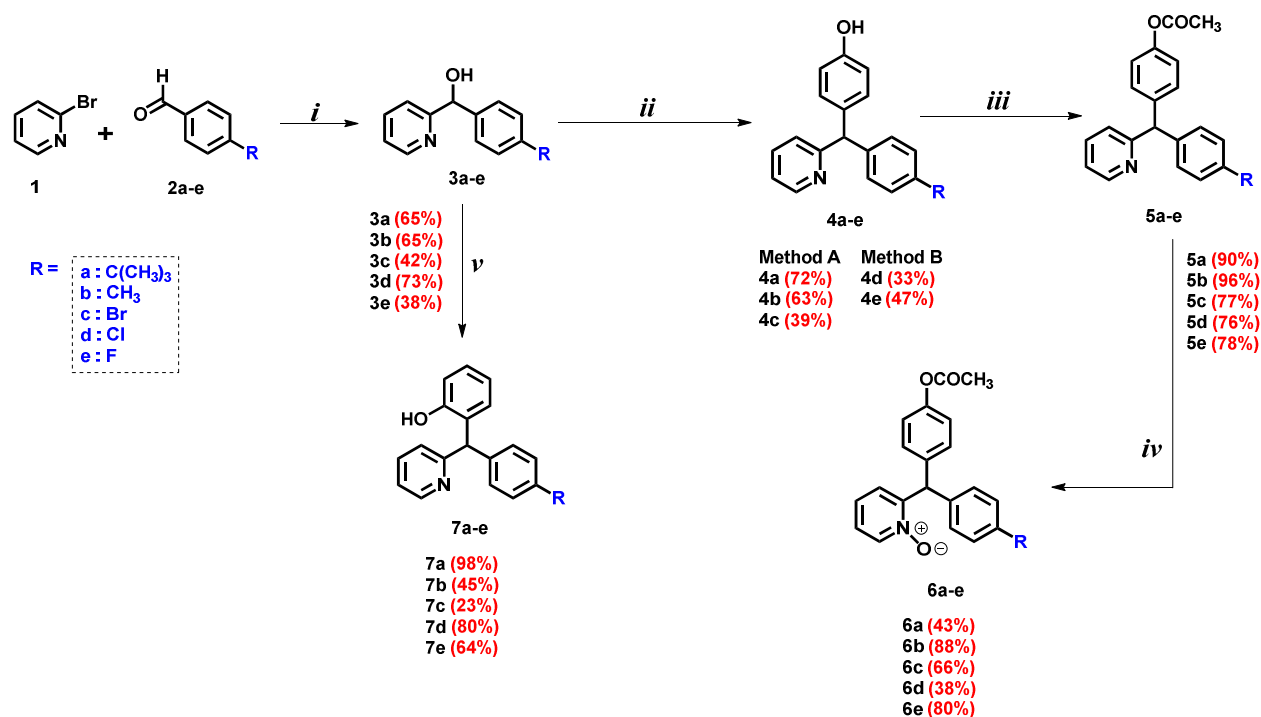
122 Considering the aforementioned evidence that endows TAMs as an interesting scaffold
123 in medicinal chemistry, added to the pharmacological relevance of targeting AhR [21],
124 led to the hypothesis pursued herein. That is, TAM class of compounds could modulate
125 AhR **activation** with potential therapeutic applicability in malignancies, immunological
126 and inflammatory processes. Hence, novel TAMs were synthesized and their AhR-
127 mediated transcriptional activity in AhR-HepG2 cells was assayed *in vitro*. The
128 differential effects displayed by the set of compounds allowed to suggest theoretical
129 contributions of the substituents in the AhR modulatory effects. ADME properties were
130 predicted and the binding affinity preliminarily studied using computational methods for
131 the most significant AhR activators identified.

2. Results and Discussion

2.1. Synthesis of triarylmethanes

The syntheses of triarylmethanes derivatives are shown in Schemes 1-4. Details about the synthetic protocol and chemical characterization of all intermediates are given in the Supplementary Information (SI-1).

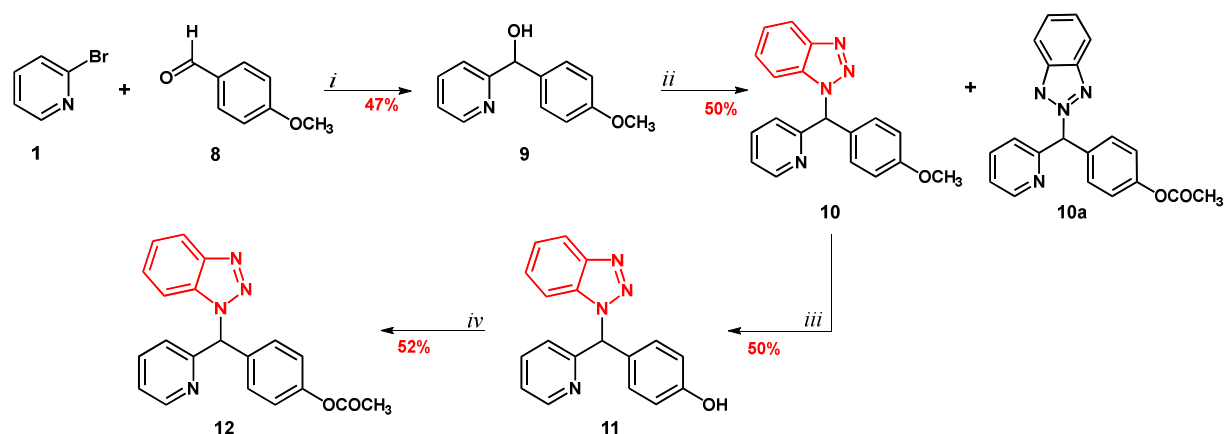
The synthesis of the *p,p*-*N*-oxides **6a-e** and *o,p*-diarylmethylpyridines **7a-e** were carried out following the synthetic pathways represented in Scheme 1. First, synthesis of the corresponding carbinols **3a-e** was performed from 2-bromopyridine **1** and the corresponding aromatic aldehydes **2a-e**, by a bromine-lithium exchange following the procedure of Seto et al. 2004 [46] or by a bromine-magnesium exchange using isopropylmagnesium chloride in tetrahydrofuran at room temperature [47].



Scheme 1. Synthesis of *p,p*- and *o,p*- triarylmethanes. (i) *i*-PrMgCl (1 M) in 2-Me-THF, anh THF, 2 h, rt, Ar; or *n*-BuLi, anh THF, -78°C/rt, Ar. (ii) phenol, H₂SO₄ (4 eq.), nitrobenzene, method A or B (A: 5 min at 80 °C, then at rt. B: from 0 °C to rt), Ar (iii) Ac₂O, NaOH, ≤15 h at 20 °C or 40 °C (iv) *m*-CPBA, anh DCM, 2 h at 20 °C. (v) phenol, H₂SO₄ (20 eq.), nitrobenzene at 80°C, Ar, 5 min.

The key step to obtain the desired TAMs involved a regioselective Friedel-Crafts hydroxyalkylation of the corresponding carbinol **3a-e** with phenol in nitrobenzene under acidic activation [48]. The *p,p* regioisomers **4a-e** were obtained with 4 equivalents of sulfuric acid at 80 °C in a range of 33% to 72% yield. The *o,p* compounds **7a-e** were obtained with 20 equivalents of catalyst at 0 °C in a range of 23% to 98% yield. Acetates **5a-e** were obtained by treating the corresponding triarylmethanes derivatives with acetic anhydride in the presence of sodium hydroxide at room temperature. After workup, the desired compounds **5a-e** were isolated in a range of 76% to 98% yield and pure enough to be used in the next step without any supplementary purification as suggested ¹H NMR analysis. *N*-oxide derivatives **6a-e** were prepared from the corresponding acetates by oxidation with *m*-chloroperbenzoic acid in dichloromethane at room temperature. After 2-3 h of reaction, *N*-oxide derivatives **6a-e** were isolated with a prior purification by flash column chromatography (FCC) on silica gel with non-optimized yields in a range of 38% to 88%.

The syntheses of the benzotriazolyl triarylmethanes **10-12** were carried out following the synthetic pathways represented in Scheme 2.



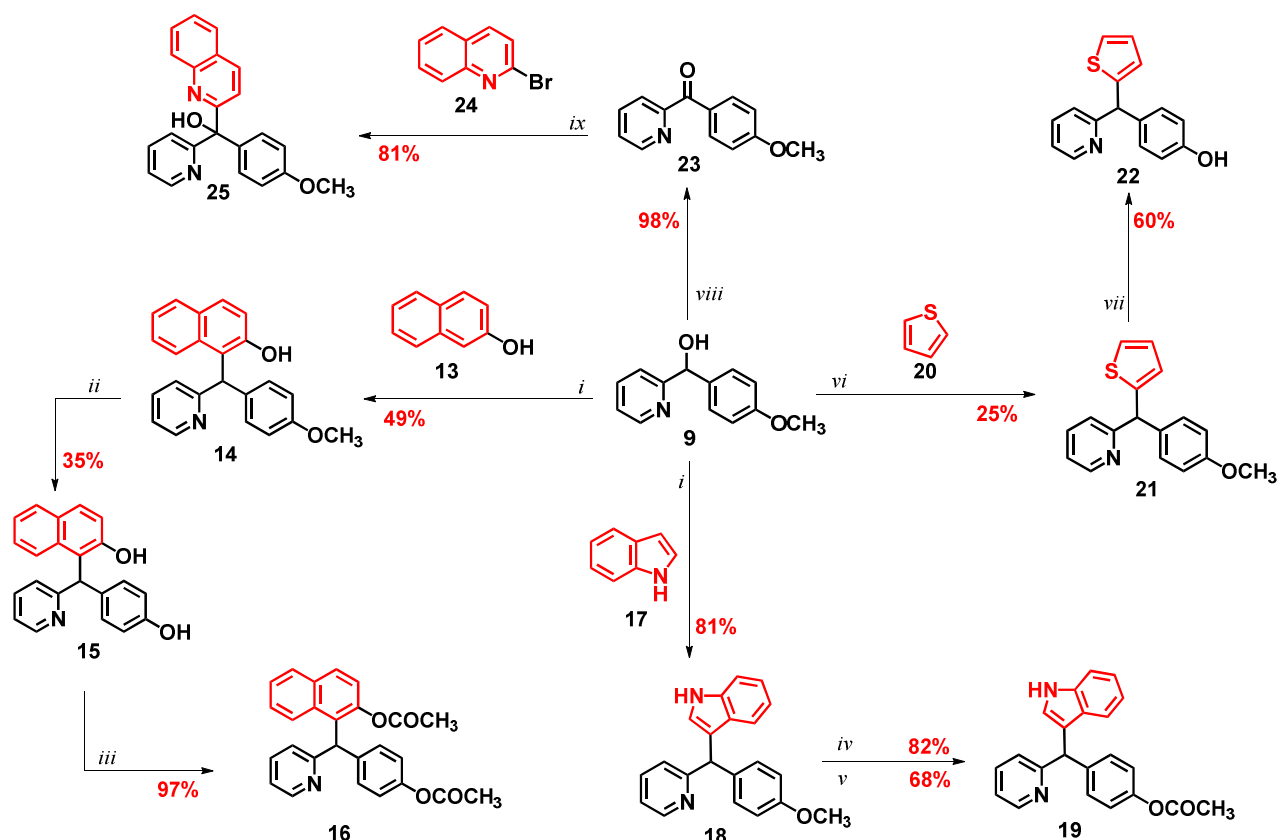
Scheme 2. Synthesis of benzotriazolyl triarylmethanes. (i) *n*-BuLi, anh THF, -78°C/rt. (ii) benzotriazole, PTSA monohydrate, C₈F₁₈, 104 °C, 24 h (iii) BBr₃, DCM, 6 h, from 0 °C to rt., Ar (iv) Ac₂O, NaOH, 24 h, from 0 °C to rt.

First, the synthesis of the (4-methoxyphenyl)(pyridin-2-yl)methanol **9** was performed by a bromine-lithium exchange as previously described for compounds **3** from 2-bromopyridine **1** and *p*-anisaldehyde **8** in anhydrous tetrahydrofuran. Pyridylaryl-

benzotriazol **10** was prepared from benzotriazole and the corresponding diarylmethanol **9** in the presence of a catalytic amount of *p*-toluenesulfonic acid in perfluorooctane (C₈F₁₈). In these conditions, the desired regioisomer **10** was obtained in 50% yield in high purity (HPLC, 95%). The regioisomer **10a** was also isolated and its characterization is described in the SI-1. An optimization of this procedure could probably improve the obtained yield.

The dimethoxylated compound **11** was synthesized by reaction with boron tribromide in dichloromethane. The reaction was conveniently carried out by mixing the reagents at 0°C in an inert solvent and then allowing the mixture to warm up to room temperature during 6 h. Under these conditions the 4-((1H-benzo[d][1,2,3]triazol-1-yl)(pyridin-2-yl)methyl)phenol **11** was obtained in 50% yield. The corresponding acetate derivative **12** was obtained by treating **11** with acetic anhydride in the presence of sodium hydroxide at room temperature. After workup and purification by FCC, the desired compound **12** was isolated in 52% yield.

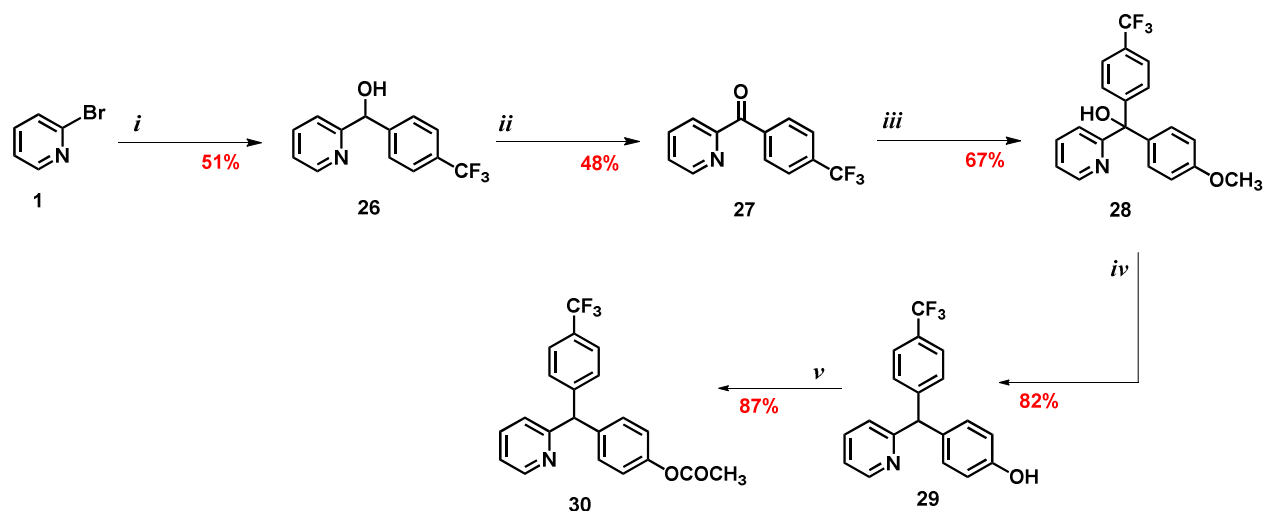
The synthesis of the TAMs bearing heteroaromatic rings (naphtol, indole, quinoline or thiophene) are outlined in Scheme 3. Unsymmetrical naphtol (**14**, **15**), pyridylaryl indoles (**18,19**), and thiophene (**21**, **22**) were synthesized under acid conditions by condensation of the corresponding heterocycle with (4-methoxyphenyl)(pyridin-2-yl)methanol **9** previously obtained by a lithium-bromine exchange as described in Scheme 2. On the other hand, TAM **25** bearing a quinoline fragment was prepared from the corresponding aryl ketone **23** previously synthesized from the carbinol **9** in excellent yield (98%) *via* a base-promoted aerobic oxidation using air as a free and clean oxidant [49]. The other desired TAMs (**16**, **19**) were prepared using sequence series of including methoxy group deprotection followed by acylation as indicated conditions in Scheme 3.



Scheme 3. Synthesis of naphthol, indole, thiophene and quinoline triarylmethanes. (*i*) $\text{NH}_2\text{SO}_3\text{H}$, DCE, 20 h, at 85 °C, Ar (*ii*) HI, AcOH , 5.5 h at 100 °C, Ar (*iii*) Ac_2O , NaOH, 24 h, from 0 °C to rt. (*iv*) BBr_3 , DCM, 19 h, from 0 °C to rt (*v*) **18a**, Ac_2O , NaOH, 3.5 h, from 0 °C to rt. (*vi*) $\text{CH}_3\text{SO}_3\text{H}$, DCE, MW 2 h at 80 °C (*vii*) BBr_3 , DCM, 19 h, from 0 °C to rt., Ar (*viii*) O_2 , NaOH, toluene at 110 °C (*ix*) prior mix of *n*-BuLi and **24** in anhyd THF, 1.5 h at -78 °C, Ar, then **23** in dry THF, 17 h at rt.

The synthesis of the TAMs bearing trifluoromethyl group was carried out following the synthetic pathways represented in Scheme 4. The synthesis of the pyridin-2-yl(4-(trifluoromethyl)phenyl)methanol **26** and the corresponding arylketone **27** was performed following the same procedure described in Scheme 1. Then, TAM **28** was obtained by a halogen-metal exchange from 4-bromoanisole in 67% yield. Demethoxylation was conveniently carried out with hydroiodic acid in acetic acid at reflux. Under these conditions the 4-(pyridin-2-yl(4-(trifluoromethyl)phenyl)methyl)phenol **29** was obtained in 82% yield. The acetate derivative **30** was obtained by treating **29** with acetic anhydride in presence of sodium hydroxide at room temperature. After workup and purification by FCC, the desired

212 compound 4-(pyridin-2-yl(4-(trifluoromethyl)phenyl) methylphenyl acetate **30** was
 213 isolated in 87% yield.



214
 215 **Scheme 4.** Synthesis of TAMs bearing trifluoromethyl group. (i) prior mix of *n*-BuLi and 2-bromopyridine
 216 in anh THF at -78 °C, Ar, then 4-(trifluoromethyl)benzaldehyde, 17 h at rt. (ii) NaOH, O₂, toluene, reflux,
 217 24 h (iii) prior mix of *n*-BuLi and 4-bromoanisole in anh THF at -78 °C, Ar and then **27** (iv) HI 57%, AcOH,
 218 reflux, Ar (v) Ac₂O, NaOH, 4 h, from 0 °C to rt.

219 All compounds biologically evaluated were obtained in high purity (HPLC or NMR,
 220 generally > 95%).

221 2.2. Biological Evaluation

222 2.2.1. Cell viability

223 The effects on cell viability caused by the synthesized TAMs on AhR-HepG2 cell line
 224 were determined by the 2-(3,5-diphenyltetrazol-2-yl)-4,5-dimethyl-1,3-thiazole
 225 bromide (MTT) assay, which constitutes a valuable method to study cell proliferation,
 226 cytotoxicity and chemosensitivity *in vitro* [50]. The cell viability percentages obtained for
 227 32 novel TAMs and the drug BSD are shown in Figure 1. The adopted criterium
 228 considered as cytotoxic was a reduction of cell viability above 15% upon treatment with
 229 TAMs.

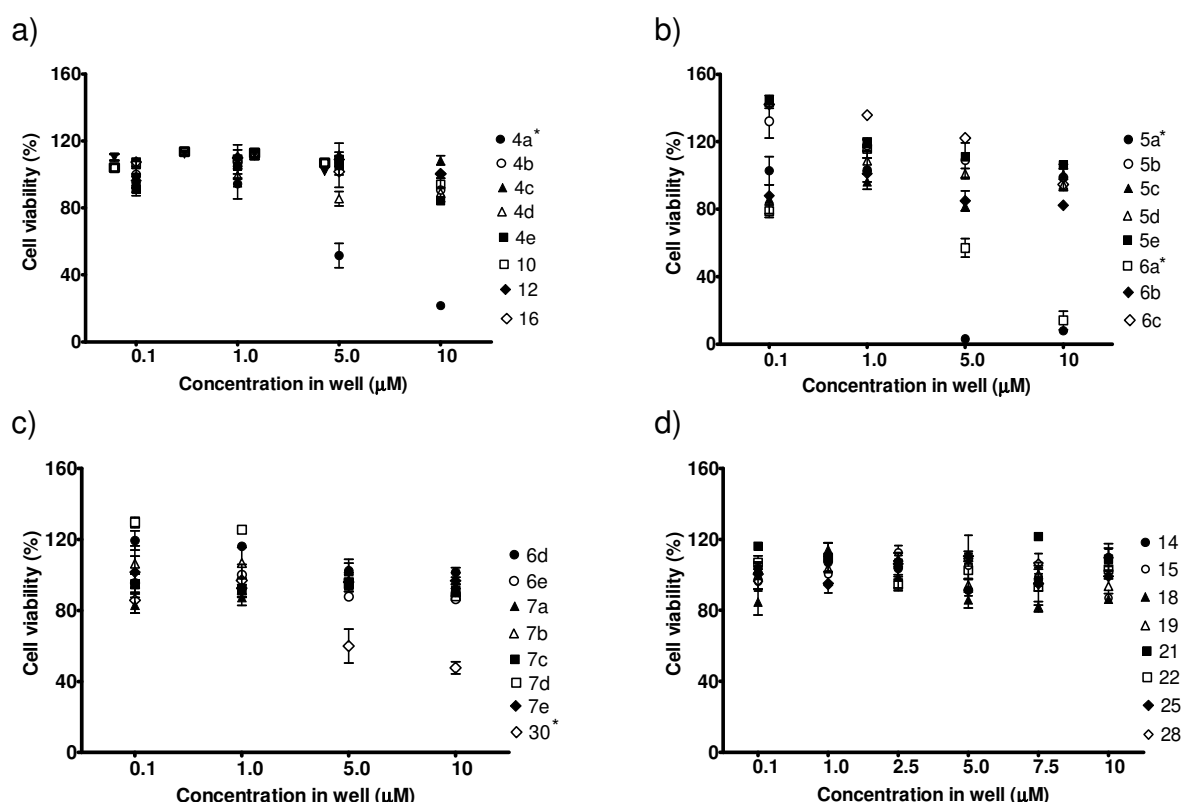


Figure 1. Viability percentages of cells exposed to the TAMs by MTT assay. a) Compounds **4 a-e**, **10**, **12**, **16**, b) Compounds **5 a-e** and **6 a-c**, c) Compounds **6d**, **6e**, **7 a-e** and **30**, d) Compounds **14**, **15**, **18**, **19**, **21**, **22**, **25** and **28**. All compounds were assayed at 0.1 μM, 1.0 μM, 5.0 μM and 10.0 μM, and compounds in d) were also tested at 2.5 μM and 7.5 μM. Each chart represents the mean percentage \pm SEM from at least three independent experiments ($n = 3$). Cell viability lower than 85% was considered cytotoxic. * $p < 0.05$ significantly different from vehicle control (using one-way ANOVA followed by Dunnett's post-test).

The eight TAMs **14**, **15**, **18**, **19**, **21**, **22**, **25** and **28** were studied in more detail due to their AhR agonist effects as will be described later. For these compounds, no cytotoxic effect was observed at the six assayed concentrations. The same conditions but longer exposure times (48 h and 72 h) in the MTT test revealed similar results (data not shown) than those obtained after 24 h of treatment (Figure 1d).

The TAMs **4a**, **5a**, **6a** and **30** were found cytotoxic over 5 μM. The strongest cytotoxicity was caused by compound **4a**, whose reduction of cell viability was above 90%, while comparable reductions (~50%) of cell viability were observed for compounds **5a**, **6a** and **30**. The concentration limits established in the AhR transcriptional activity bioassay only considered no cytotoxic concentrations of the tested TAMs.

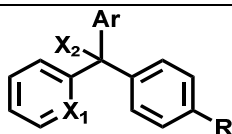
2.2.2. AhR transcriptional activity

Standard Positive Controls. During the validation and optimization of the *in vitro* method, sigmoidal dose-response curves of the endogenous AhR agonist FICZ were obtained with concentrations from 0.01-18.0 μM ($R^2 = 0.99$), according to the recommendations of the AhR-HepG2 cell line provider (See SI-2). Similarly, the antagonist bioassay was validated with the inhibition curve of the AhR antagonist 2-methyl-2H-pyrazole-3-carboxylic acid (CH223191), obtained by co-exposure the EC_{50} of FICZ and concentrations from 1-30 μM of the CH223191 as described elsewhere [51].

The maximum induction of AhR transcription caused by FICZ was up to 30 folds at the maximum concentration tested (18 μM). From the dose-response curve of AhR agonist, the estimated EC_{50} of FICZ in the cell model was 9.06 μM . Meanwhile, in presence of FICZ concentration at the EC_{50} , the antagonist compound CH223191 reduced to half the transcriptional activity of AhR at the maximum concentration tested (30 μM). From the dose-response curve of AhR inhibition, the estimated IC_{50} of CH223191 was 2.43 μM , consistent with data reported in the literature [52].

TAM compounds. Results of AhR agonist and AhR antagonist assays are presented in Table 1 for all the studied compounds, that include the 32 novel TAMs synthesized, the commercial TAM drug BSD and the positive controls. Dose response-curves are provided as SI-2.

Table 1. AhR-mediated transcriptional activity of the 32 rationally designed TAMs **4-7 [a-e]**, **10, 12, 14-16, 18, 19, 21, 22, 25, 28, 30**, the drug bisacodyl and the agonist (FICZ) and antagonist (CH223191) controls.



AhR-HepG2 transcriptional activity									
ID	Ar	R	X ₁	X ₂	[μM] ^a	Agonist RPC (%) ±SEM ^b	EC ₅₀ (μM) ±SEM ^c	Antagonist RPC (%) ±SEM ^b	Activity Criteria ^d
4a	Phe (4-C(CH ₃) ₃)	OH	N	H	1.0	6.89±0.29	ND	113.44±3.16	Inactive
4b	Phe (4-CH ₃)	OH	N	H	10.0	7.09±0.35	>100	138.98±4.72	Inactive
4c	Phe (4-Br)	OH	N	H	10.0	7.71±0.56	>100	168.82±7.81	Inactive
4d	Phe (4-Cl)	OH	N	H	10.0	6.59±0.37	>100	200.45±7.41	Inactive
4e	Phe (4-F)	OH	N	H	10.0	7.79±0.52	>400	150.92±7.29	Inactive
5a	Phe (4-C(CH ₃) ₃)	OCOCH ₃	N	H	1.0	5.32±0.29	ND	112.56±2.01	Inactive
5b	Phe (4-CH ₃)	OCOCH ₃	N	H	10.0	9.42±0.46	>100	203.94±4.05	Inactive
5c	Phe (4-Br)	OCOCH ₃	N	H	10.0	6.32±0.13	>1000	143.15±6.44	Inactive
5d	Phe (4-Cl)	OCOCH ₃	N	H	10.0	6.26±0.10	>1000	128.16±5.01	Inactive
5e	Phe (4-F)	OCOCH ₃	N	H	10.0	8.77±0.33	>100	118.36±5.34	Inactive
6a	Phe (4-C(CH ₃) ₃)	OCOCH ₃	N ⁺ O ⁻	H	1.0	6.10±0.23	ND	120.3±2.55	Inactive
6b	Phe (4-CH ₃)	OCOCH ₃	N ⁺ O ⁻	H	10.0	6.28±0.18	>200	93.35±1.09	Inactive
6c	Phe (4-Br)	OCOCH ₃	N ⁺ O ⁻	H	10.0	8.80±0.52	>100	106.22±3.50	Inactive
6d	Phe (4-Cl)	OCOCH ₃	N ⁺ O ⁻	H	10.0	7.78±0.28	>200	78.81±3.89	Inactive
6e	Phe (4-F)	OCOCH ₃	N ⁺ O ⁻	H	10.0	6.51±0.31	>1000	92.41±2.75	Inactive
7a	Phe (2-OH)	(CH ₃) ₃ C	N	H	10.0	6.81±0.19	>1000	196.65±7.59	Inactive
7b	Phe (2-OH)	CH ₃	N	H	10.0	6.93±0.15	>100	114.43±6.55	Inactive
7c	Phe (2-OH)	Br	N	H	10.0	7.99±0.17	>1000	117.10±3.45	Inactive
7d	Phe (2-OH)	Cl	N	H	10.0	7.18±0.16	>1000	114.57±5.72	Inactive
7e	Phe (2-OH)	F	N	H	10.0	6.89±0.14	>1000	111.59±3.21	Inactive
10	1H-benzotriazole	OCH ₃	N	H	10.0	8.86±0.26	>100	163.53±7.29	Inactive
12	1H-benzotriazole	OCOCH ₃	N	H	10.0	9.23±0.24	>100	141.94±6.44	Inactive
14	1-Naph(2-OH)	OCH ₃	N	H	10.0	39.70±0.76	53.62±0.22	142.31±2.78	Agonist
15	1-Naph(2-OH)	OH	N	H	5.0	28.57±0.51	>50	168.86±5.74	Agonist
16	1-Naph(2-OCOCH ₃)	OCOCH ₃	N	H	10.0	5.17±0.25	>200	143.80±1.99	Inactive
18	3-indole	OCH ₃	N	H	10.0	114.20±0.80	21.72±0.32	182.99±5.12	Agonist
19	3-indole	OCOCH ₃	N	H	10.0	76.95±0.63	27.86±0.15	226.23±7.45	Agonist
21	2-thiophene	OCH ₃	N	H	10.0	10.54±0.41	>50	136.57±2.70	Agonist
22	2-thiophene	OH	N	H	10.0	111.01±0.86	13.16±0.08	202.27±4.42	Agonist
25	2-quinoline	OCH ₃	N	OH	10.0	53.78±0.37	19.88±0.08	272.13±5.51	Agonist
28	Phe(4-CF ₃)	OCH ₃	N	OH	10.0	26.60±0.89	52.03±0.29	242.95±5.42	Agonist
30	Phe(4-CF ₃)	OCOCH ₃	N	H	1.0	7.71±0.22	ND	117.24±3.81	Inactive
BSD	Phe(4-OCOCH ₃)	OCOCH ₃	N	H	10.0	6.58±0.19	>1000	107.20±3.03	Inactive
Control	FICZ		-		18.0	100%	9.06±0.02	-	Agonist
Control	CH223191		-		30.0	-	(IC ₅₀) 2.43±0.18	54.50±0.79	Antagonist

^a Maximum concentration tested in the absence of limitations due to cytotoxicity or insolubility. ^b Average of the percentages of the maximum response relative to the positive control (RPC_{Max}) ± SEM of AhR agonist/antagonist activity from at least three independent experiments (n=3). ^c

In the AhR reporter gene assay, the maximum effect observed corresponded to the maximum concentration tested for all TAMs except for **15** and **18**. Compounds **4a**, **5a**, **6a** and **30** were assayed at non-cytotoxic concentrations (up to 1 µM) and they were unable to induce or blockage AhR transcriptional activity in this cell model.

AhR agonist assay. The eight TAMs **14**, **15**, **18**, **19**, **21**, **22**, **25** and **28** were identified as agonists of AhR (RPC_{max}> 10%) while the rest of them and the BSD were classified as inactive AhR agonists (Table 1). The agonist effectiveness of the active compounds compared to FICZ followed the order: **18** ≈ **22** > **19** > **25** > **14** > **28** ≈ **15** > **21**. Compounds **18** and **22** were more active as agonist than FICZ at a comparable exposure concentration showing an RPC_{max} of 114.2% and 111.0%, respectively.

In cases where a dose-response curve of agonism was achieved, the half effective concentration (EC₅₀) was estimated as a measure of the potency of active compounds. As reported in Table 1, compound **22** (EC₅₀ = 13.16 µM) was suggested as the most potent AhR agonist. Compounds **25** and **18** showed comparable half effective concentrations of 19.88 µM and 21.72 µM, respectively, while compound **19** was less potent (EC₅₀ = 27.86 µM). The EC₅₀ estimated for compounds **14** and **28** were 53.62 µM and 52.03 µM, respectively. Lastly, it was not possible to obtain a dose-response curve for compounds **15** nor **21**.

AhR antagonist assay. None of the tested compounds showed antagonist effects on AhR activation. However, additive effects and probably synergism in presence of FICZ were observed for most of the agonist compounds. Interestingly, the level of AhR transcriptional response in presence of FICZ was not proportional to the effectiveness of compounds individually tested as agonists. Thus, a remarkable high induction during the co-exposure was registered for compounds **25** (RPC_{max} = 272.13%) and **28** (RPC_{max} = 242.95%) despite they were not by themselves among the strongest activators of AhR. Similarly, a notable induction of AhR **activation** in presence of FICZ during the antagonist assay was showed by the inactive compounds **5b**, **4d** and **7a** (RPC_{max} 203.94%, 200.45% and 196.65%, respectively).

2.3. SAR considerations

The AhR-mediated transactivation induced by the TAMs allowed a comprehensive structure-activity relationship (SAR) analysis. The key structural features of the active TAMs and their AhR agonist effects expressed as fold responses are shown in Figure 2.

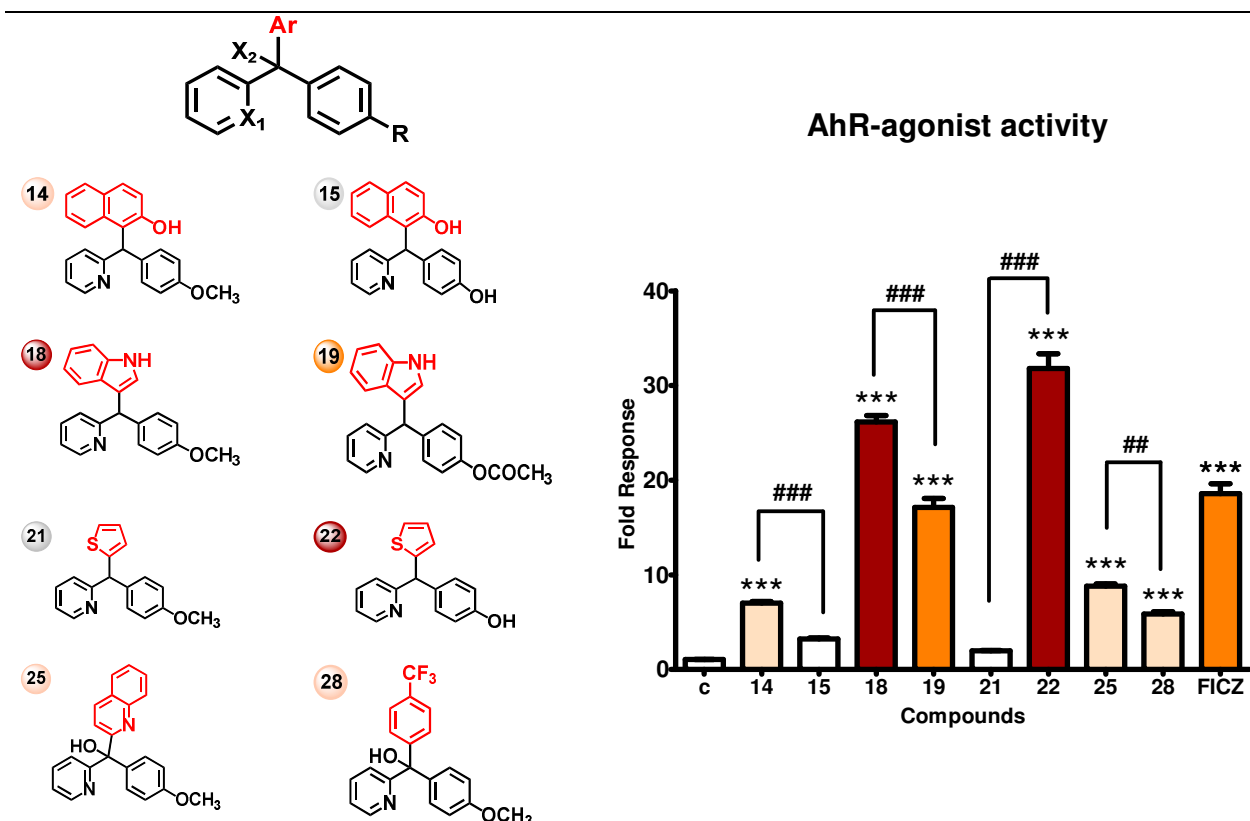


Figure 2. Maximum AhR agonist activity induced in cells by compounds **14**, **15**, **18**, **19**, **21**, **22**, **25** and **28**. General structure and agonist compounds are represented at the left. Data are expressed as fold responses, as compared to non-induced cells (*i.e.* vehicle control (c)). The bar chart at the right shows mean fold response \pm SEM ($n = 4$) as: ≥ 25 folds (red), between 10-20 folds (orange), ≤ 10 folds and significant (light orange), < 10 folds and not significant (white). The levels of significance were determined using one-way ANOVA, followed by Dunnett's post-test when compared to vehicle control ($***p < 0.001$) or by Bonferroni post-test when compared between pairs of structural analogous ($##p < 0.01$, $###p < 0.001$).

X₁, X₂ substitution. Regarding X₁, the occurrence of a pyridine ring (**14**, **15**, **18**, **19**, **21**, **22**, **25**, **28**) was important for AhR agonist activity similarly to some other compounds reported *in vivo* as CYP1A1 inducers [54]. The *N*-oxidation had no influence on AhR

activation, noticeable when comparing the TAMs **5a-e** vs. the corresponding *N*-oxides **6a-e**. None of the substituted phenyls at **Ar** showed any effect on AhR except for **28** in which the introduction of a hydroxyl group at **X₂** position turned it moderately active. Compound **25** bearing a quinoline and a hydroxyl group at **X₂** also exhibited significant AhR agonist induction.

R substitution. The presence of different oxygenated functional group at **R** does not appear to determine the agonist effects on AhR of the synthesized TAMs as it has been reported for others aromatic compounds in the literature [55]. Most of the active compounds in this study carry a hydroxyl or methoxy group at **R**. The methoxy substitution in most cases was a better feature to exhibit AhR agonist activity (**14** vs. **15** and **18** vs. **19**). However, the free hydroxyl group in **22** resulted in a 30-fold increase of the AhR agonism when compared with the methoxylated derivative **21**.

Ar substitution. The AhR-agonist activity was crucially influenced by the third aromatic or heteroaromatic system occupying **Ar**. Thus, the most potent AhR agonism was exhibited by TAMs with heteroaromatic moiety such as thiophene (**22**), indole (**18**, **19**) and quinoline (**25**). Otherwise, derivatives with a naphthol substituent (**14**, **15**) displayed some AhR agonist ability although considerably weaker than the rest of heteroaromatic derivatives (except for **21**) as shown in Figure 2. Curiously, compounds bearing a benzotriazole moiety (**10**, **12**) were found inactive. It should be notice that even though **15** and **21** were considered agonists according to the RPC_{max} threshold (Table 1), their induced fold response was not significant compared to the vehicle control as shown in Figure 2.

On the other hand, the introduction of heteroaromatic substituent at **Ar** were in no case harmful to cells according to the cell viability study (Figure 1). Most of the substituted phenyl derivatives at **Ar** that were causing cytotoxicity at the highest concentrations tested (**4a**, **5a**, **6a**) are bearing a tertbutyl functional group.

Consistent to the above results, phloroglucinol TAMs have shown better safety index and anti-HIV effects when bearing an heteroaromatic moiety [42]. Additionally, indole-containing chemicals have long been recognized as AhR ligands from endogenous and

dietary sources, sustaining the strong agonism displayed by **18** and **19** [19,56].
 Although the thiophene ring in TAM-class of compounds has been suggested as an
 attractive moiety for antimycobacterial activity [57], it is not commonly found in either
 classical or nonclassical AhR modulators identified to date [58]. Thus, to our knowledge,
 the agonist effects on AhR transcriptional activity of thiophene derivatives are
 suggested herein for the first time.

2.4. Computational studies

2.4.1. Molecular Docking

The binding to AhR of the strongest TAM agonist identified (**22**) was compared by
 means of molecular docking analysis with the known ligand/agonist compounds FICZ
 and TCDD. In the absence of a crystalized structure of AhR-LBD, the structurally related
 PAS-B domain of HIF2 α was used for molecular docking analysis (details are provided
 as SI-3). The best poses obtained for the three ligands during the docking simulations
 are represented in Figure 3.

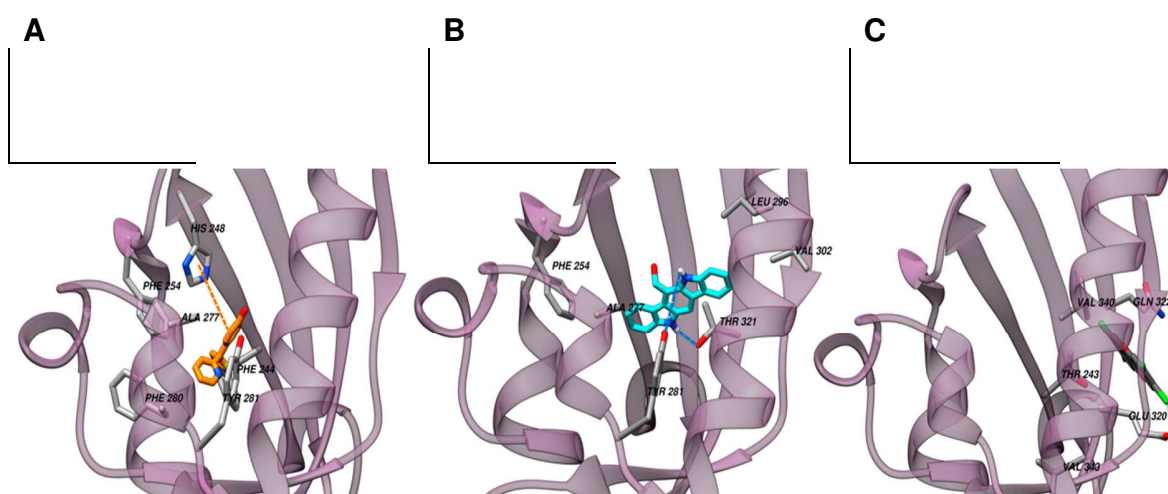


Figure 3. Representation of molecular docking and the molecular interactions between HIF2 α (PBD ID: 3F1O) and **22** (A), FICZ (B) and TCDD (C). The structure of the protein is represented as transparent lilac ribbons and the best pose obtained for **22**, FICZ and TCDD are displayed as sticks. The residues involved in hydrophobic interactions are labelled. π -Cation (orange), hydrogen bond (blue) and halogen bond (green) interactions are represented in dot lines. (color online only)

The three docked ligands (**22**, FICZ and TCDD) seem to concurred in the internal cavity of the crystallized PAS-B heterodimer as expected [10]. While **22** and FICZ were predicted to bound with AhR-LBD in a similar region of the cavity, the best pose estimated for TCDD binding seem to lie in a different region as shown in Figure 3. Details on the residues involved in the molecular docking for each ligand are provided in Supplementary Information (SI-3). Furthermore, the hydrophobic interactions in the predicted protein/ligand complex for **22** as well as for the endogenous agonist FICZ shared PHE 254 and ALA 277 residues. π -Cation interactions with HIS 248, hydrogen bond with TYR 281 and THR 321, and halogen bond with GLU 320 were also identified for **22**, FICZ and TCDD respectively as represented in Figure 3. The posted results suggested differences in the predictive binding for these three ligands that could ultimately lead to distinct biological responses [13]. A comparison between the binding energies and interactions modes of compounds **22** and **21** did not provided plausible rationalization for the remarkable activity differences *in vitro* identified (see Section 2, SI-3).

On the other hand, AhR ligands often modulate other transcription factors, particularly nuclear receptors [59,60]. Therefore, as a preliminary off-targeting screening, the binding capacity of compound **22** in ER, Androgen Receptor (AR), Progesterone Receptor (PR) and Pregnane X Receptor (PXR) was analyzed by molecular docking. A comparison between **22** and well-known ligands of each receptor did not reveal any apparent binding resemblances. Although the binding energies of **22** were in most cases similar to those exhibited by the specific ligand for each receptor, the pocket and binding sites were different in all cases (Details are provided in Section 4, SI-3).

2.4.2. Druglikeness and ADME profile

Characterizing the druglikeness as well as the bioavailability are important steps toward the prioritization in drug discovery [61]. Therefore, physicochemical properties (Table 2) were predicted *in silico* for the six novel synthesized TAMs with the most significant AhR agonist activity. Additional properties are provided in SI-3.

Table 2. Physicochemical properties and druglikeness criteria of the AhR-agonist TAMs and the drug bisacodyl.

ID	#rtvFG ^a	MW [g/mol] ^b	Dipole ^c	SASA [Å ²] ^d	Volume [Å ³] ^e	TPSA ^f	Donor HB ^g	Accept HB ^h	Polrz [Å ³] ⁱ	logP o/w ^j	logS [S: mol/dm ³] ^k	Lipinski's rule of five ^l
14	0	341.41	0.68	599.04	1081.50	42.35	1	2.50	38.39	5.32	-5.46	1
18	0	314.39	1.75	578.44	1034.32	37.91	1	1.75	36.98	5.36	-5.51	1
19	1	342.40	1.75	625.36	1111.64	54.98	1	3.50	40.02	4.82	-5.74	0
22	0	267.35	3.53	503.96	869.78	50.36	1	1.75	29.76	4.09	-4.32	0
25	0	342.40	6.52	615.79	1090.79	61.36	1	3.50	38.90	4.95	-5.41	0
28	0	359.35	7.33	606.32	1064.55	42.35	1	2.50	36.68	5.57	-6.12	1
BSD	2	361.40	7.66	658.56	1169.98	65.49	0	6.00	40.99	3.66	-4.74	0

^a #rtvFG: Number of reactive functional groups in the structure of the molecule (listed in Experimental Section). Recommended values: 0-2.

^b MW: Molecular weight of the molecule. Recommended values: 130-725 g/mol.

^c Dipole: Computed dipole moment of the molecule. Recommended values: 1.0-12.5.

^d SASA: Total solvent accessible surface area. Recommended values: 300-1000 Å² using a probe with a 1.4 Å radius.

^e Volume: Total solvent-accessible volume. Recommended values: 500-2000 Å³ using a probe with a 1.4 Å radius.

^f TPSA: Topological polar surface area

^g Donor HB: Estimated number of hydrogen bonds that would be donated by the solute to water molecules in an aqueous solution. Recommended values: 0-6.

^h Accept HB: Estimated number of hydrogen bonds that would be accepted by the solute from water molecules in an aqueous solution. Recommended values: 2-20

ⁱ Polrz: Predicted polarizability. Recommended values: 13-70 Å³.

^j logP o/w: Predicted logarithm of octanol/water partition coefficient. Recommended values: -2.0 to 6.5.

^k logS: Predicted logarithm of solubility (S expressed in mol/dm³). Recommended values: -6.5 to 0.5.

^l Lipinski's rule of five (druglikeness): Number of violations of Lipinski's rule of five: MW < 500, logP o/w < 5, donor HB ≤ 5, accept HB ≤ 10. Maximum: 4 violations.

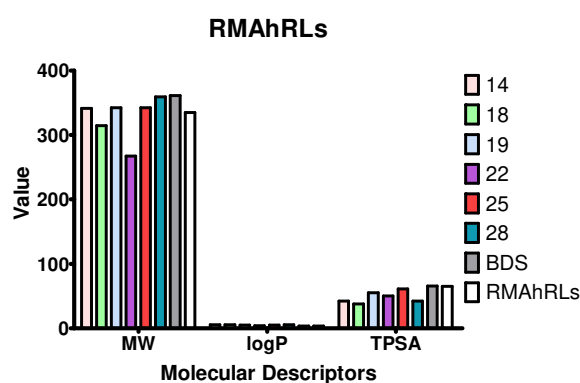
The presence of reactive functional groups (#rtvFG) has been related to decomposition, reactivity and toxicity *in vivo*. Therefore, this molecular descriptor serves as an alert system of structural groups such as azo, diazo, carbonate, aluminum or silicon (full list in SI-3). All the agonist TAMs were consistent the recommended criterium for drug-like compounds. They all were free from potentially reactive functional groups except for **19**. Interestingly, the TAM drug bisacodyl possessed two. The molecular weights, the computed dipole moments, the topological polar surface area (TPSA) and the total solvent accessible surface area (SASA) and volume, the polarizability as well as the estimated number of hydrogen bonds (HB) that would be donated or accepted in an aqueous solution were predicted within the recommended values for all the studied TAMs.

The octanol/water partition coefficient (logP o/w) directly influences the effects of chemical entities on biological systems, particularly their pharmacokinetics and pharmacodynamics [62]. Similarly, the aqueous solubility (logS) of a compound influences its ability to reach the site of action and produce any kind of effect. According to the predicted logP o/w and logS, all the agonist TAMs met the recommended range for druglikeness. Finally, Table 2 shows the Lipinski's rule of five

as a global criterium of druglikeness that suggests the limits of some physicochemical properties as follow: MW < 500, logP o/w < 5, donor HB ≤ 5, accpt HB ≤ 10. Hence, none of the agonist TAMs showed more than one violation of such rule and only the predicted logP o/w for the TAMs **14**, **18** and **28** was slightly higher than 5.

In order to analyze the six agonist compounds in the context of rapidly metabolized AhR ligands (RMAhRLs) or Selective AhR modulators (SAhRMs), a comparative analysis was performed based on their physicochemical profiles, as proposed by Dolciemi D. *et al* [63]. The mean values ± SD of the molecular descriptors suggested for RMAhRLs are MW (335±91), log P o/w (3.46±1.10) and TPSA (65.1±24.8), while those for SAhRMs are MW (307±77), log P o/w (4.24±2.24) and TPSA (43.7±34) [63]. Comparisons performed using one-way ANOVA (p<0.05) followed by Dunnett's post-test of the TAMs within the RMAhRLs and SAhRMs context, revealed no significant differences, as represented in Figure 4 a) and b), respectively. Therefore, the studied TAMs cannot be classified as SAhRMs or RMAhRLs according to this criterion.

a)



b)

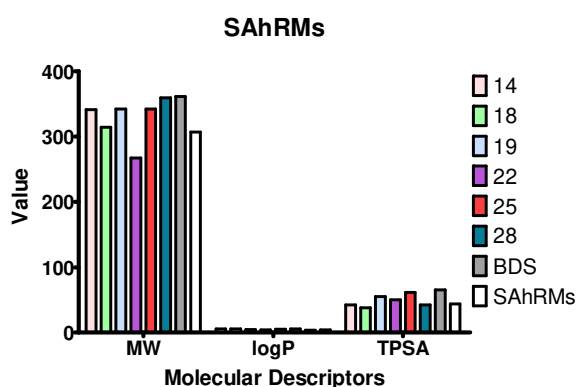


Figure 4. Mean values of the molecular descriptors MW, logP and TPSA for compounds **14**, **18**, **19**, **22**, **25** and **28** suggested to classify rapidly metabolized AhR ligands (RMAhRLs) and Selective AhR modulators (SAhRMs) [63]. One-way ANOVA (p<0.05) followed by Dunnett's post-test did not revealed significant differences between TAMs and RMAhRLs or SAhRMs, respectively.

On the other hand, predictive results of some properties contributing to the ADME profile of the AhR-agonist TAMs, are shown in Table 3.

Table 3. Prediction of ADME descriptors for the AhR-agonist TAMs and the drug bisacodyl

ID	Caco-2 [nm/sec] ^a	MDCK [nm/sec] ^b	logBB ^c	logKp [nm/sec] ^d	logKh _{sa} [nm/sec] ^e	J _m [μg cm ⁻² h ⁻¹] ^f	HOA ^g	#Metab ^h	Jorgensen's rule of three ⁱ
14	4561.02	2551.05	-0.07	-0.05	0.87	1.06	3	5	0
18	5349.67	3031.00	0.07	-0.07	0.93	0.83	3	4	0
19	2083.59	1093.83	-0.37	-0.88	0.80	0.08	3	3	1
22	2157.45	1872.28	-0.19	-1.07	0.47	1.11	3	5	0
25	4130.44	2291.76	-0.12	-0.08	0.70	1.12	3	4	0
28	5013.57	10000.00	0.26	-0.34	0.82	0.12	3	4	1
BSD	846.79	413.32	-0.87	-1.81	0.20	0.10	3	3	0

^a Caco-2 (model for the gut-blood barrier): Predicted apparent Caco-2 cell permeability (non-active transport) [nm/sec]. Criteria: <25 poor permeability, >500 great permeability.

^b MDCK (mimic for the blood-brain barrier): Predicted apparent MDCK cell permeability (non-active transport) [nm/sec]. Criteria: <25 poor permeability, >500 great permeability.

^c logBB: Predicted brain/blood partition coefficient (model for orally delivery drugs). Recommended values: from -3.0 to 1.2.

^d logKP: Predicted skin permeability. Recommended values: from -8.0 to -1.0.

^e logKh_{sa}: Predicted binding to human serum albumin. Recommended values: from -1.5 to 1.5.

^f J_m: Predicted maximum transdermal transport rate obtain from: $K_p \times MW \times S$ (μg cm⁻² h⁻¹)

^g HOA (Human Oral Absorption): Predicted qualitative human oral absorption: low (1), medium (2), high (3).

^h Metab: Number of likely metabolic reactions (listed in SI-3). Recommended values: 1-8.

ⁱ Jorgensen's rule of three (oral availability): Fewer (and preferably no) violations of the follow: logS > -5.7, Caco-2 > 22 nm/sec, #PrimaryMetabolites < 7.

Considering the predicted parameters collectively related to oral bioavailability (Caco-2 permeability, Human Oral Absorption (HOA) and Jorgensen's rule of three), it can be concluded that the AhR-agonist TAMs synthesized probably have good permeability to cross the gut-blood barrier, a high human oral absorption and only **19** and **28** violated the solubility criterium of Jorgensen's rule. Adequate binding to human serum albumin (logKh_{sa}) as well as an appropriated number of metabolic reactions (#Metab) were predicted for all the TAMs. Lastly, the apparent capacity to cross the brain/blood barrier (logBB) was predicted as good for all the studied TAMs while the predicted skin permeability (logKp) was in acceptable limit only for the strongest AhR-agonist **22** and BSD.

3. Conclusions

TAM compounds were straightforwardly synthesized and characterized by means of efficient synthetic strategies in this work. The effects of 32 newly TAM derivatives as potential modulators of the emerging pharmacological target AhR were determined *in vitro* using a novel secreted luciferase assay system. The bioassays revealed an

exclusive agonism of eight derivatives and a lack of antagonist activity on **AhR activation** across the TAM set. Heteroaromatic or naphthol moieties crucially determined the occurrence of AhR agonism and the thiophene derivative **22** was the most potent agonist compound on AhR-mediated transcription yielding over 30-fold response, comparable to the endogenous metabolite FICZ. The structural adequacy, absence of cytotoxicity as well as druglikeness and favorable ADME profile, allow to suggest **22** as a new lead compound in the study of AhR-mediated transcription. In general, these results could provide valuable insights to design new potent AhR modulators based on the TAM scaffold.

4. Experimental Section

4.1. Chemistry

4.1.1. Materials and Methods

All reagents were obtained from commercial sources unless otherwise noted and used as received. Heated experiments were conducted using thermostatically controlled oil baths. Reaction requiring anhydrous conditions were performed under an atmosphere oxygen-free in oven-dried glassware. Drying of the products was carried out under reduced pressure using a vacuum pump and/or a desiccant heated to 40°C in the presence of P₂O₅. All reactions were monitored by analytical thin layer chromatography (TLC) or by Gas chromatography-Mass spectrometry (GC-MS). TLC was performed on aluminium sheets, silica gel coated with fluorescent indicator F₂₅₄, Merck. TLC plates were visualized using irradiation with light at 254 nm or in an iodine chamber as appropriate. FCC was carried out when necessary using silica gel 60 (particle size 0.040-0.063 mm, Merck). The eluent mixture is specified for each purification.

4.1.2. Physical measurements

Melting points (Mp) were determined on a Leica VMHB system Kofler apparatus. The structure of the products prepared by different methods was checked by comparison of their NMR, IR and MS data and by the TLC behavior. ¹H and ¹³C-NMR spectra were acquired on a Bruker BioSpin GmbH spectrometer 400 MHz, at room temperature.

Chemical shifts are reported in δ units, parts per million (ppm). Coupling constants (J) are measured in hertz (Hz). Splitting patterns are designed as follows: s, singlet; d, doublet; dd, doublet of doublets; dm, doublet of multiplets, ddd, doublet of doublets of doublets; m, multiplet; br, broad. Various 2D techniques and DEPT experiments were used to establish the structures and to assign the signals. For the assignments of the NMR signals, we use the convention presented in Figure 4. GC-MS analyses were performed with an Agilent 6890N instrument equipped with a 12 m x 0.20 mm dimethyl polysiloxane capillary column and an Agilent 5973N MS detector-column temperature gradient 80-300°C (method 160): 160°C (1 min), 180°C to 260°C (10°C/min), 260°C (4 min); (method 180): 180°C (1 min), 180°C to 300°C (10°C/min), 300°C (2 min), gradient 200-300°C (method 200): 200°C (1 min), 200°C to 300°C (10°C/min), 300°C (4 min). Low-resolution mass spectra (LRMS) resulting from ionization by electronic impact. Infrared spectra were recorded over the 400-4000 cm^{-1} range with an Agilent Technologies Cary 630 FTIR/ ATR/ ZnSe spectrometer. High-resolution mass spectra (HRMS) analyses were acquired on a Thermo Scientific LTQ Orbitrap mass spectrometer. The HPLC analyses were carried out on a normal phase column Hypersil Si (length: 150 mm, diameter: 4.6 mm, stationary phase: 5 μm) and a reverse phase column Hypersil ODS C18 (length: 150 mm, diameter: 4.60 mm, stationary phase: 5 μm) using a Water 2998 Photodiode Array Detector (260-370 nm) and an isocratic system of elution. The retention time (R_t) is expressed in min in the decimal system. HPLC purity were determined on the Hypersil Si column, using *n*-heptane/ethyl acetate 7/3 with a flow rate of 0.8 mL per min and UV detection at $\lambda = 262\text{-}264$ nm, unless otherwise notified.

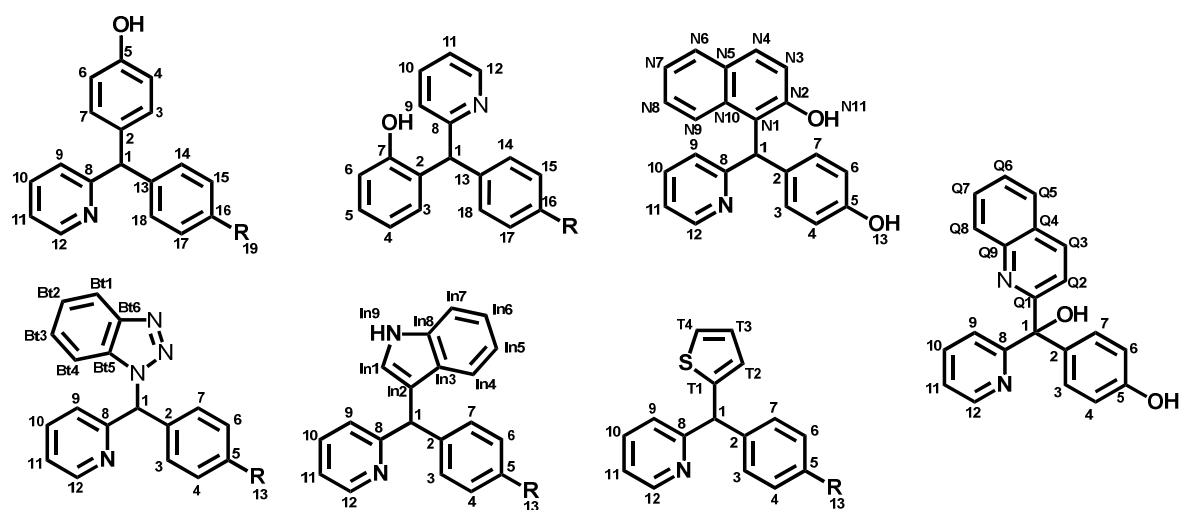


Figure 4. Convention adopted to assign signals of ^1H and ^{13}C -NMR spectra.

Only the 32 TAM compounds evaluated *in vitro* are described herein. Intermediates and other TAMs obtained are detailed as SI-1.

4.1.3. General procedure for the preparation of *p,p*-triarylmethanes

Method A: To a solution of the corresponding carbinol (1 eq.) and phenol (1.2 eq.) in nitrobenzene (0.4 M) was added dropwise concentrated sulfuric acid (4 eq.) at 0°C. The reaction progress was monitored by GC-MS and TLC (eluent DCM/MeOH 90/10). After 5 min at 80 °C the reaction was cooled to room temperature and neutralized with a saturated solution of NaHCO_3 (pH 7-8), then extracted with ethyl acetate three times. The combined organic phases were dried over anhydrous Na_2SO_4 , filtered and concentrated. The crude residue was purified by FCC on silica gel (eluent gradient DCM, DCM/MeOH 98/2, DCM/MeOH 90/10) to afford the corresponding *p,p* triarylmethane: Yields: **4a** (72%), **4b** (63%) and **4c** (39%).

Method B: To a solution of the corresponding carbinol (1 eq.) and phenol (1.2 eq.) in nitrobenzene (0.4 M) was added dropwise concentrated sulfuric acid (4 eq.) at 0°C. The reaction progress was monitored by GC-MS and TLC (eluent CyHex/ EtOAc 50/50). After stirring at 0°C the reaction was cooled to room temperature and neutralized with a saturated solution of NaHCO_3 (formation of a gum which solubilizes once pH 7-8 is reached), then extracted with ethyl acetate four times. The combined organic phases

were washed with brine, dried over anhydrous Na₂SO₄, filtered and concentrated. The crude residue was purified by FCC on silica gel (eluent gradient DCM, DCM/MeOH 98/2, DCM/MeOH 90/10) to afford the corresponding *p,p* triarylmethane: Yields: **4d** (33%) and **4e** (47%).

4.1.3.1. 4-((4-(tert-butyl)phenyl)(pyridin-2-yl)methyl)phenol (4a). Yield: 96 mg, 0.30 mmol, white solid, 72%. 13 mg (0.04 mmol, 9.6%) of 2-((4-(tert-butyl)phenyl)(pyridin-2-yl)methyl)phenol are also isolated, (Method A). Mp = 154-156 °C. **TLC** CyHex/EtOAc 50/50, R_f = 0.54, DCM/MeOH 90/10, R_f = 0.80; **¹H NMR (DMSO d₆, 400 mHz)** (δ ppm) 1.24 (s, 9H, H₂₀), 5.49 (s, 1H, H₁), 6.69 (d, 2H, J_{ortho} = 8 Hz, H₄, H₆), 7.01 (d, 2H, J_{ortho} = 8 Hz, H₇, H₃), 7.11 (d, 2H, J_{ortho} = 8 Hz, H₁₄, H₁₈), 7.18 - 7.24 (m, 2H, H₉, H₁₁), 7.30 (d, 2H, J_{ortho} = 8 Hz, H₁₅, H₁₇), 7.71 (ddd, 1H, J₁₀₋₉ = J₁₀₋₁₁ = 8 Hz, J₁₀₋₁₂ = 4 Hz, H₁₀), 8.52 (ddd, 1H, J₁₂₋₁₁ = 4.7 Hz, J₁₂₋₁₀ = 1.8 Hz, J₁₂₋₉ = 0.95 Hz, H₁₂), 9.27 (s, 1H, OH); **¹³C NMR (DMSO d₆, 100 mHz)** (δ ppm) 31.12 (C₁₉), 34.03 (C₂₀), 57.06 (C₁), 114.96 (C₆, C₄), 121.38 (C₁₁), 123.37 (C₉), 124.87 (C₁₅, C₁₇), 128.60 (C₁₄, C₁₈), 129.88 (C₃, C₇), 133.31 (C₂), 136.56 (C₁₀), 140.59 (C₁₃), 148.22 (C₁₆), 149.02 (C₁₂), 155.58 (C₅), 163.15 (C₈); **GC-MS** method 180, R_t = 7.82 min, *m/z* 317 [M⁺] (100), 302 [M⁺ - CH₃] (30), 286 [M⁺ - 2 CH₃] (5), 260 [M⁺ - C(CH₃)₃] (19), 239 [OHPhCH_t-BuPh]⁺ (23), 224 [OHPhCH_t-BuPh⁺ - CH₃] (8); **IR** (ATR) (cm⁻¹) 3058, 3020 (νCsp²-H), 2957 (νCsp³-H), 1615, 1600, 1510 (νC=C), 1167 (νC-O), 810 (δCsp²-H *p*-disubst), 755 (δCsp²-H *o*-disubst); **HPLC** purity: 96%, (Hypersyl Si, *n*-heptane/EtOAc 30/70, flow rate 0.80 mL/min, λ_{max} = 264 nm, R_t = 2.84 min).

4.1.3.2. 4-(pyridin-2-yl(*p*-tolyl)methyl)phenol (4b). Yield: 73 mg, 0.26 mmol, beige solid, 63%. 18 mg (0.07 mmol, 15%) of 2-(pyridin-2-yl(*p*-tolyl)methyl)phenol are also isolated, (Method A). Mp = 156-158 °C. **TLC** CyHex/EtOAc 50/50, R_f = 0.44, DCM/MeOH 90/10, R_f = 0.53; **¹H NMR (DMSO d₆, 400 mHz)** (δ ppm) 2.24 (s, 3H, H₁₉), 5.50 (s, 1H, H₁), 6.69 (d, 2H, J_{ortho} = 8.5 Hz, H₄, H₆), 6.99 (d, 2H, J_{ortho} = 8.5 Hz, H₇, H₃), 7.03-7.11 (m, 4H, H₁₄, H₁₅, H₁₈, H₁₇), 7.16-7.24 (m, 2H, H₉, H₁₁), 7.70 (ddd, 1H, J₁₀₋₉ = J₁₀₋₁₁ = 7.7 Hz, J₁₀₋₁₂ = 1.80 Hz, H₁₀), 8.51 (ddd, 1H, J₁₂₋₁₁ = 5 Hz, J₁₂₋₁₀ = 2.8 Hz, J₁₂₋₉ = 0.8 Hz, H₁₂), 9.24 (s, 1H, OH); **¹³C NMR (DMSO d₆, 100 mHz)** (δ ppm) 20.56 (C₁₉), 57.12 (C₁), 114.98 (C₆, C₄), 121.40 (C₁₁), 123.38 (C₉), 128.78 (C₁₄, C₁₅, C₁₇, C₁₈),

129.91 (C₃, C₇), 133.40 (C₁₆), 135.05 (C₂), 136.57 (C₁₀), 140.63 (C₁₃), 149.05 (C₁₂), 155.70 (C₅), 163.21 (C₈); **GC-MS** method 180, R_t = 7.22 min, m/z 274 [M⁺] (100), 259 [M⁺ - CH₃] (12), 197 [OHPhCHPhCH₃]⁺(34), 181 [OHPhCHPhCH₃⁺ - OH] (24), 167 [PhCHPy]⁺, (8), 78 [Py]⁺(4); **IR** (ATR) (cm⁻¹) 3018, 3005 (νCsp²-H), 2915 (νCsp³-H), 1614, 1592, 1508 (νC=C), 1233 (νC-O), 754 (δCsp²-H o-disubst); **HPLC** purity: 98%, (Hypersyl Si, *n*-heptane/EtOAc 30/70, flow rate 0.80 mL/min, λ_{max} = 264 nm, R_t = 3.00 min).

4.1.3.3. 4-((4-bromophenyl)(pyridin-2-yl)methyl)phenol (4c). Yield: 51 mg, 0.15 mmol, oil, 39%, (Method A). **TLC** DCM/MeOH 90/10, R_f = 0.60; **¹H NMR (DMSO d₆, 400 MHz)** (δ ppm) 5.55 (s, 1H, H₁), 6.69 (d, 2H, J_{ortho} = 8.70 Hz, H₄, H₆), 7.00 (d, 2H, J_{ortho} = 8.5 Hz, H₇, H₃), 7.14 (d, 2H, J_{ortho} = 8.2 Hz, H₁₄, H₁₈), 7.20-7.28 (m, 2H, H₉, H₁₁), 7.46 (d, 2H, J_{ortho} = 8.3 Hz, H₁₅, H₁₇), 7.73 (ddd, 1H, J₁₀₋₉ = J₁₀₋₁₁ = 7.7 Hz, J₁₀₋₁₂ = 1.8 Hz, H₁₀), 8.53 (dd, 1H, J₁₂₋₁₁ = 5.3 Hz, J₁₂₋₁₀ = 1.9 Hz, H₁₂), 9.32 (s, 1H, OH); **¹³C NMR (DMSO d₆, 100 MHz)** (δ ppm) 56.56 (C₁), 115.15 (C₆, C₄), 119.32 (C₁₆), 121.68 (C₁₁), 123.58 (C₉), 129.94 (C₃, C₇), 131.02 (C₁₅, C₁₇), 131.23 (C₁₄, C₁₈), 132.79 (C₂), 136.83 (C₁₀), 143.16 (C₁₃), 149.21 (C₁₂), 159.91 (C₇), 162.44 (C₈); **GC-MS** method 180, R_t = 8.81 min, m/z 340 [M⁺] (100), 324 [M⁺ - OH] (3), 259 [M⁺ - Br] (52), 181 [OHPhCH₂Ph]⁺(85), 167 [PhCH₂Py]⁺(21), 78 [Py]⁺ (15); **IR** (ATR) (cm⁻¹) 3055, 3018 (νCsp²-H), 2924 (νCsp³-H), 1593, 1511, 1486 (νC=C), 1168 (νC-O); **HPLC** purity: 95%, (Hypersyl Si, *n*-heptane/EtOAc 30/70, flow rate 0.80 mL/min, λ_{max} = 263 nm, R_t = 3.00 min).

4.1.3.4. 4-((4-chlorophenyl)(pyridin-2-yl)methyl)phenol (4d). Yield: 865 mg, 2.94 mmol, white solid, 33%, (Method B). Mp = 170-171 °C. **TLC** CyHex/EtOAc 50/50, R_f = 0.49, DCM/MeOH 90/10, R_f = 0.70; **¹H NMR (DMSO d₆, 400 MHz)** (δ ppm) 5.57 (s, 1H, H₁), 6.70 (d, 2H, J_{ortho} = 8.6 Hz, H₄, H₆), 7 (d, 2H, J_{ortho} = 8.6 Hz, H₇, H₃), 7.19-7.25 (d + m, 4H, J_{ortho} = 8.5 Hz, H₉, H₁₁, H₁₄, H₁₈), 7.34 (d, 2H, J_{ortho} = 8.5 Hz, H₁₅, H₁₇), 7.73 (ddd, 1H, J₁₀₋₉ = J₁₀₋₁₁ = 7.6 Hz, J₁₀₋₁₂ = 1.9 Hz, H₁₀), 8.53 (dd, 1H, J₁₂₋₁₁ = 5.6 Hz, J₁₂₋₁₀ = 2.2 Hz, H₁₂), 9.31 (s, 1H, OH); **¹³C NMR (DMSO d₆, 100 MHz)** (δ ppm) 56.48 (C₁), 115.12 (C₄, C₆), 121.64 (C₁₁), 123.55 (C₉), 128.07 (C₁₅, C₁₇), 129.91 (C₃, C₇), 130.77 (C₁₄, C₁₈),

130.80 (C₁₆), 132.85 (C₂), 136.80 (C₁₀), 142.70 (C₁₃), 149.19 (C₁₂), 155.90 (C₅), 162.50 (C₈); **GC-MS** method 180, R_t = 8.04 min, *m/z* 295 [M⁺] (100), 280 [M⁺-OH] (2), 259 [M⁺-Cl] (25), 217 [OHPhCHPhCl]⁺(36), 201 [OHPhCHPhCl⁺-OH] (9), 181 [OHPhCHPhCl⁺-Cl] (35), 167 [PhCHPy]⁺(14), 78 [Py]⁺ (7); **IR** (ATR) (cm⁻¹) 3054 (νO-H), ν 3019 (νCsp²-H), 2928 (νCsp³-H), 1615, 1592, 1510 (νC=C), 1235 (νC-O), 806 (δCsp²-H p-disubst), 756 (δCsp²-H o-disubst), 624(νC-Cl); **HPLC** purity: 95%, (Hypersyl Si, *n*-heptane/EtOAc 30/70, flow rate 0.80 mL/min, λ_{max} = 263 nm, R_t = 3.01 min).

4.1.3.5. 4-((4-fluorophenyl)(pyridin-2-yl)methyl)phenol (4e). Yield: 89 mg, 0.32 mmol, yellow oil, 47%, (Method B). **TLC** CyHex/EtOAc 50/50, R_f = 0.44, DCM/MeOH 90/10, R_f = 0.70; **¹H NMR (DMSO d₆, 400 MHz)** (δ ppm) 5.58 (s, 1H, H₁), 6.73 (d, 2H, J_{ortho} = 8.5 Hz, H₄, H₆), 7.02 (d, 2H, J_{ortho} = 8.5 Hz, H₇, H₃), 7.05-7.14 (m, 2H, H₉, H₁₁), 7.17-7.27 (m, 4H, H₁₄, H₁₅, H₁₇, H₁₈), 7.70 (ddd, 1H, J₁₀₋₉ = J₁₀₋₁₁ = 7.8 Hz, J₁₀₋₁₂ = 2 Hz, H₁₀), 8.53 (dd, 1H, J₁₂₋₁₁ = 4.8 Hz, J₁₂₋₁₀ = 1.7 Hz, H₁₂); **¹³C NMR (DMSO d₆, 100 MHz)** (δ ppm) 56.64 (C₁), 114.81 (d, 2C, J_{C-F} = 21 Hz, C₁₅, C₁₇), 115.24 (C₄, C₆), 121.68 (C₁₁), 123.59 (C₉), 130.02 (C₃, C₇), 130.83 (d, 2C, J_{C-F} = 8 Hz, C₁₄, C₁₈), 133.31 (C₂), 136.85 (C₁₀), 139.70 (d, 1C, J_{C-F} = 3 Hz, C₁₃), 149.25 (C₁₂), 155.95 (C₅), 160.65 (d, 1C, J_{C-F} = 240 Hz, C₁₆), 162.89 (C₈); **GC-MS** method 180, R_t = 6.37 min, *m/z* 278 [M⁺] (100), 261 [M⁺-OH] (30), 201 [OHPhCHPhF]⁺(42), 183 [OHPhCHPhCl⁺-F] (23), 78 [Py]⁺ (4); **IR** (ATR) (cm⁻¹) 3056, 3005 (νCsp²-H), 1592, 1506 (νC=C), 1221 (νC-O), 811 (δCsp²-H p-disubst), 757 (δCsp²-H o-disubst); **HPLC** purity: 100%, (Hypersyl Si, *n*-heptane/EtOAc 30/70, flow rate 0.80 mL/min, λ_{max} = 264 nm, R_t = 3.07 min).

4.1.4. General procedure for the preparation of triarylmethane acetates

To a solution of the corresponding compound (1 eq.) in acetic anhydride (110 eq.) was added an aqueous solution of sodium hydroxide 1 M (1.30 eq.) at 20 °C or 40 °C. The reaction progress was monitored by GC-MS and TLC (eluent CyHex/EtOAc 90/10). After stirring at room temperature, the reaction mixture was concentrated, and ethyl acetate was added. The solution was washed with water, an aqueous solution of NaHCO₃ then with brine and water. Then the organic phases were dried over anhydrous

Na₂SO₄, filtered and concentrated. The expected compounds were isolated, and purity was checked by NMR. Yields: **5a** (90%), **5b** (96%), **5c** (77%), **5d** (76%), and **5e** (78%).

4.1.4.1. 4-((4-(tert-butyl)phenyl)(pyridin-2-yl)methyl)phenyl acetate (5a). The reaction was performed during 4 h at 20 °C then 15 h at 40 °C. Yield: 524 mg, 0.35 mmol, brown oil, 90%. **TLC** CyHex/EtOAc 50/50, R_f = 0.73, DCM/MeOH 90/10, R_f = 0.20; **¹H NMR (DMSO d₆, 400 mHz)** (δ ppm) 1.25 (s, 9H, H₁₉), 2.25 (s, 3H, H₂₁), 5.65 (s, 1H, H₁), 7.04 (d, 2H, J_{ortho} = 8.6 Hz, H₄, H₆), 7.17 (d, 2H, J_{ortho} = 8.3 Hz, H₁₄, H₁₈), 7.23-7.29 (m, 4H, H₃, H₇, H₉, H₁₁), 7.32 (d, 2H, J_{ortho} = 8.4 Hz, H₁₅, H₁₇), 7.74 (ddd, 1H, J₁₀₋₉ = J₁₀₋₁₁ = 7.6 Hz, J₁₀₋₁₂ = 2 Hz, H₁₀), 8.51-8.56 (m, 1H, H₁₂); **¹³C NMR (DMSO d₆, 100 mHz)** (δ ppm) 20.79 (C₂₁), 31.09 (C₁₉), 34.06 (C₂₀), 56.91 (C₁), 121.48 (C₄, C₆), 121.65 (C₁₁), 123.58 (C₉), 125.06 (C₁₅, C₁₇), 128.58 (C₁₄, C₁₈), 129.91 (C₃, C₇), 136.79 (C₁₀), 139.88 (C₂), 140.61 (C₁₃), 148.55 (C₁₆), 148.77 (C₅), 149.17 (C₁₂), 162.33 (C₈), 169.23 (C₂₂); **GC-MS** method 180, R_t = 9.38 min, *m/z* 359 [M⁺] (99), 344 [M⁺ - CH₃] (11), 316 [M⁺ - 2 CH₃] (100), 302 [M⁺ - C(CH₃)₃] (33), 239 [OHPhCHt-BuPh]⁺ (35), 224 [OHPhCHt-BuPh⁺ - CH₃] (14), 209 [OHPhCHt-BuPh⁺ - 2 CH₃] (25), 193 [OHPhCHt-BuPh⁺ - C(CH₃)₃] (9), 167 [PhCHPy]⁺ (23); **IR** (ATR) (cm⁻¹) 3053 (νCsp²-H), 2960, 2905, 2868 (νCsp³-H), 1759 (νC=O), 1587, 1504, 1467 (νC=C), 1192 (νC-O), 749 (δCsp²-H p-disubst).

4.1.4.2. 4-(pyridin-2-yl(p-tolyl)methyl)phenyl acetate (5b). The reaction was performed during 2 h 20 min at 20 °C. Yield: 542 mg, 1.51 mmol, brown oil, 96%. **TLC** CyHex/EtOAc 50/50, R_f = 0.74, DCM/MeOH 90/10, R_f = 0.80; **¹H NMR (DMSO d₆, 400 mHz)** (δ ppm) 2.25 (s, 3H, H₂₀), 5.72 (s, 1H, H₁), 7.06 (d, 2H, J_{ortho} = 8.6 Hz, H₄, H₆), 7.21 (d, 2H, J_{ortho} = 8.4 Hz, H₁₄, H₁₈), 7.24-7.26 (m, 3H, H₃, H₇, H₁₁), 7.31 (dd, 1H, J₉₋₁₀ = 8 Hz, J₉₋₁₁ = 2 Hz, H₉), 7.51 (d, 2H, J_{ortho} = 8.4 Hz, H₁₅, H₁₇), 7.76 (ddd, 1H, J₁₀₋₉ = J₁₀₋₁₁ = 7.6 Hz, J₁₀₋₁₂ = 1.80 Hz, H₁₀), 8.56 (ddd, 1H, J₁₂₋₁₁ = 7.6 Hz, J₁₂₋₁₀ = 2.7 Hz, J₁₂₋₉ = 0.9 Hz, H₁₂); **¹³C NMR (DMSO d₆, 100 mHz)** (δ ppm) 20.83 (C₂₀), 56.40 (C₁), 119.64 (C₁₆), 121.68 (C₄, C₆), 121.90 (C₁₁), 123.76 (C₉), 129.94 (C₃, C₇), 131.19 (C₁₄, C₁₈), 131.24 (C₁₅, C₁₇), 137.02 (C₁₀), 140.08 (C₂), 142.39 (C₁₃), 148.97 (C₅), 149.35 (C₁₂), 161.66 (C₈), 169.24 (C₁₉); **GC-MS** method 180, *m/z* R_t = 9.46 min, 382 [M⁺] (61), 340 [M⁺ - COCH₃] (100), 261 [M⁺ - Cl - COCH₃] (38), 184 [OPhCH₂Ph]⁺ (46), 167 [PhCH₂Ph]⁺ (24);

624 **IR** (ATR) (cm⁻¹) 3061, 3029, 3009 (νCsp²-H), 1754 (νC=O), 1585, 1504, 1487 (νC=C),
625 1202 (νC-O), 763 (δCsp²-H p-disubst); **HPLC** purity: 98%, (Hypersyl Si, *n*-
626 heptane/EtOAc 30/70, flow rate 0.80 mL/min, λ_{max} = 262 nm, R_t = 2.79 min).

627 **4.1.4.3. 4-((4-bromophenyl)(pyridin-2-yl)methyl)phenyl acetate (5c).** The reaction
628 was performed during 1 h at 20 °C. Yield: 344 mg, 0.90 mmol, brown oil, 77%.
629 **TLC** CyHex/EtOAc 50/50, R_f = 0.82; **¹H NMR (DMSO d₆, 400 mHz)** (δ ppm) 2.25 (s,
630 3H, H₂₀), 5.74 (s, 1H, H₁), 7.07 (d, 2H, J_{ortho} = 8.6 Hz, H₄, H₆), 7.24-7.29 (m, 5H, H₃, H₇,
631 H₁₁, H₁₄, H₁₈), 7.31 (dd, 1H, J₉₋₁₀ = 7.8 Hz, J₉₋₁₁ = 1.20 Hz, H₉), 7.38 (d, 2H, J_{ortho} = 8.5
632 Hz, H₁₅, H₁₇), 7.76 (dd, 1H, J₁₀₋₁₁ = 7.8 Hz, J₁₀₋₁₂ = 1.9 Hz, H₁₀), 8.56 (ddd, 1H, J₁₂₋₁₁ =
633 7.5 Hz, J₁₂₋₁₀ = 2.7 Hz, J₁₂₋₉ = 0.9 Hz, H₁₂); **¹³C NMR (DMSO d₆, 100 mHz)** (δ ppm)
634 20.83 (C₂₀), 56.36 (C₁), 121.68 (C₄, C₆), 121.90 (C₁₁), 123.75 (C₉), 128.27 (C₁₅, C₁₇),
635 129.94 (C₃, C₇), 130.85 (C₁₄, C₁₈), 131.11 (C₁₆), 137.70 (C₁₀), 140.16 (C₂), 141.95 (C₁₃),
636 148.97 (C₅), 149.35 (C₁₂), 161.73 (C₈), 169.24 (C₁₉); **GC-MS** method 180, R_t = 8.67 min
637 *m/z* 338 [M⁺] (54), 294 [M⁺ - COCH₃] (100), 259 [M⁺ - Py] (17), 217 [OPhCH₂PhCl]⁺ (28),
638 202 [PyCH₂PhCl]⁺ (7), 184 [OPhCH₂Ph]⁺ (18), 167 [PhCH₂Ph]⁺ (13); **IR** (ATR) (cm⁻¹)
639 3055, 3007 (νCsp²-H), 2917 (νCsp³-H), 1754 (νC=O), 1585, 1505, 1466 (νC=C), 1202
640 (νC-O), 817 (δCsp²-H o-disubst), 763 (δCsp²-H p-disubst); **HPLC** purity: 95%,
641 (Hypersyl Si, *n*-heptane/EtOAc 30/70, flow rate 0.80 mL/min, λ_{max} = 262 nm, R_t = 2.78
642 min).

643 **4.1.4.4. 4-((4-chlorophenyl)(pyridin-2-yl)methyl)phenyl acetate (5d).** The reaction
644 was performed during 1 h at 20 °C. Yield: 349 mg, 1.03 mmol, orange oil, 76%.
645 **TLC** CyHex/EtOAc 50/50, R_f = 0.74, CyHex/EtOAc 50/50, , R_f = 0.74; **¹H NMR (DMSO**
646 **d₆, 400 mHz)** (δ ppm) 2.25 (s, 3H, H₂₀), 5.73 (s, 1H, H₁), 7.05 (d, 2H, J₄₋₆ = 8.6 Hz, H₄,
647 H₆), 7.15 (dd, 2H, J_{ortho} = J_{H-F} = 8.9 Hz, H₁₅, H₁₇), 7.23-7.31 (m, 6H, H₃, H₇, H₉, H₁₁, H₁₄,
648 H₁₈), 7.76 (ddd, 1H, J₁₀₋₉ = J₁₀₋₁₁ = 7.7 Hz, J₁₀₋₁₂ = 1.9 Hz, H₁₀), 8.55-8.57 (ddd, 1H, J₁₂₋₉
649 = 0.80 Hz, J₁₂₋₁₀ = 1.8 Hz, J₁₁₋₁₂ = 4.8 Hz, H₁₂); **¹³C NMR (DMSO d₆, 100 mHz)** (δ ppm)
650 20.83 (C₂₀), 56.28 (C₁), 115.04 (d, 2C, J_{C-F} = 20.90 Hz, C₁₅, C₁₇), 121.63 (C₄, C₆),
651 121.84 (C₁₁), 123.69 (C₉), 129.90 (C₃, C₇), 130.82 (d, 2C, J_{C-F} = 7.9 Hz, C₁₄, C₁₈),
652 136.98 (C₁₀), 139.09 (d, 2C, J_{C-F} = 3.20 Hz, C₁₃), 140.49 (C₂), 148.91 (C₅), 149.33 (C₁₂),

653 160.82 (d, 1C, J_{C-F} = 239.60 Hz, C₁₆), 169.25 (C₈), 172.06 (C₁₉); **GC-MS** method 180, R_t
654 = 7.18 min, m/z , 321 [M⁺] (6), 278 [M⁺ - CH₃CO] (100), 183 [PyCHPhO]⁺(15); **IR** (ATR)
655 (cm⁻¹) 3051, 3006 (νCsp²-H), 2927 (νCsp³-H), 1754 (νC=O), 1571, 1588, 1503 (νC=C),
656 1192 (νC-O), 1160 (νC-F), 819 (δCsp²-H o-disubst), 750 (δCsp²-H p-disubst); **HPLC**
657 purity: 97%, (Hypersyl Si, *n*-heptane/EtOAc 30/70, flow rate 0.80 mL/min, λ_{max} = 262
658 nm, R_t = 2.84 min).

659 **4.1.4.5. 4-((4-fluorophenyl)(pyridin-2-yl)methyl)phenyl acetate (5e).** The reaction
660 was performed during 3 h at 40 °C. Yield: 470 mg, 1.46 mmol, brown oil, 78%. **TLC**
661 CyHex/EtOAc 50/50, R_f = 0.60; **¹H NMR (DMSO d₆, 400 mHz)** (δ ppm) 2.25 (s, 3H,
662 H₂₀), 5.73 (s, 1H, H₁), 7.05 (d, 2H, J_{4-6} = 8.6 Hz, H₄, H₆), 7.15 (dd, 2H, J_{ortho} = J_{H-F} = 8.9
663 Hz, H₁₅, H₁₇), 7.23-7.31 (m, 6H, H₃, H₇, H₉, H₁₁, H₁₄, H₁₈), 7.76 (ddd, 1H, J_{10-9} = J_{10-11} =
664 7.7 Hz, J_{10-12} = 1.9 Hz, H₁₀), 8.55-8.57 (ddd, 1H, J_{12-9} = 0.80 Hz, J_{12-10} = 1.8 Hz, J_{11-12} =
665 4.8 Hz, H₁₂); **¹³C NMR (DMSO d₆, 100 mHz)** (δ ppm) 20.83 (C₂₀), 56.28 (C₁), 115.04 (d,
666 2C, J_{C-F} = 20.90 Hz, C₁₅, C₁₇), 121.63 (C₄, C₆), 121.84 (C₁₁), 123.69 (C₉), 129.90 (C₃,
667 C₇), 130.82 (d, 2C, J_{C-F} = 7.9 Hz, C₁₄, C₁₈), 136.98 (C₁₀), 139.09 (d, 2C, J_{C-F} = 3.20 Hz,
668 C₁₃), 140.49 (C₂), 148.91 (C₅), 149.33 (C₁₂), 160.82 (d, 1C, J_{C-F} = 239.60 Hz, C₁₆),
669 169.25 (C₈), 172.06 (C₁₉); **GC-MS** method 180, R_t = 7.18 min, m/z , 321 [M⁺] (6), 278 [M⁺
670 - CH₃CO] (100), 183 [PyCHPhO]⁺(15); **IR** (ATR) (cm⁻¹) 3051, 3006 (νCsp²-H), 2927
671 (νCsp³-H), 1754 (νC=O), 1571, 1588, 1503 (νC=C), 1192 (νC-O), 1160 (νC-F), 819
672 (δCsp²-H o-disubst), 750 (δCsp²-H p-disubst); **HPLC** purity: 97%, (Hypersyl Si, *n*-
673 heptane/EtOAc 30/70, flow rate 0.80 mL/min, λ_{max} = 262 nm, R_t = 2.84 min).

674 **4.1.5. General procedure for the preparation of triarylmethane acetate *N*-oxides**

675 To a solution of the corresponding triarylmethane acetate (1 eq.) in anhydrous
676 dichloromethane (0.22 M), was added in one portion *m*-chloroperbenzoic acid (3 eq.).
677 The suspension was stirred at room temperature. The reaction medium became a clear
678 solution and then pale yellow milky one. The reaction progress was monitored by GC-
679 MS and TLC (eluent CyHex/EtOAc 60/40). At the end of the reaction, the reaction
680 mixture was neutralized by a 40% aqueous solution of KOH (pH 7-8) then diluted with
681 distilled water and extracted with dichloromethane four times. The combined organic

phases were dried over anhydrous Na₂SO₄, filtered and concentrated. The crude product was purified by FCC on silica gel (eluent DCM/MeOH 97/3) to afford the corresponding *N*-oxides: Yields: **6a** (43%), **6b** (88%), **6c** (66%), **6d** (38%), and **6e** (80%).

4.1.5.1. 2-((4-acetoxyphenyl)(4-(tert-butyl)phenyl)methyl)pyridine 1-oxide (6a). The reaction was performed during 2 h at 20 °C. Yield: 45 mg, 0.12 mmol, light yellow oil, 43%. **TLC** DCM/MeOH 97/3, R_f = 0.20; **¹H NMR (DMSO d₆, 400 mHz)** (δ ppm) 1.27 (s, 9H, H₂₀), 2.26 (s, 3H, H₂₂), 6.13 (s, 1H, H₁), 6.98-7.02 (m, 3H, H₁₁, H₁₄, H₁₈), 7.07-7.12 (m, 4H, H₃, H₄, H₆, H₇), 7.29-7.38 (m, 4H, H₉, H₁₀, H₁₅, H₁₇), 8.27 (dd, 1H, J₁₂₋₁₁ = 5.4 Hz, J₁₂₋₉ = 0.8 Hz, H₁₂); **¹³C NMR (DMSO d₆, 100 mHz)** (δ ppm) 20.84 (C₂₂), 31.12 (C₁₉), 34.17 (C₂₀), 48.71 (C₁), 121.87 (C₄, C₆), 124.63 (C₉, C₁₀), 125.42 (C₁₅, C₁₇), 126.51 (C₁₁), 128.66 (C₁₄, C₁₈), 129.86 (C₃, C₇), 137.43 (C₂), 138.11 (C₁₃), 139.20 (C₁₂), 149.13 (C₈, C₁₆), 152.55 (C₅), 169.19 (C₂₁); **IR (ATR)** (cm⁻¹) 3054 (νCsp²-H), 2962, 2954 (νCsp³-H), 1759 (νC=O), 1506, 1486, 1431 (νC=C), 1250 (νN-O), 1183 (νC-O), 852 (δCsp²-H o-disubst), 762 (δCsp²-H p-disubst); **HPLC** purity: 99%, (Hypersil ODS C18, MeOH/H₂O 90/10, flow rate 0.80 mL/min, λ_{max} = 264 nm, R_t = 2.47 min).

4.1.5.2. 2-((4-acetoxyphenyl)(p-tolyl)methyl)pyridine 1-oxide (6b). The reaction was performed during 2 h at 20 °C. Yield: 92 mg, 0.28 mmol, white solid, 88%. Mp = 164-166 °C. **TLC** DCM/MeOH 97/3, R_f = 0.30; **¹H NMR (DMSO d₆, 400 mHz)** (δ ppm) 2.26 (s, 3H, H₂₁), 2.29 (s, 3H, H₁₉), 6.12 (s, 1H, H₁), 6.96-6.98 (m, 3H, H₁₁, H₁₄, H₁₈), 7.08 (s, 4H, H₃, H₄, H₆, H₇), 7.15 (d, 2H, J_{ortho} = 7.8 Hz, H₁₅, H₁₇), 7.29 (ddd, 1H, J₁₀₋₉ = 7.7 Hz, J₁₀₋₁₁ = 7.8 Hz, J₁₀₋₁₂ = 1.30 Hz, H₁₀), 7.35 (ddd, 1H, J₉₋₁₀ = 7 Hz, J₉₋₁₁ = 6.4, J₉₋₁₂ = 2.2 Hz, H₉), 8.27 (dd, 1H, J₁₂₋₁₀ = 6.4 Hz, J₁₂₋₉ = 1.04 Hz, H₁₂); **¹³C NMR (DMSO d₆, 100 mHz)** (δ ppm) 20.61 (C₂₁), 20.86 (C₁₉), 48.80 (C₁), 121.87 (C₄, C₆), 124.65 (C₉, C₁₀), 126.55 (C₁₁), 128.90 (C₁₄, C₁₈), 129.24 (C₃, C₇), 129.85 (C₁₅, C₁₇), 136.05 (C₁₆), 137.47 (C₂), 138.16 (C₁₃), 139.21 (C₁₂), 149.15 (C₈), 152.59 (C₅), 169.21 (C₂₀); **LRMS** (ESI, CV=30) 356 [M+23]⁺ (100), 357 [M+H+23]⁺ (15), 689 [2M+23]⁺ (12); **IR (ATR)** (cm⁻¹) 3071, 3049 (νCsp²-H), 2921 (νCsp³-H), 1756 (νC=O), 1607, 1501, 1488 (νC=C), 1250 (νN-O), 1202 (νC-O), 838 (δCsp²-H o-disubst), 769 (δCsp²-H p-disubst); **HPLC** purity:

711 97%, (Hypersil ODS C18, MeOH/H₂O 90/10, flow rate 0.80 mL/min, λ_{max} = 263 nm, R_t
712 = 2.38 min).

713 **4.1.5.3. 2-((4-acetoxyphenyl)(4-bromophenyl)methyl)pyridine 1-oxide (6c).** The
714 reaction was performed during 2 h 30 min at 20 °C. After purification by FCC, the
715 product was solubilized in dichloromethane and then washed three times with
716 NaHCO₃/Na₂CO₃ aqueous solution (1:1) to remove the *m*-chloroperbenzoic acid
717 residue. Yield: 78 mg, 0.20 mmol, yellow oil, 66%. **TLC** DCM/MeOH 97/3, R_f = 0.36; **¹H**
718 **NMR (DMSO d₆, 400 mHz)** (δ ppm) 2.27 (s, 3H, H₂₀), 6.14 (s, 1H, H₁), 7.10 (dd, 1H, J₉₋₁₀ = 7.8 Hz, J₉₋₁₁ = 2.1 Hz, H₉), 7.06 (d, 2H, J_{ortho} = 8.4 Hz, H₁₄, H₁₈), 7.11 (s, 4H, H₃, H₄,
719 H₆, H₇), 7.31 (ddd, 1H, J₁₀₋₉ = 7.8 Hz, J₁₀₋₁₁ = 7.7 Hz, J₁₀₋₁₂ = 1.3 Hz, H₁₀), 7.38 (ddd, 1H,
720 J₁₁₋₁₀ = 7.7 Hz, J₁₁₋₁₂ = 7.4 Hz, J₁₁₋₉ = 2.1 Hz, H₁₁), 7.54 (d, 2H, J_{ortho} = 8.5 Hz, H₁₄, H₁₈),
721 8.30 (ddd, 1H, J₁₂₋₁₁ = 7.4 Hz, J₁₂₋₁₀ = 2.8 Hz, J₁₂₋₉ = 1 Hz, H₁₂); **¹³C NMR (DMSO d₆,**
722 **100 mHz)** (δ ppm) 20.85 (C₂₀), 48.74 (C₁), 120.07 (C₁₆), 122.02 (C₄, C₆), 124.81 (C₁₁),
723 124.88 (C₁₀), 126.55 (C₉), 129.99 (C₃, C₇), 131.10 (C₁₄, C₁₈), 131.52 (C₁₅, C₁₇), 137.45
724 (C₂), 139.26 (C₁₂), 139.92 (C₁₃), 149.34 (C₈), 151.91 (C₅), 169.17 (C₁₉); **LRMS** (ESI,
725 CV=30) 420 [M+23]⁺ (100), 689 [2M+23]⁺ (12); **IR** (ATR) (cm⁻¹) 3083 (ν Csp²-H), 1754
726 (ν C=O), 1505, 1484, 1428 (ν C=C), 1248 (ν N-O), 1201 (ν C-O), 850 (δ Csp²-H *o*-disubst),
727 771 (δ Csp²-H *p*-disubst); **HPLC** purity: 96%, (Hypersil ODS C18, MeOH/H₂O 90/1, flow
728 rate 0,8 mL/min, λ_{max} = 264 nm, R_t = 2.42 min).

730 **4.1.5.4. 2-((4-acetoxyphenyl)(4-chlorophenyl)methyl)pyridine 1-oxide (6d).** The
731 reaction was performed during 2 h 30 min at 20 °C. After purification by FCC, the
732 product was solubilized in dichloromethane and then washed three times with
733 NaHCO₃/Na₂CO₃ aqueous solution (1:1) to remove the *m*-chloroperbenzoic acid
734 residue. Yield: 40 mg, 0.11 mmol, yellow oil, 38%. **TLC** DCM/MeOH 97/3, R_f = 0.38; **¹H**
735 **NMR (DMSO d₆, 400 mHz)** (δ ppm) 2.27 (s, 3H, H₂₀), 6.15 (s, 1H, H₁), 6.97 (dd, 1H, J₉₋₁₀ = 7.8 Hz, J₉₋₁₁ = 2.1 Hz, H₉), 7.11 (d, 2H, J_{ortho} = 8.4 Hz, H₁₄, H₁₈), 7.11 (s, 4H, H₃, H₄,
736 H₆, H₇), 7.32 (ddd, 1H, J₁₀₋₉ = 7.8 Hz, J₁₀₋₁₁ = 7.7 Hz, J₁₀₋₁₂ = 1.3 Hz, H₁₀), 7.36 - 7.42
737 (m, 1H, H₁₁), 7.31 (d, 2H, J_{ortho} = 8.5 Hz, H₁₄, H₁₈), 8.29 (ddd, 1H, J₁₂₋₁₁ = 7.3 Hz, J₁₂₋₁₀ =
738 2.8 Hz, J₁₂₋₉ = 1 Hz, H₁₂); **¹³C NMR (DMSO d₆, 100 mHz)** (δ ppm) 20.84 (C₂₀), 48.67
739

(C₁), 122.02 (C₄, C₆), 124.81 (C₁₁), 124.87 (C₁₀), 126.55 (C₉), 128.60 (C₁₅, C₁₇), 129.99 (C₃, C₇), 130.74 (C₁₄, C₁₈), 131.54 (C₁₆), 137.52 (C₂), 139.27 (C₁₂), 139.49 (C₁₃), 149.34 (C₈), 151.98 (C₅), 169.17 (C₁₉); **IR** (ATR) (cm⁻¹) 3080, 3050 (νCsp²-H), 1755(νC=O), 1506, 1487, 1430 (νC=C), 1251 (νN-O), 1200 (νC-O), 857 (δCsp²-H o-disubst), 765 (δCsp²-H p-disubst); **HPLC** purity: 96%, (Hypersil ODS C18, MeOH/H₂O 90/10, flow rate 0.80 mL/min, λ_{max} = 264 nm, R_t = 2.38 min).

4.1.5.5. 2-((4-acetoxyphenyl)(4-fluorophenyl)methyl)pyridine 1-oxide (6e). The reaction was performed during 4 h 30 min at 20 °C. Yield: 220 mg, 0.65 mmol, yellow solid, 80%. Mp = 226-224 °C. **TLC** DCM/MeOH 97/3, R_f = 0.20; **¹H NMR (DMSO d₆, 400 MHz)** (δ ppm) 2.26 (s, 3H, H₂₀), 6.17 (s, 1H, H₁), 6.98 (dd, 1H, J₉₋₁₁ = 2 Hz, J₉₋₁₀ = 7.8 Hz, H₉), 7.10 (s, 4H, H₄, H₆, H₁₅, H₁₇), 7.12-7.20 (m, 4H, H₃, H₇, H₁₄, H₁₈), 7.31 (ddd, 1H, J₁₀₋₉ = J₁₀₋₁₁ = 7.7 Hz, J₁₀₋₁₂ = 1.2 Hz, H₁₀), 7.37 (ddd, 1H, J₁₁₋₁₀ = J₁₁₋₁₂ = 7.7 Hz, J₁₁₋₉ = 2.1 Hz, H₁₁), 8.28 (dd, 1H, J₁₂₋₁₁ = 6.4 Hz, J₁₂₋₉ = 1.0 Hz, H₁₂); **¹³C NMR (DMSO d₆, 100 MHz)** (δ ppm) 20.85 (C₂₀), 48.49 (C₁), 115.42 (d, 2C, J_{C-F} = 20.60 Hz, C₁₅, C₁₇), 121.98 (C₄, C₆), 124.79 (C₁₀, C₁₁), 126.53 (C₉), 129.90 (C₃, C₇), 130.85 (d, 2C, J_{C-F} = 8.30 Hz, C₁₄, C₁₈), 136.59 (d, 1C, J_{C-F} = 2.40 Hz, C₁₃), 137.86 (C₂), 139.26 (C₁₂), 149.28 (C₅), 152.29 (C₈), 161.08 (d, 1C, J_{C-F} = 241.90 Hz, C₁₆), 169.19 (C₁₉); **LRMS** (ESI, CV=30) 360 (100) [M+23]⁺, 361 360 (100) [M+H+23]⁺; **IR** (ATR) (cm⁻¹) 3066 (νCsp²-H), ν 2922 (νCsp³-H), 1753 (νC=O), 1603, 1504, 1427 (νC=C), 1275 (νN-O), 1193 (νC-O), 1160 (νC-F), 843 (δCsp²-H o-disubst), 765 (δCsp²-H p-disubst); **HPLC** purity: 97%, (Hypersil ODS C18, MeOH/H₂O 90/10, flow rate 0.80 mL/min, λ_{max} = 264 nm, R_t = 2.25 min).

4.1.6. General procedure for the preparation of *o,p*-triarylmethanes

To a solution of the corresponding carbinol (1 eq.) and phenol (1.2 eq.) in nitrobenzene (0.40 M) was added dropwise concentrated sulfuric acid (20 eq.) at 0 °C. The reaction progress was monitored by GC-MS and TLC (eluent DCM/MeOH 90/10). After 5 min at 80 °C the reaction was cooled to room temperature and neutralized with a saturated solution of NaHCO₃ (pH 7-8), then extracted with ethyl acetate three times. The combined organic phases were dried over anhydrous Na₂SO₄, filtered and

concentrated. The crude residue was purified by FCC on silica gel (eluent gradient DCM, DCM/MeOH 95/5, DCM/MeOH 90/10) to afford the corresponding *o,p*-triarylmethane: Yields: **7a** (98%), **7b** (45%), **7c** (23%), **7d** (80%), and **7e** (64%).

4.1.6.1. 2-((4-(*tert*-butyl)phenyl)(pyridin-2-yl)methyl)phenol (7a). Yield: 134 mg, 0.42 mmol, beige solid, 98%, Mp = 202-204 °C. **TLC** DCM/MeOH 90/10, R_f = 0.16; **¹H NMR (DMSO d₆, 400 mHz)** (δ ppm) 1.25 (s, 9H, H₁₉), 5.54 (s, 1H, H₁), 6.71 (d, 1H, J_{ortho} = 8.4 Hz, H₆), 7.07 (dd, 1H, J₄₋₆ = 2.3 Hz, J_{ortho} = 8.50 Hz, H₄), 7.13 (d, 2H, J_{ortho} = 8.2 Hz, H₁₄, H₁₈), 7.20-7.27 (m, 2H, H₉, H₁₁), 7.29-7.36 (m, 4H, H₁₅, H₁₇, H₅, H₃), 7.74 (ddd, 1H, J₁₀₋₉ = J₁₀₋₁₁ = 7.7 Hz, J₁₀₋₁₂ = 2 Hz, H₁₀), 8.54 (ddd, 1H, J₁₂₋₁₁ = 4.7 Hz, J₁₂₋₁₀ = 1.8 Hz, J₁₂₋₉ = 0.9 Hz, H₁₂), 10.38 (s, 1H, OH); **¹³C NMR (DMSO d₆, 100 mHz)** (δ ppm) 31.13 (C₁₉), 34.05 (C₂₀), 56.84 (C₁), 116.17 (C₆), 121.50 (C₁₁), 123.42 (C₉), 124.97 (C₁₅, C₁₇), 127.24 (C₃, C₅), 128.58 (C₁₄, C₁₈), 130.37 (C₂), 131.42 (C₄), 136.68 (C₁₀), 140.19 (C₁₃), 148.34 (C₁₆), 149.11 (C₁₂), 151.73 (C₇), 162.77 (C₈); **LRMS** (ESI, CV=30) 318.18 (50) [M+H]⁺; **IR** (ATR) (cm⁻¹) 3454 (νO-H), 3057 (νCsp²-H), ν 2959, 2904 (νCsp³-H), 1489, 1592, 1473 (νC=C), 1168 (νC-O).

4.1.6.2. 2-(pyridin-2-yl(*p*-tolyl)methyl)phenol (7b). Yield: 53 mg, 0.21 mmol, beige solid, 45%, Mp = 210-212 °C. **TLC** DCM/MeOH 90/10, R_f = 0.20, DCM/MeOH 90/10, R_f = 0.10-0.20; **¹H NMR (DMSO d₆, 400 mHz)** (δ ppm) 2.26 (s, 3H, H₁₉), 5.54 (s, 1H, H₁), 6.70 (d, 1H, J_{ortho} = 8.4 Hz, H₆), 7.03 (dd, 1H, J₄₋₃ = J₄₋₅ = 8.5 Hz, J₄₋₆ = 2.3 Hz, H₄), 7.05-7.13 (m, 5H, H₁₄, H₁₅, H₁₈, H₁₇, H₃), 7.19-7.25 (m, 2H, H₅, H₁₁), 7.29 (d, 1H, J₉₋₁₀ = 2.3 Hz, H₉), 7.73 (ddd, 1H, J₁₀₋₉ = J₁₀₋₁₁ = 7.7 Hz, J₁₀₋₁₂ = 1.9 Hz, H₁₀), 8.53 (ddd, 1H, J₁₂₋₁₁ = 7.5 Hz, J₁₂₋₁₀ = 4.8 Hz, J₁₂₋₉ = 0.9 Hz, H₁₂), 10.38 (s, 1H, OH); **¹³C NMR (DMSO d₆, 100 mHz)** (δ ppm) 20.61 (C₁₉), 56.91 (C₁), 116.28 (C₆), 121.54 (C₉), 123.46 (C₅), 127.30 (C₃), 128.83 (C₂), 128.89 (C₁₄, C₁₅, C₁₇, C₁₈, C₁₁), 130.40 (C₁₆), 131.51 (C₄), 135.22 (C₁₃), 136.71 (C₁₀), 140.27 (C₇), 149.16 (C₁₂), 162.87 (C₈); **LRMS** (ESI, CV=30) 298 (100) [M+23]⁺; **IR** (ATR) (cm⁻¹) 3418 (νO-H), ν 3052, 3007 (νCsp²-H), 2922 (νCsp³-H), 1590, 1509, 1474 (νC=C), 1166 (νC-O), 830 (δCsp²-H *p*-disubst).

4.1.6.3. 2-((4-bromophenyl)(pyridin-2-yl)methyl)phenol (7c). Yield: 31 mg, 0.09 mmol, orange oil, 23%. **TLC** DCM/MeOH 90/10, R_f = 0.10; **¹H NMR (DMSO d₆, 400**

798 **mHz**) (δ ppm) 5.61 (s, 1H, H₁), 6.73 (d, 1H, J_{ortho} = 8.4 Hz, H₆), 7.06 (ddd, 1H, J₄₋₅ = J₄₋₃
799 = 8.4 Hz, J₄₋₆ = 2.4 Hz, H₄), 7.14-7.20 (m, 3H, H₁₄, H₁₈, H₅), 7.22-7.29 (m, 2H, H₉, H₁₁),
800 7.32 (d, 1H, J₃₋₅ = 2.30 Hz, H₃), 7.49 (d, 2H, J_{ortho} = 8.5 Hz, H₁₅, H₁₇), 7.75 (ddd, 1H, J₁₀₋₉
801 = J₁₀₋₁₁ = 7.7 Hz, J₁₀₋₁₂ = 1.9 Hz, H₁₀), 8.54 (ddd, 1H, J₁₂₋₁₁ = 4.8 Hz, J₁₂₋₁₀ = 1.8 Hz,
802 J₁₂₋₉ = 0.9 Hz, H₁₂), 10.40 (s, 1H, OH); **¹³C NMR (DMSO d₆, 100 mHz)** (δ ppm) 56.26
803 (C₁), 116.40 (C₆), 119.44 (C₁₆), 121.77 (C₁₁), 123.64 (C₉), 127.33 (C₃, C₅), 130.53 (C₂),
804 131 (C₁₅, C₁₇), 131.08 (C₁₄, C₁₈), 131.24 (C₄), 136.93 (C₁₀), 142.77 (C₁₃), 149.22 (C₁₂),
805 151.94 (C₇), 162.07 (C₈); **IR (ATR)** (cm⁻¹) 3403 (νO-H), ν 3068, 2926 (νCsp²-H), 2922
806 (νCsp³-H), 1590, 1486 (νC=C), 1164 (νC-O).

807 **4.1.6.4. 2-((4-chlorophenyl)(pyridin-2-yl)methyl)phenol (7d).** Yield: 106 mg, 0.36
808 mmol, beige solid, 80%, Mp = 200-202 °C. **TLC** DCM/MeOH 90/10, R_f = 0.21; **¹H**
809 **NMR (DMSO d₆, 400 mHz)** (δ ppm) 5.65 (s, 1H, H₁), 6.73 (d, 1H, J_{ortho} = 8.4 Hz, H₆),
810 7.06 (dd, 1H, J_{ortho} = 8.6 Hz, J₄₋₆ = 2.5 Hz, H₄), 7.23 (d, 2H, J_{ortho} = 8.4 Hz, H₁₄, H₁₈),
811 7.26-7.32 (m, 4H, H₉, H₁₁, H₃, H₅), 7.37 (d, 2H, J_{ortho} = 8.5 Hz, H₁₅, H₁₇), 7.80 (ddd, 1H,
812 J₁₀₋₉ = J₁₀₋₁₁ = 7.7 Hz, J₁₀₋₁₂ = 1.8 Hz, H₁₀), 8.57 (dd, 1H, J₁₂₋₁₁ = 5.5 Hz, J₁₂₋₁₀ = 1.8 Hz,
813 H₁₂), 10.41 (s, 1H, OH); **¹³C NMR (DMSO d₆, 100 mHz)** (δ ppm) 56 (C₁), 116.46 (C₆),
814 121.98 (C₁₁), 123.83 (C₉), 127.37 (C₃, C₅), 128.22 (C₁₅, C₁₇), 130.56 (C₂), 130.86 (C₁₄,
815 C₁₈), 131.47 (C₄), 132.55 (C₁₆), 137.47 (C₁₀), 142.13 (C₁₃), 148.96 (C₁₂), 152 (C₇),
816 161.85 (C₈); **IR (ATR)** (cm⁻¹) 3422 (νO-H), 3064 (νCsp²-H), 2957 (νCsp³-H), 1591,
817 1488, 1450 (νC=C), 1163 (νC-O), 818 (δCsp²-H p-disubst), 623 (νC-Cl).

818 **4.1.6.5. 2-((4-fluorophenyl)(pyridin-2-yl)methyl)phenol (7e).** Yield: 78 mg, 0.28
819 mmol, light yellow solid, 64%, Mp = 222-224 °C. **TLC** DCM/MeOH 90/10, R_f = 0.39; **¹H**
820 **NMR (DMSO d₆, 400 mHz)** (δ ppm) 5.62 (s, 1H, H₁), 6.71 (d, 1H, J_{ortho} = 8.5 Hz, H₆),
821 7.06 (dd, 1H, J₃₋₄ = J₄₋₅ = 8.5 Hz, J₄₋₆ = 2.2 Hz, H₄), 7.09-7.16 (m, 2H, H₁₄, H₁₈), 7.22-
822 7.28 (m, 4H, H₉, H₁₁, H₁₅, H₁₇), 7.31 (d, 2H, J_{ortho} = 2.1 Hz, H₃, H₅), 7.75 (ddd, 1H, J₁₀₋₉ =
823 J₁₀₋₁₁ = 7.7 Hz, J₁₀₋₁₂ = 1.9 Hz, H₁₀), 8.54 (dd, 1H, J₁₂₋₁₁ = 4.8 Hz, J₁₂₋₁₀ = 1.9 Hz, H₁₂);
824 **¹³C NMR (DMSO d₆, 100 mHz)** (δ ppm) 56.18 (C₁), 114.83 (C₁₅, C₁₇), 115.04 (C₆),
825 121.70 (C₁₁), 123.57 (C₅, C₃), 127.30 (C₉), 130.52 (C₂), 130.83 (C₁₄, C₁₈), 131.43 (C₄),
826 136.88 (C₁₀), 139.47 (C₁₃), 149.27 (C₁₂), 157.33 (C₇), 159.54 (C₁₆), 162.46 (C₈); **IR**

(ATR) (cm⁻¹) 3424 (νO-H), 3064 (νCsp²-H), 1595, 1506, 1432 (νC=C), 1156 (νC-O), 809 (δCsp²-H p-disubst), 750 (δCsp²-H o-disubst).

4.1.7. Preparation of benzotriazole-triarylmethanes

A mixture of benzotriazole (5 mmol, 1 eq.), (4-methoxyphenyl)(pyridin-2-yl)methanol **9** (4.6 mmol, 1 eq.) and *p*-toluenesulfonic acid monohydrate (13 mmol, 2.8 eq.) was stirred and refluxed overnight in perfluorooctane (20 mL, bp 104°C) under argon. The perfluorocarbon fluid was removed on cooling. A solution of methanol saturated with KOH (20 mL) was added to the remaining solid and sonication was applied until solubilization was complete. Methanol was removed under vacuum and water (20 mL) was added. The mixture was extracted with ethyl acetate four times. The combined organic phases were dried over Na₂SO₄, filtered and concentrated. The crude product was purified by FCC on silica gel (eluent CyHex/ EtOAc, 60/40) and afforded the desired compound **10** as a beige solid. The regioisomer 2-((4-methoxyphenyl)(pyridin-2-yl)methyl)-2,3-dihydro-1H-benzo[d][1,2,3]triazole **10a** was also isolated and characterized (see SI-1).

4.1.7.1. 1-((4-methoxyphenyl)(pyridin-2-yl)methyl)-1H-benzo[d][1,2,3] triazole (**10**).

Yield: 730 mg (50%). Mp = 170-172 °C. **TLC** CyHex/EtOAc 60/40, R_f = 0.20; **¹H NMR (DMSO d₆, 400 mHz)** (δ ppm) 3.78 (s, 3H, CH₃), 7.00 (d, 2H, J_{ortho} = 8.8 Hz, H₄, H₆), 7.32-7.38 (m, 3H, H₃, H₇, H₉), 7.39 (ddd, 1H, J₁₁₋₁₀ = 7.6 Hz, J₁₁₋₁₂ = 4.5 Hz, J₁₁₋₉ = 0.9 Hz, H₁₁), 7.42 (m, 1H, H_{BT3}), 7.50 (ddd, 1H, J_{BT2-BT1} = 8.3 Hz, J_{BT2-BT3} = 6.9 Hz, J_{BT2-BT4} = 1 Hz, H_{BT2}), 7.61 (dt, 1H, J_{BT4-BT3} = 8.4 Hz, H_{BT4}), 7.69 (s, 1H, H₁), 7.88 (ddd, 1H, J₁₀₋₉ = 7.8 Hz, J₁₀₋₁₁ = 7.7 Hz, J₁₀₋₁₂ = 1.8 Hz, H₁₀), 8.09 (dd, 1H, J_{BT1-BT2} = J_{BT4-BT3} = 8.3 Hz, J_{BT1-BT3} = J_{BT4-BT2} = 1.8 Hz, H_{BT1}), 8.56 (ddd, 1H, J₁₂₋₁₁ = 4.8 Hz, J₁₂₋₁₀ = 1.8 Hz, J₁₂₋₉ = 0.8 Hz, H₁₂); **¹³C NMR (DMSO d₆, 100 mHz)** (δ ppm) 55.12 (C₁₃), 66.10 (C₁), 111.23 (C_{BT4}), 114.02 (C₆, C₄), 119.20 (C_{BT1}), 122.71 (C₁₁), 123.19 (C₉), 123.97 (C_{BT2}), 127.30 (C_{BT3}), 129.12 (C_{BT5}), 130.15 (C₇ and C₃), 133.08 (C₂), 137.30 (C₁₀), 145.23 (C_{BT6}), 149.37 (C₁₂), 157.44 (C₅), 159.14 (C₈); **IR** (ATR) (cm⁻¹) 3054, 3005 (νCsp²-H), 2933, 2905 (νCsp³-H), 2837 (νOMe), 1609, 1587, 1510, 1463 (νC=C), 1243 (νC - O); **GC-MS** method 200, R_t = 8.83 min *m/z*: 316 [M]⁺(5), 198 [PyCHPhOCH₃]⁺(100), 79 [PyH]⁺(10); **HPLC**: purity:

95%, (Hypersil 250, 5 μ m, A165, Isooctane/EtOAc 70/30, flow rate 1.20 mL/min, λ_{max} = 260 nm, R_t = 12.3 min).

4.1.7.2. 4-((1H-benzo[d][1,2,3]triazol-1-yl)(pyridin-2-yl)methyl)phenyl acetate (**12**).

To a previously synthesized solution of 4-((1H-benzo[d][1,2,3]triazol-1-yl)(pyridin-2-yl)methyl)phenol **11** (0.19 mmol, 1 eq.) (see SI-1) in acetic anhydride (40 mmol, 210 eq.) at 0 °C was slowly added a solution of NaOH 1 M (0.6 mmol, 3.1 eq.). The mixture was stirred for 24 h at room temperature, concentrated under vacuum and water was added (10 mL). The mixture was extracted with ethyl acetate three times then the organic phases were neutralized with saturated NaHCO₃ solution (pH \approx 8), washed with brine and then dried over Na₂SO₄. The product was purified by FCC (eluent DCM/MeOH, 95/5) to afford **12** as a white solid.

Yield: 33.6 mg (52%). Mp = 172-174 °C. **TLC** DCM/MeOH 95/5, R_f = 0.2; **¹H NMR (DMSO d₆, 400 MHz)** (δ ppm) 2.26 (s, 3H, CH₃), 7.17 (d, 2H, J_{ortho} = 8.6 Hz, H₄, H₆), 7.31 (d, 1H, J_{11-10} = 7.7 Hz, H₉), 7.36 (ddd, 1H, J_{11-10} = 4.8, J_{11-12} = 4.7 Hz, J_{11-9} = 1.1 Hz, H₁₁), 7.39-7.42 (m, 1H, H_{Bt2}), 7.43 (d, 2H, J_{ortho} = 8.6 Hz, H₃, H₇), 7.47-7.51 (m, 1H, H_{Bt3}), 7.64 (dt, 1H, $J_{\text{Bt4-Bt3}}$ = 8.4 Hz, H_{Bt4}), 7.75 (s, 1H, H₁), 7.86 (ddd, 1H, J_{10-9} = 7.7 Hz, J_{10-11} = 7.7 Hz, J_{10-12} = 1.8 Hz, H₁₀), 8.09 (dd, 1H, $J_{\text{Bt1-Bt2}}$ = $J_{\text{Bt4-Bt3}}$ = 8.3 Hz, $J_{\text{Bt1-Bt3}}$ = $J_{\text{Bt4-Bt2}}$ = 1.6 Hz, H_{Bt1}), 8.56 (ddd, 1H, J_{12-11} = 4.8 Hz, J_{12-10} = 1.8 Hz, J_{12-9} = 0.85 Hz, H₁₂); **¹³C NMR (DMSO d₆, 100 MHz)** (δ ppm) 20.80 (CH₃), 65.85 (C₁), 111.10 (C_{Bt4}), 122.06 (C₆, C₄), 119.20 (C_{Bt1}), 122.84 (C₉), 123.37 (C₁₁), 124.12 (C_{Bt2}), 127.18 (C_{Bt3}), 130.02 (C₇ and C₃), 133.09 (C₂), 134.72 (C_{Bt5}), 137.44 (C₁₀), 145.21 (C_{Bt6}), 149.46 (C₁₂), 150.31 (C₅), 157.00 (C₈), 169.09 (C=O); **IR** (ATR) (cm⁻¹) 3054, 3005 ($\nu_{\text{Csp2-H}}$), 2923, 2904 ($\nu_{\text{Csp3-H}}$), 1750 ($\nu_{\text{C-O}}$), 1610, 1588, 1509 ($\nu_{\text{C=C}}$), 1245 ($\nu_{\text{C-O}}$), 835 ($\delta_{\text{Csp2-H p-disubst}}$), 772 ($\delta_{\text{Csp2-H o-disubst}}$); **GC-MS**: method 200, R_t = 9.92 min m/z : 344 [M]⁺(12), 226 [M-Bt]⁺ (25), 184 [PyCHNH-Ph]⁺(100); **HRMS**: calcd. for C₂₀H₁₆N₄O₂ [M+Na]⁺ (367.1165), found (367.1165).

4.1.8. Preparation of naphthol triarylmethanes

4.1.8.1. 1-((4-methoxyphenyl)(pyridin-2-yl)methyl)naphthalen-2-ol (**14**).

2-Naphtol **13** (2.70 mmol, 1.2 eq.) was mixed with (4-methoxyphenyl)(pyridin-2-yl)methanol (2.30 mmol 1.5 eq.) in dichloroethane (2.5 mL) and sulfamic acid (3.45 mmol, 1.5 eq.) under argon. The mixture was heated at 85 °C for 20 h. After reaction completion, the reaction mixture was cooled at room temperature, neutralized with a saturated solution of NaHCO₃ (pH ≈ 8) and extracted with dichloromethane three times. The organic layers were dried over MgSO₄, filtered and concentrated under vacuum. The product was purified by FCC on silica gel (DCM 100%) to afford **14** as a whitish solid.

Yield: 38.5 mg (49%). Mp = 158-160 °C. **TLC** CyHex/EtOAc 60/40, R_f 0.2; **¹H NMR (DMSO d₆, 400 mHz)** (δ ppm) δ 3.67 (s, 3H, CH₃), 6.48 (s, 1H, H₁), 6.79 (d, 2H, J_{ortho} = 8.7 Hz, H₄, H₆), 7.43 (d, 2H, J_{ortho} = 8.7 Hz, H₃, H₇), 7.15 (d, 1H, J_{N3-N4} = 8.8 Hz, H_{N3}), 7.25 (ddd, 1H, J_{N7-N6} = 7.9 Hz, J_{N7-N8} = 6.8 Hz, J_{N7-N9} = 0.85 Hz, H_{N7}), 7.29 (ddd, 1H, J₁₁₋₁₀ = 7.5, J₁₁₋₁₂ = 4.9 Hz, J₁₁₋₉ = 1.1 Hz, H₁₁), 7.36 (ddd, 1H, J_{N8-N9} = 8.5, J_{N9-N8} = 7.9 Hz, J_{N8-N6} = 1.3 Hz, H_{N8}), 7.51 (d, 1H, J₉₋₁₀ = 7.9 Hz, H₉), 7.74 (d, 1H, J_{N3-N4} = 7.9 Hz, H_{N4}), 7.80 (d, 1H, J_{N6-N7} = 7.9 Hz, H_{N6}), 7.78-7.83 (m, 1H, H₁₀), 8.18 (d, 1H, J_{N9-N8} = 7.9 Hz, H_{N9}), 8.52 (ddd, 1H, J₁₂₋₁₁ = 4.9 Hz, J₁₂₋₁₀ = 1.8 Hz, J₁₂₋₉ = 0.7 Hz, H₁₂), 11.13 (s, 1H, OH); **¹³C NMR (DMSO d₆, 100 mHz)** (δ ppm) 48.08 (C₁), 54.92 (CH₃), 113.39 (C₆, C₄), 119.91 (C_{N3}), 120.34 (C_{N1}), 121.89 (C_{N9}), 122.27 (C₉), 123.20 (C_{N7}), 124.07 (C₁₁), 126.16 (C_{N8}), 128.50 (C_{N6}), 128.57 (C_{N5}), 128.90 (C_{N4}), 129.24 (C₇ and C₃), 133.37 (C_{N10}), 133.69 (C₂), 137.59 (C₁₀), 148.10 (C₁₂), 153.63 (C_{N2}), 157.41 (C₅), 163.00 (C₈); **GC-MS**: method 180, R_t = 11.64 min m/z: 341 [M]⁺(100), 324 [M-OH]⁺(90), 393 [M-47]⁺(15); **IR** (ATR) (cm⁻¹) 3031 (νCsp²-H), 2952, 2929 (νCsp³-H), 2834 (νOMe), 1618, 1597, 1507 (νC=C), 1243 (νC-O); **HRMS**: calcd. for C₂₃H₁₉NO₂ [M+H]⁺ (342.1489), found (342.1489).

4.1.8.2. 1-((4-hydroxyphenyl)(pyridin-2-yl)methyl)naphthalen-2-ol (**15**).

To a solution of **14** (0.6 mmol, 1 eq.) in glacial acetic acid (2.5 mL) under argon, was added 0.6 mL of stabilized hydriodic acid (d = 1.701, 57%, 4.5 mmol, 7.5 eq.). The mixture was refluxed (T = 100 °C) for 5 h 30 then neutralized with a saturated solution of NaHCO₃ (pH ≈ 8). Then the mixture was extracted with ethyl acetate (3 x 20 mL),

dried over Na₂SO₄ and filtrated. The filtrate was concentrated under vacuum and purified by FCC on silica gel (CyHex/EtOAc, 60/ 40) to provide **15** as a yellow solid. Yield: 70.10 mg (35%). Mp = 218-220 °C. **TLC** CyHex/EtOAc 60/40, R_f 0.45; **¹H NMR (DMSO d₆, 400 mHz)** (δ ppm) 3.67 (s, 3H, CH₃), 6.48 (s, 1H, H₁), 6.62 (d, 2H, J_{ortho} = 8.5 Hz, H₄, H₆), 6.83 (d, 2H, J_{ortho} = 8.5 Hz, H₃, H₇), 7.14 (d, 1H, J_{N3-N4} = 7.1 Hz, H_{N3}), 7.23-7.31 (m, 2H, H_{N7} and H₁₁), 7.37 m, 1H, H_{N8}), 7.53 (d, 1H, J₉₋₁₀ = 7.8 Hz, H₉), 7.73 (d, 1H, J_{N3-N4} = 7.1 Hz, H_{N4}), 7.77-7.83 (m, 2H, H_{N6} and H₁₀), 8.19 (d, 1H, J_{N9-N8} = 8.6 Hz, H_{N9}), 8.50-8.54 (m, 1H, H₁₂), 9.19 (s, 1H, OH), 11.20 (s, 1H, OH); **¹³C NMR (DMSO d₆, 100 mHz)** (δ ppm) 48.12 (C₁), 114.77 (C₆, C₄), 119.99 (C_{N3}), 120.50 (C_{N1}), 121.85 (C_{N9}), 122.23 (C₉), 123.20 (C_{N7}), 124.09 (C₁₁), 126.12 (C_{N8}), 128.48 (C_{N6}), 128.56 (C_{N5}), 128.80 (C_{N4}), 129.14 (C₇, C₃), 131.92 (C_{N10}), 133.42 (C₂), 137.59 (C₁₀), 148.03 (C₁₂), 153.67 (C_{N2}), 155.44 (C₅), 163.21 (C₈); **GC-MS**: method 200, R_t = 9.12 min *m/z*: 327 [M]⁺(90), 310 [M-OH]⁺(100); **IR** (ATR) (cm⁻¹) 3339 (νO-H), 3077, 3016 (νCsp²-H), 1616, 1591, 1511 (νC=C), 1410 (δ C-O), 1227(νC-O), 801 (δCsp²-H p-disubst), 740 (δCsp²-H o-disubst); **HRMS**: calcd. for C₂₂H₁₇NO₂ [M+H]⁺ (328.1332), found (328.1332).

4.1.8.3. 4-((2-acetoxynaphthalen-1-yl)(pyridin-2-yl)methyl)phenyl acetate (**16**)

To a stirred solution of **15** (0.12 mmol, 1 eq.) in acetic anhydride (13 mmol, 110 eq.) at 0°C, was slowly added a solution of NaOH 1 M (0.3 mmol, 2.6 eq.). The mixture was stirred for 24 h at room temperature, concentrated under vacuum and dissolved in 10 mL of water. The reaction mixture was extracted with ethyl acetate three times, neutralized with saturated NaHCO₃ solution (pH ≈ 8). The combined organic phases were washed with brine dried over Na₂SO₄, filtered and concentrated. FCC on silica gel (CyHex/EtOAc, 50/50) afforded **16** as a transparent oil.

Yield: 47.70 mg (97%). **TLC** CyHex/EtOAc 70/30, R_f 0.60; **¹H NMR (DMSO d₆, 400 mHz)** (δ ppm) 1.84 (s, 3H, CH₃), 2.24 (s, 3H, CH₃), 3.67, 6.54 (s, 1H, H₁), 7.79 (d, 2H, J_{ortho} = 8.6 Hz, H₄, H₆), 7.09 (d, 1H, J_{N3-N4} = 7.9 Hz, H_{N3}), 7.22 (d, 2H, J_{ortho} = 8.6 Hz, H₃, H₇), 7.20-7.24 (m, 1H, H₁₁), 7.30 (d, 1H, J₉₋₁₀ = 8.9 Hz, H₉), 7.43- 7.51 (m, 2H, H_{N7}, H_{N8}), 7.72 (ddd, 1H, J₁₀₋₉ = 7.7, J₁₀₋₁₁ = 7.8 Hz, J₁₀₋₁₂ = 1.2 Hz, H₁₀), 7.92 (d, 1H, J_{N6-N7} = 8.9 Hz, H_{N6}), 7.94-7.97 (m, 1H, H_{N4}), 8.16-8.21 (m, 1H, H₉), 8.47 (ddd, 1H, J₁₂₋₁₁ = 4.9 Hz,

942 $J_{12-10} = 1.9$ Hz, $J_{12-9} = 0.9$ Hz, H_{12}); **^{13}C NMR (DMSO d_6 , 100 MHz)** (δ ppm) 25.66 and
 943 26.05 (CH_3), 55.24 (C_1), 126.73 (C_6 , C_4), 126.93 ($\text{C}_{\text{N}3}$), 128.32 (C_9), 130.19 ($\text{C}_{\text{N}9}$), 130.56
 944 ($\text{C}_{\text{N}7}$), 131.80 ($\text{C}_{\text{N}8}$), 133.76 ($\text{C}_{\text{N}5}$), 133.85 ($\text{C}_{\text{N}4}$ and $\text{C}_{\text{N}6}$), 129.14 (C_7 , C_3), 137.01 ($\text{C}_{\text{N}1}$),
 945 137.58 ($\text{C}_{\text{N}10}$), 141.94 (C_{10}), 143.90 (C_2), 152.00 ($\text{C}_{\text{N}2}$), 154.05 (C_5), 154.15 (C_{12}),
 946 167.21 (C_8), 173.90 and 174.46 ($\text{C}=\text{O}$); **GC-MS**: method 180, $R_t = 12.39$ min m/z : 411
 947 $[\text{M}]^+(1)$, 369 $[\text{M}-\text{Ac}]^+(3)$, 252 $[\text{PyCHPhNaph}]^+(100)$; **IR** (ATR) (cm^{-1}) 3059 ($\nu\text{Csp}^2\text{-H}$).
 948 2926 ($\nu\text{Csp}^3\text{-H}$), 1749 ($\nu\text{C}=\text{O}$), 1572, 1503, 1469 ($\nu\text{C}=\text{C}$), 1180 ($\nu\text{C}-\text{O}$), 811 ($\delta\text{Csp}^2\text{-H}$
 949 p -disubst). **HRMS**: calcd. for $\text{C}_{26}\text{H}_{21}\text{NO}_4$ $[\text{M}+\text{Na}]^+$ (434.1363), found (434.1363).

950 4.1.9. Preparation of indole triarylmethanes

951 4.1.9.1. 3-((4-methoxyphenyl)(pyridin-2-yl)methyl)-3a,7a-dihydro-1H-indole (18)

952 Indole **17** (4.7 mmol, 2 eq.) was mixed with (4-methoxyphenyl)(pyridin-2-yl)methanol **9**
 953 (2.3 mmol, 1 eq.), dichloroethane (2.5 mL) and sulfamic acid (2.3 mmol, 1 eq.) under
 954 argon. The mixture was heated at 85°C during 20 h. After reaction, the mixture was
 955 cooled to room temperature. A solution of methanol saturated with NaOH (20 mL) was
 956 added to the remaining solid and sonication was applied until complete solubilization.
 957 Methanol was removed under vacuum and water (20 mL) was added. The mixture was
 958 extracted with dichloromethane three times. The combined organic phases were dried
 959 over Na_2SO_4 , filtered and concentrated. FCC on silica gel (CyHex/EtOAc, 50/50)
 960 afforded **18** as a brown solid.

961 Yield: 59 mg (81%). Mp = $136\text{--}138^\circ\text{C}$. **TLC**: CyHex/EtOAc 50/50, R_f 0.4; **^1H NMR**
 962 **(DMSO d_6 , 400 MHz)** (δ ppm) 3.70 (s, 3H, CH_3), 5.69 (s, 1H, H_1), 6.84 (d, 2H, $J_{\text{ortho}} =$
 963 8.7 Hz, H_4 , H_6), 6.82–6.88 (m, 2H, $H_{\text{In}1}$, $H_{\text{In}6}$), 7.0 (ddd, 1H, $J_{\text{In}7-\text{In}6} = 8.0$ Hz, $J_{\text{In}7-\text{In}5} = 7.0$
 964 Hz, $J_{\text{In}7-\text{In}4} = 1.1$ Hz, $H_{\text{In}7}$), 7.14 (d, 1H, $J_{11-10} = 7.7$ Hz, H_{11}), 7.20 (ddd, 1H, $J_{9-10} = 7.8$ Hz,
 965 $J_{9-11} = 4.9$ Hz, $J_{9-12} = 1.1$ Hz, H_9), 7.23 (d, 2H, $J_{\text{ortho}} = 8.6$ Hz, H_3 , H_7), 7.29 (dt, 1H, $J_{\text{In}4-\text{In}5}$
 966 = 8.9 Hz, $H_{\text{In}4}$), 7.35 (dt, 1H, $N_{\text{In}5}$, $J_{\text{In}5-\text{In}4} = 8.9$ Hz, $H_{\text{In}5}$), 7.68 (ddd, 1H, $J_{10-9} = 7.7$ Hz,
 967 $J_{10-11} = 7.7$ Hz, $J_{10-12} = 1.8$ Hz, H_{10}), 8.51 (ddd, 1H, $J_{12-11} = 4.9$ Hz, $J_{12-10} = 1.9$ Hz, $J_{12-9} =$
 968 0.8 Hz, H_{12}), 10.9 (s, 1H, NH); **^{13}C NMR (DMSO d_6 , 100 MHz)** (δ ppm) 49.08 (C_1), 55.92
 969 (CH_3), 111.49 ($\text{C}_{\text{In}4}$), 114.56 ($\text{C}_{\text{In}2}$), 118.50 (C_{11}), 119.72 (C_9), 120.09 ($\text{C}_{\text{In}7}$), 120.36 (C_6 ,
 970 C_4), 122.56 ($\text{C}_{\text{In}5}$), 122.90 ($\text{C}_{\text{In}1}$), 122.94 ($\text{C}_{\text{In}6}$), 128.42 ($\text{C}_{\text{In}3}$), 130.56 (C_7 , C_3), 135.40

971 (C₂), 136.80 (C₁₀), 139.81 (C_{ln8}), 148.80 (C₅), 149.08 (C₁₂), 160.89 (C₈); **GC-MS:**
972 method 160, *R_t* = 13.14 min *m/z*: 314 [M]⁺(90), 299 [M-15]⁺(10), 236
973 [InCHPhOCH₃]⁺(100); **IR** (ATR) (cm⁻¹) 3412 (νN-H). 3052, 3009 (νCsp²-H), 2920
974 (νCsp³-H), 2857 (νOMe), 1592, 1507, 1456 (νC=C), 1246 (νC - O), 743 (δCsp²-H o-
975 disubst); **HRMS**: calcd. for C₂₁H₁₈N₂O [M+H]⁺ (315.1492), found (315.1492).

976 **4.1.9.2. 4-((3a,7a-dihydro-1H-indol-3-yl)(pyridin-2-yl)methyl)phenyl acetate (19)**

977 To a stirred solution of **18a** (1.6 mmol, 1 eq.) in acetic anhydride (183 mmol, 115 eq.) at
978 0 °C, was slowly added a solution of NaOH 1 M (2.15 mmol, 1.3 eq.). The mixture was
979 stirred for 3 h 30 at room temperature and concentrated under vacuum and dissolved in
980 10 mL of water. The reaction mixture was extracted with ethyl acetate three times and
981 neutralized with saturated NaHCO₃ solution (pH ≈ 8). The combined organic phases
982 were washed with brine, drying over Na₂SO₄, filtered and concentrated. FCC on silica
983 gel (CyHex/EtOAc, 30/70) afforded **19** as a light brown solid.

984 Yield: 39 mg (68%). Mp = 152-154 °C. **TLC** CyHex/EtOAc 30/70, *R_f* 0.60; **¹H NMR**
985 **(DMSO d₆, 400 MHz)** (δ ppm) 2.23 (s, 3H, CH₃), 5.78 (s, 1H, H₁), 6.85- 6.87 (m, 1H,
986 H_{ln1}), 6.88- 6.89 (m, 1H, H_{ln6}), 7.02 (d, 2H, *J*_{ortho} = 8.7 Hz, H₄, H₆), 7.03 (dd, 1H, *J*_{ln7- ln6} =
987 8.0 Hz, *J*_{ln7- ln5} = 7.0 Hz, *J*_{ln7- ln4} = 1.1 Hz, H_{ln7}), 7.14 (d, 1H, *J*₁₁₋₁₀ = 7.9 Hz, H₁₁), 7.22
988 (ddd, 1H, *J*₉₋₁₀ = 7.5 Hz, *J*₉₋₁₁ = 4.8 Hz, *J*₉₋₁₂ = 1.1 Hz, H₉), 7.32 (m, 2H, H_{ln4}, H_{ln5}), 7.35
989 (d, 2H, *J*_{ortho} = 8.7 Hz, H₃, H₇), 7.71 (ddd, 1H, *J*₁₀₋₉ = 8.6 Hz, *J*₁₀₋₁₁ = 7.6 Hz, *J*₁₀₋₁₂ = 1.9
990 Hz, H₁₀), 8.51 (ddd, 1H, *J*₁₂₋₁₁ = 4.8 Hz, *J*₁₂₋₁₀ = 1.8 Hz, *J*₁₂₋₉ = 0.8 Hz, H₁₂), 10.94 (s, 1H,
991 NH); **¹³C NMR (DMSO d₆, 100 MHz)** (δ ppm) 20.80 (CH₃), 49.82 (C₁), 111.49 (C_{ln4}),
992 116.56 (C_{ln2}), 118.42 (C₁₁), 118.72 (C₉), 121.09 (C_{ln7}), 121.36 (C₆, C₄), 121.56 (C_{ln5}),
993 122.91 (C_{ln1}), 123.94 (C_{ln6}), 126.42 (C_{ln3}), 129.56 (C₇, C₃), 136.40 (C₂), 136.70 (C₁₀),
994 140.81 (C_{ln8}), 148.70 (C₅), 149.06 (C₁₂), 162.89 (C₈), 169.24 (C=O); **GC-MS**: method
995 180, *R_t* = 11.76 min *m/z*: 342 [M]⁺(90), 300 [M- COCH₃]⁺ (100), 264 [M-PyH]⁺(15), 222
996 [PyCHln]⁺(100); **IR** (ATR) (cm⁻¹) 3408 (νN-H). 3060 (νCsp² - H), 2989 (νCsp³ - H), 1749
997 (νC=O), 1589, 1570, 1505 (νC=C), 1223 (νC - O), 743 (δCsp²-H o-disubst); **HRMS**:
998 calcd. for C₂₂H₁₈N₂O₂ [M+Na]⁺ (365.1260), found (365.1260).

4.1.10. Preparation of thiophen triarylmethanes

4.1.10.1. 2-((4-methoxyphenyl)(thiophen-2-yl)methyl)pyridine (**21**)

A mixture of (4-methoxyphenyl) (pyridin-2-yl)methanol **9** (1.3 mmol, 1 eq.), thiophene **20** (13 mmol, 10 eq.) and methanesulfonic acid (0.7 mL, d = 1.48, 10 mmol, 8 eq.) in dichloroethane (6 mL) was placed in a vial. The vial was sealed, and the mixture was stirred and submitted to microwave irradiation for 2 h (300 W power, T = 80 °C). The mixture was neutralized with saturated NaHCO₃ solution (pH ≈ 8), extracted with dichloromethane (4 x 30 mL) and dried MgSO₄. Concentration under vacuum over SiO₂ (10 mL) and purification on FCC (CyHex/ EtOAc, 70/30) afforded **21** as greenish oil.

Yield: 80 mg (25%). **TLC** CyHex/EtOAc 70/30, R_f 0.4; **¹H NMR (DMSO d₆, 400 MHz)** (δ ppm) 3.71 (s, 3H, CH₃), 5.80 (s, 1H, H₁), 6.80 (dt, 1H, J_{T2-T3} = 3.5 Hz, J_{T2-T4} = 2.4 Hz, H_{T2}), 6.86 (d, 2H, J_{ortho} = 8.8 Hz, H₄, H₆), 6.93 (dd, 1H, J_{T3-T2} = 3.5 Hz, J_{T3-T4} = 5.1 Hz, H_{T3}), 7.23-7.27 (m, 1H, H_{T4}), 7.25 (d, 2H, J_{ortho} = 8.8 Hz, H₃, H₇), 7.34 (d, 1H, J_{H11-10} = 7.8 Hz, H₁₁), 7.38 (m, 1H, H₉), 7.74 (ddd, 1H, J_{H10-9} = 7.7 Hz, J_{H10-11} = 7.7 Hz, J_{H10-12} = 1.9 Hz, H₁₀), 8.51 (ddd, 1H, J_{H12-11} = 4.8 Hz, J_{H12-10} = 1.8 Hz, J_{H12-9} = 0.8 Hz, H₁₂); **¹³C NMR (DMSO d₆, 100 MHz)** (δ ppm) 52.53 (C₁), 54.99 (CH₃), 113.64 (C₄, C₆), 121.10 (C₁₁), 122.18 (C₉), 125.10 (C_{T4}), 125.10 (C_{T2}), 126.41 (C_{T3}), 129.47 (C₃, C₇), 135.09 (C₂), 136.93 (C₁₀), 146.68 (C_{T1}), 149.12 (C₁₂), 157.90 (C₅), 162.89 (C₈); **GC-MS**: method 160, R_t = 8.06 min m/z: 281 [M]⁺(100), 266 [M-CH₃]⁺(25), 203 [ThCHPhOCH₃]⁺(100); **IR** (ATR) (cm⁻¹) 3081, 3048 3005 (νCsp²-H), 2962, 2932 (νCsp³-H), 2837 (νOMe), 1604, 1584, 1509 (νC=C), 1242(νC-O), 808 (δCsp²-H p-disubst), 702 (δCsp²-H o-disubst); **HRMS**: calcd. for C₁₇H₁₅NOS [M+H]⁺ (282.0947), found (282.0946).

4.1.10.2. 4-(pyridin-2-yl(thiophen-2-yl)methyl)phenol (**22**)

To a stirred solution of **21** (0.5 mmol, 1 eq.) in anhydrous dichloromethane (7 mL) under argon at 0°C, was added dropwise a 1 M solution of BBr₃ in dichloromethane (2.4 mmol, 5 eq.). After 19 h at room temperature, MeOH (10 mL) was added. The solution was dried over Na₂SO₄, filtrated and concentrated under vacuum over SiO₂ (10 mL). The dry

1026 SiO₂ powder was loaded onto a silica gel column and eluted (DCM/MeOH, 95/5).
1027 Concentration under vacuum afforded **22** as a black oil.

1028 Yield: 80 mg (60%). **TLC** DCM/MeOH 95/5, *R_f* 0.3; **¹H NMR (DMSO d₆, 400 mHz)** (δ
1029 ppm) 5.72 (s, 1H, H₁), 6.67 (d, 2H, *J*_{ortho} = 8.6 Hz, H₄, H₆), 6.80 (dt, 1H, *J*_{T2-T3} = 3.4 Hz,
1030 *J*_{T2-T4} = 2.1 Hz, H_{T2}), 6.93 (dd, 1H, *J*_{T3-T2} = 3.5 Hz, *J*_{T3-T4} = 5.1 Hz, H_{T3}), 7.11 (d, 2H, *J*_{ortho}
1031 = 8.6 Hz, H₃, H₇), 7.24 (dd, 1H, *J*_{T4-T3} = 7.5 Hz, *J*_{T4-T2} = 2.1 Hz, H_{T4}), 7.32 (d, 1H, *J*₁₁₋₁₀ =
1032 7.9 Hz, H₁₁), 7.36 (m, 1H, H₉), 7.73 (ddd, 1H, *J*₁₀₋₉ = 7.7 Hz, *J*₁₀₋₁₁ = 7.7 Hz, *J*₁₀₋₁₂ = 1.9
1033 Hz, H₁₀), 8.53 (ddd, 1H, *J*₁₂₋₁₁ = 4.9 Hz, *J*₁₂₋₁₀ = 1.8 Hz, *J*₁₂₋₉ = 0.9 Hz, H₁₂); **¹³C NMR**
1034 **(DMSO d₆, 100 mHz)** (δ ppm) (δ ppm) 50.50 (C₁), 114.68 (C₄, C₆), 120.10 (C₁₁), 122.20
1035 (C₉), 125.24 (C_{T4}), 125.36 (C_{T2}), 126.40 (C_{T3}), 130.47 (C₃, C₇), 135.45 (C₂), 136.83
1036 (C₁₀), 146.74 (C_{T1}), 149.10 (C₁₂), 157.76 (C₅), 162.40 (C₈); **GC-MS**: method 180, *R_t* =
1037 6.5 min *m/z*: 267 [M]⁺(100); **IR** (ATR) (cm⁻¹) 3400 (νC-O), 3001 (νCsp²-H), 1590, 1511
1038 (νC=C), 1249(νC-O), 816 (δCsp²-H p-disubst), 751(δCsp²-H o-disubst); **HRMS**: calcd.
1039 for C₁₆H₁₃NOS [M+H]⁺ (268.0791), found (268.0790).

1040 **4.1.11. Preparation of quinoline triarylmethane**

1041 **4.1.11.1. (4-methoxyphenyl)(pyridin-2-yl)(quinolin-2-yl)methanol (25)**

1042 *n*-Butyllithium in hexane (1.6 M, 2.5 mmol, 1.3 eq.) was added dropwise to a stirred
1043 solution of 2-bromoquinoline **24** (2.2 mmol, 1.1 eq.) in anhydrous tetrahydrofuran (2 mL)
1044 at -78°C under argon. After 1 h 30, (4-methoxyphenyl)(pyridin-2-yl)methanone **23** (1.9
1045 mmol, 1 eq.) in dry tetrahydrofuran (3 mL) was added dropwise. After 17 h at room
1046 temperature, water (10 mL) was added. The reaction mixture was extracted with ethyl
1047 acetate three times, dried over Na₂SO₄, filtered and concentrated. FCC (CyHex/EtOAc,
1048 80/20) afforded **25** as a brown oil.

1049 Yield: 53 mg (81%). **TLC** CyHex/EtOAc 80/20, *R_f* 0.3; **¹H NMR (DMSO d₆, 400 mHz)** (δ
1050 ppm) 3.70 (s, 3H, CH₃), 6.85 (d, 2H, *J*_{ortho} = 8.9 Hz, H₄, H₆), 7.06 (s, 1H, OH), 7.24 (d,
1051 2H, *J*_{ortho} = 8.9 Hz, H₃, H₇), 7.29 (ddd, 1H, *J*₁₁₋₁₀ = 7.7 Hz, *J*₁₁₋₁₂ = 4.8 Hz, *J*₁₁₋₉ = 1.1 Hz,
1052 H₁₁), 7.59 (ddd, 1H, *J*_{Q6-Q5} = 8 Hz, *J*_{Q6-Q7} = 6.9 Hz, *J*_{Q6-Q8} = 1.1 Hz, H_{Q6}), 7.72-7.77(m,
1053 3H, H₉, H_{Q2}, H_{Q5}), 7.82 (ddd, 1H, *J*₁₀₋₉ = 7.8 Hz, *J*₁₀₋₁₁ = 7.4 Hz, *J*₁₀₋₁₂ = 1.9 Hz, H₁₀),

7.94-7.97(m, 2H, H_{Q7}, H_{Q8}), 8.32 (d, 1H, J_{Q3-Q2} = 8.0 Hz, H_{Q3}), 8.49 (ddd, 1H, J₁₂₋₁₁ = 4.8 Hz, J₁₂₋₁₀ = 1.8 Hz, J₁₂₋₉ = 0.9 Hz, H₁₂); **¹³C NMR (DMSO d₆, 100 mHz)** (δ ppm) 54.98 (CH₃), 90.63 (C₁), 113.01(C₄, C₆), 121.23 (C₁₁), 122.24 and 122.28 (C_{Q2}, C_{Q5}), 126.67 (C_{Q8}), 126.79 (C_{Q4}), 127.69 (C_{Q7}), 128.49 (C₁₁), 128.77 (C₃ and C₇), 129.70 (C₉), 136.15 (C₁₀), 136.74 (C_{Q3}), 137.86 (C₂), 145.16 (C_{Q9}), 147.49 (C₁₂), 158.15 (C₈), 163.81 (C_{Q1}), 163.99 (C₅); **GC-MS**: method 180, *R*_t = 10.71 min *m/z*: 342 [M]⁺(75), 325 [M-OH]⁺(75), 128 [C₉H₆N]⁺(75); **IR** (ATR) (cm⁻¹) 3408 (νO-H). 3031, 3025 (νCsp²H), 2992 (νCsp³-H), 2851 (νOMe), 1580, 1587, 1509 (νC=C), 1220(νC-O), 742 (δCsp²-H o-disubst); **HRMS**: calcd. for C₂₂H₁₈N₂O₂ [M+H]⁺ (343.1368), found (343.1367).

4.1.12. Preparation of triarylmethanes bearing trifluoromethyl

4.1.12.1. (4-methoxyphenyl)(pyridin-2-yl)(4-(trifluoromethyl)phenyl)methanol (28)

n-Butyllithium in hexane (1.6 M, 2.8 mmol, 1.6 eq.) was added dropwise to a stirred solution of 4-bromoanisole (2.5 mmol, 1.4 eq.) in anhydrous tetrahydrofuran (2 mL) at -78°C under argon. After 1½ h, pyridin-2-yl(4-(trifluoromethyl)phenyl)methanone **27** (1.7 mmol, 1 eq.) dissolved in dry tetrahydrofuran (1 mL) was added dropwise. After 17 h at room temperature, water (30 mL) was added. Extraction with ethyl acetate (4 x 30 mL), drying over Na₂SO₄, concentration under vacuum and column chromatography (CyHex/EtOAc, 70/30) afforded **28** as a white solid.

Yield: 39 mg (67%). Mp = 98-100 °C. **TLC** CyHex/EtOAc 70/30, *R*_f 0.5; **¹H NMR (DMSO d₆, 400 mHz)** (δ ppm) 3.55 (s, 3H, CH₃), 6.45 (s, 1H, OH), 6.70 (d, 2H, J_{ortho} = 9.0 Hz, H₁₆, H₁₈), 6.90 (d, 2H, J_{ortho} = 9.0 Hz, H₁₅, H₁₉), 7.15 (ddd, 1H, J₁₁₋₁₀ = 7.6 Hz, J₁₁₋₁₂ = 4.8 Hz, J₁₁₋₉ = 1.1 Hz, H₁₁), 7.30 (d, 2H, J_{ortho} = 8.2 Hz, H₃, H₇), 7.50 (d, 2H, J_{ortho} = 8.2 Hz, H₄, H₆), 7.48 (d, 1H, J₉₋₁₀ = 8.1 Hz, H₉), 7.60 (ddd, 1H, J₁₀₋₉ = 7.9 Hz, J₁₀₋₁₁ = 7.5 Hz, J₁₀₋₁₂ = 1.9 Hz, H₁₀), 8.31 (ddd, 1H, J₁₂₋₁₁ = 4.7 Hz, J₁₂₋₁₀ = 1. Hz, J₁₂₋₉ = 0.84 Hz, H₁₂); **¹³C NMR (DMSO d₆, 100 mHz)** (δ ppm) 54.98 (CH₃), 80.15 (C₁), 112.94 (C₁₆, C₁₈), 121.30 (C₉), 122.04 (C₁₁), 124.21 and 124.25 (C₄, C₆), 126.60 (C₃, C₇), 128.94 (C₁₅, C₁₉), 129.10 (CF₃), 136.75 (C₁₀), 138.60 (C₅), 147.91 (C₁₂), 151.90 (C₂), 137.86 (C₅), 158.09 (C₁₇), 164.59 (C₈); **GC-MS**: method 160, *R*_t = 8.59 min *m/z* 359 [M]⁺(100), 281 [HOPhCOHPhCF₃]⁺ (43), 252 [CH₃OPhCH₂PhCF₃]⁺ (20), 173 [OCPhCF₃]⁺ (65); **IR**

(ATR) (cm^{-1}) 3423 (νOH), 3012 ($\nu\text{Csp}^2\text{-H}$), 2934 ($\nu\text{Csp}^3\text{-H}$), 2854 (νOMe), 1612, 1590, 1525 ($\nu\text{C}=\text{C}$), 1324 ($\nu\text{C-O}$), 1109 ($\nu\text{C-O-C}$), 1065 ($\nu\text{C-F}$), 831 ($\delta\text{Csp}^2\text{-H}$ p-disubst); **HRMS**: calcd. for $\text{C}_{20}\text{H}_{16}\text{F}_3\text{NO}_2$ $[\text{M}+\text{H}]^+$ (360.1206), found (360.1206).

4.1.12.2. 4-(hydroxy(pyridin-2-yl)(4-(trifluoromethyl)phenyl)methyl)phenyl acetate (30)

To a stirred solution of 4-(pyridin-2-yl(4-(trifluoromethyl)phenyl)methyl)phenol **29** (0.4 mmol, 1 eq.) in acetic anhydride (44 mmol, 110 eq.) was slowly added a solution of NaOH 1 M (0.5 mmol, 1.3 eq.) at 0 °C. The mixture was stirred for 4 h at room temperature then neutralized with a saturated solution of NaHCO_3 ($\text{pH} \approx 8$). Acetone was added (10 mL) and the mixture was stirred for another 30 min (a white precipitate of sodium acetate formed). The mixture was extracted with ethyl acetate three times, dried with Na_2SO_4 , filtrated and concentrated under vacuum. FCC on silica gel (CyHex/EtOAc, 50/50) afforded **30** as a yellow oil.

Yield: 130 mg (87%). **TLC**: CyHex/EtOAc 50/50, R_f 0.45; **^1H NMR (DMSO d_6 , 400 MHz)** (δ ppm) 2.30 (s, 3H, CH_3), 6.45 (s, 1H, C_1), 7.07 (d, 2H, $J_{\text{ortho}} = 8.6$ Hz, H_{16} , H_{18}), 7.24-7.30 (m, 3H, H_{11} , H_{15} , H_{19}), 7.33 (d, 1H, $J_{9-10} = 7.9$ Hz, H_9), 7.47 (d, 2H, $J_{\text{ortho}} = 8.4$ Hz, H_3 , H_7), 7.67 (d, 2H, $J_{\text{ortho}} = 8.2$ Hz, H_4 , H_6), 7.76 (ddd, 1H, $J_{10-9} = 8.6$ Hz, $J_{10-11} = 7.6$ Hz, $J_{10-12} = 1.9$ Hz, H_{10}), 8.57 (ddd, 1H, $J_{12-11} = 4.8$ Hz, $J_{12-10} = 1.9$ Hz, $J_{12-9} = 0.9$ Hz, H_{12}); **^{13}C NMR (DMSO d_6 , 100 MHz)** (δ ppm) 20.78 (CH_3), 56.65 (C_1), 121.72 (C_{16} , C_{18}), 121.95 (C_{11}), 122.93 (C_9), 123.83 (C_4 , C_6), 129.73 (C_3 , C_7), 129.79 (C_{15} , C_{19}), 129.96 (CF_3), 136.83 (C_{10}), 139.70 (C_5), 147.66 (C_{14}), 149.04 (C_2), 149.36 (C_{12}), 161.31 (C_{17}), 169.16 (C_8), 170.29 ($\text{C}=\text{O}$); **GC-MS**: method 180, $R_t = 6.96$ min m/z 371 $[\text{M}^+]$ (50), 328 $[\text{M-Ac}]^+$ (100); **IR** (ATR) (cm^{-1}) 3051 ($\nu\text{Csp}^2\text{-H}$), 2931 ($\nu\text{Csp}^3\text{-H}$), 1755 ($\nu\text{C}=\text{O}$), 1618, 1588, 1505 ($\nu\text{C}=\text{C}$), 1323 ($\nu\text{C-O}$), 1108 ($\nu\text{C-O-C}$), 1066 ($\nu\text{C-F}$), 823 ($\delta\text{Csp}^2\text{-H}$ p-disubst); **HRMS**: calcd. for $\text{C}_{21}\text{H}_{16}\text{F}_3\text{O}_2\text{Na}$ $[\text{M}+23]^+$ (394.1025), found (394.1026).

1108 **4.2. AhR transcriptional activity**

1109 **4.2.1. Materials**

1110 Unless otherwise specified, chemical reagents and biological products for *in vitro*
1111 assays were obtained from Gibco, Life Technologies (Thermo Fisher Scientific Inc),
1112 MilliporeSigma (Merck KGaA) or InvivoGen. Fungible material was provided by Falcon®,
1113 Corning® or Eppendorf®.

1114 **4.2.2. Cell Culture**

1115 *Cell-Line and luciferase assay system.* AhR-Lucia™ Human liver carcinoma HepG2
1116 (AhR-HepG2) reporter cells were obtained from InvivoGen engineered to detect
1117 endogenous AhR expression. This cell line is stably transfected with a pSELECT-zeo-
1118 Lucia plasmid that contains the resistance marker to the antibiotic Zeocin™. EF-
1119 1α/HTLV composite promoter is combined to the elongation factor 1 alpha core
1120 promoter and the 5' untranslated region of the Human T-cell Leukemia Virus. The
1121 secreted luciferase Lucia™ is expressed by a synthetic reporter gene codon optimized
1122 for prolonged mammalian cell expression. The promoter is coupled with the human
1123 *Cyp1a1* gene entire regulatory sequence, that contains six XREs. The secreted
1124 coelenterazine Lucia™ is a novel luciferase reporter technology that does not involve
1125 cells lysis to measure the bioluminescence.

1126 *Quality and sterility.* Quality control of the reporter activity and guaranteed of
1127 mycoplasma-free contamination was provided by the cell line suppliers. Additional
1128 routinely inspections were conducted as standard quality control procedures to avoid
1129 mycoplasma, fungi, yeast and/or viruses' contamination. All the experiments were
1130 steered with less than 20 passages after thawing as recommended. The cell culture
1131 facilities from the Central Service for Experimental Research (SCSIE) at the University
1132 of Valencia where the experiments were conducted have certified proficiency to
1133 maintain, subculturing and guarantee aseptic conditions.

1134 *Maintenance.* AhR-HepG2 cells were handled and cultured according to supplier's
1135 information under strict sterility conditions in T-75 culture flasks under an aqueous

saturated atmosphere with 5% CO₂ at 37 °C. The growth medium was prepared as follow: to Minimum Essential Medium (MEM) containing non-essential amino acids (NEAA) was added 10% (v/v) of 56 °C heat-inactivated fetal bovine serum (FBS) and a mixture of Penicillin-Streptomycin (100 U/mL-100 µg/mL). The antimicrobial formula Normocin™ (0.1 mg/mL) and, after the third passage, the selective antibiotic Zeocin™ (0.2 mg/mL) were supplemented to prevent mycoplasma, bacterial and fungal contamination.

Subculturing. Once the cells reached 85% confluency in the culture flasks, they were rinsed twice with 10 mL of PBS and later detached through the incubation with 3-5 mL of 0.25 % trypsin-EDTA during 6 min at 37 °C. After inactivation, the cell suspension was centrifugated at 1200 rpm during 5 min, the supernatant was removed, and the pellet resuspended in fresh medium. To dissociate the clumps during the passages, sterile 10 mL syringes with 18-gauge (18G) needles were used. This last step also guaranteed the accuracy of the cell counting performed by mixing 10 µL of cell suspension with 10 µL of 0.4% Trypan Blue Solution in a chamber slide read in cell counters on the Countess™ II instrument (Invitrogen™, Thermo Fisher Scientific).

4.2.3. Bioassays

Assay medium and seeding. The assay medium used was the growth medium without Normocin™ nor Zeocin™. A volume of 200 µL of cells/well was seeded into 96-wells microplates at a density of 2.0×10^5 cells/mL and incubated overnight prior to treatment.

Treatment. The 32 synthesized TAMs and the commercial TAM-drug bisacodyl were dissolved in DMSO (0.5% final maximum concentration/well). The cells were exposed during 24 h to at least 4 different concentration of the TAMs (0.1 -10 µM), depending on their cytotoxicity and/or solubility. In the agonist assay, cells were exposed to 10 µL/well of the tested compounds while in the antagonist assay, cells were treated with 10 µL/well of the tested compounds plus 10 µL/well of the EC₅₀ of FICZ.

Cell viability assay. Cell viability was assessed by the 3-(4,5-dimethylthiazolyl-2)-2,5-diphenyltetrazolium bromide (MTT) assay, which is a colorimetric method based on the reduction of the yellowish solution of the MTT tetrazolium salt to form the formazan

precipitate, as an identification of the redox potential in metabolically active cells [50]. After seeding, cells were treated with different concentrations of the tested compounds and incubated during 24-72 h. Then, the medium was discarded and 100 µL/well of 0.5 mg/mL of MTT solution was added. Plates were incubated at 37 °C allowing the transformation, the supernatant was removed, and the formazan crystals were dissolved adding 100 µL/well of DMSO. Finally, the optical density was determined by reading the absorbance at 490 nm using a microplate reader (VICTORx3, PerkinElmer Inc., USA).

AhR-transactivation assay. The induction of AhR-mediated transcriptional activity was measured by transferring 20 µL of the supernatant of stimulated cells to white sterile and flat-bottom 96-wells microplates. The QUANTI-Luc™ assay reagent containing the coelenterazine substrate for the luciferase reaction was prepared according to suppliers by pouring the lyophilized powder protected from light in sterile water. Finally, 50 µL/well of the QUANTI-Luc solution was added and the light signal produced was immediately measured in a microplate reader (VICTORx3, PerkinElmer Inc., USA).

4.2.4. Activity Results

Activity criteria. The capacity of the synthesized TAMs to activate (i.e. act as agonists) and to suppress (i.e. act as antagonists) AhR-mediated transcription was analyzed in terms of magnitude of the effects and based on the concentration at which such effects occurs. Therefore, the fold response induced (compared with vehicle control) was used to inform the magnitude of the effect while half effective/inhibitory concentrations (EC_{50} or IC_{50}) were estimated from dose-response curves of agonist or antagonist activity respectively. In the absence of a regulatory guidance for AhR, the threshold used to identify active from inactive compounds in both agonist and antagonist assays followed the OECD guideline for ER transactivation where the induced response is compared with a positive control (PC) [53]. Thus, the maximum response relative to the positive control (RPC_{max}) in this work represented the maximum fold response induced by each TAM (x) compared to the positive control FICZ.

In the AhR-agonist assay, the RPC_{max} was calculated as percentage of the maximum AhR induction of FICZ (in relative light units of the luciferase gene expression), that is

expressed as *Fold response* $PC_{Max}(FICZ)$ in Equation 1. Meanwhile, in the antagonist assay, the RPC_{max} was calculated as percentage of the effect induced by the EC_{50} of FICZ that is expressed as *Fold response* $EC_{50}(FICZ)$ in Equation 2.

Compounds showing $RPC_{max} \geq 10\%$ were considered active in the agonist bioassay while compounds with $RPC_{max} \leq 70\%$ were considered active in the antagonist bioassay.

$$Agonist\ RPC_{max}\ (%) = \frac{Fold\ response\ (x)}{Fold\ response\ PC_{Max}(FICZ)} \times 100$$

Equation 1

$$Antagonistic\ RPC_{max}\ (%) = \frac{Fold\ response\ (x)}{Fold\ response\ EC_{50}(FICZ)} \times 100$$

Equation 2

On the other hand, when it was possible, sigmoidal curves of x [log (concentration)] vs. y (Fold response) were designed constraining the Hill Slope value to 1.0 and using the *Top* and *Bottom* plateaus in the units of the y axis. The concentration of agonist required to provoke a response halfway between the baseline and maximum responses (EC_{50} or IC_{50}) was estimated from Equation 3.

$$y = Bottom + \left(\frac{Top - Bottom}{1 + 10^{(logEC_{50} - x) * Hill\ Slope}} \right)$$

Equation 3

Statistical analysis. All data informed represent means obtained from at least three independent experiments ($n = 3$) and sextuplicate in all cases. The precision of results was reported through the standard error of the mean (SEM). All active compounds were re-tested at least once again ($n = 4$) and a greater number of concentrations was evaluated (≥ 5). Statistical significance was determined with a one-way analysis of variance (ANOVA) following by Dunnett's post-test for comparison with controls or Bonferroni post-test to compare the studied compounds.

4.3. Computational Studies

4.3.1. Molecular Docking Simulations

Molecular docking analysis was performed with Autodock Vina [64] as implemented in YASARA [65]. The crystalized protein structure of HIF2 α was used for docking analysis (PDB ID 3F1O). The sequence of the PAS-B domain of HIF2 α shows the highest level of identity and similarity with AhR among all the PAS identified to date [66]. Hence, it is commonly used as template structure in molecular modeling of AhR ligand binding domain [67]. An additional evaluation of the aforementioned sequence identity and similarity is provided in Section 3, SI-3. The analyzed ligands were the strongest agonist identified **22**, the structurally related compound **21**, and the known AhR ligand/agonist compounds FICZ and TCDD. Besides, a preliminary off-targeting docking analysis of compound **22** with four nuclear receptors (ER, AR, PR and PXR) was performed.

All simulations were performed for the entirely target structure making stiff the protein and totally flexible the ligand compounds. Protein Ligand Interaction Profiler server [68] was used to predict the interactions of the best protein/ligand complex for each ligand and molecular graphics and analyses were performed with UCSF Chimera [69].

4.3.2. Druglikeness and ADME profile

The physicochemical parameters and ADME descriptors were predicted using the QikProp v5.9 Panel from Schrödinger software v11.9. Conformational averages from OPLS-AA force field were used for calculations.

Supplementary Information

SI-1. Synthesis and characterization of intermediates and non-assayed compounds.

SI-2. Dose-Response Curves.

SI-3. Computational Studies.

Corresponding Authors

E-mail: rosa.m.giner@uv.es (Rosa M. Giner).

1245 E-mail: maite.sylla@lecnam.net (Maité Sylla-Iyarreta Veitía)

1246 ***Author Contributions***

1247 The manuscript was written through contributions of all authors. All authors have given
1248 approval to the final version of the manuscript.

1249 ***Acknowledgments***

1250 This project has received funding from the European Union's Horizon 2020 research
1251 and innovation programme under the Marie Skłodowska-Curie grant agreement No.
1252 722634. The Early Stage Researcher Goya-Jorge E. of this Innovative Training Network
1253 named 'PROTECTED' (<http://protected.eu.com/>) gratefully thanks for her PhD
1254 scholarship. Authors also thank the FONGECIF for the financial support offered to
1255 Céline Rampal and Nicolas Loones during their engineering internship at Cnam.

5. References

- [1] C.A. Bradfield, E. Glover, A. Poland, Purification and N-terminal amino acid sequence of the Ah receptor from the C57BL/6J mouse, *Mol. Pharmacol.* 39 (1991) 13–19.
- [2] K.W. Bock, Aryl hydrocarbon receptor (AHR): From selected human target genes and crosstalk with transcription factors to multiple AHR functions, *Biochem. Pharmacol.* 168 (2019) 65–70. <https://doi.org/10.1016/j.bcp.2019.06.015>.
- [3] S.-H. Seok, W. Lee, L. Jiang, K. Molugu, A. Zheng, Y. Li, S. Park, C.A. Bradfield, Y. Xing, Structural hierarchy controlling dimerization and target DNA recognition in the AHR transcriptional complex, *Proc. Natl. Acad. Sci.* 114 (2017) 5431–5436. <https://doi.org/10.1073/pnas.1617035114>.
- [4] I.A. Murray, A.D. Patterson, G.H. Perdew, Aryl hydrocarbon receptor ligands in cancer: Friend and foe, *Nat. Rev. Cancer.* 14 (2014) 801–814. <https://doi.org/10.1038/nrc3846>.
- [5] E.J. Wright, K.P. De Castro, A.D. Joshi, C.J. Elferink, Canonical and non-canonical aryl hydrocarbon receptor signaling pathways *Toxicology*, *Curr. Opin. Toxicol.* 2 (2017) 87–92. <https://doi.org/10.1016/j.cotox.2017.01.001>.
- [6] L. Stejskalova, Z. Dvorak, P. Pavek, Endogenous and exogenous ligands of aryl hydrocarbon receptor: current state of art., *Curr. Drug Metab.* 12 (2011) 198–212. <https://doi.org/10.2174/138920011795016818>.
- [7] L.C. Quattrochi, R.H. Tukey, Nuclear uptake of the Ah (dioxin) receptor in response to omeprazole: Transcriptional activation of the human CYP1A1 gene, *Mol. Pharmacol.* 43 (1993) 504–508.
- [8] E.F. O'Donnell, K.S. Saili, D.C. Koch, P.R. Kopparapu, D. Farrer, W.H. Bisson, L.K. Mathew, S. Sengupta, N.I. Kerkvliet, R.L. Tanguay, S.K. Kolluri, The anti-inflammatory drug leflunomide is an agonist of the aryl hydrocarbon receptor, *PLoS One.* 5 (2010). <https://doi.org/10.1371/journal.pone.0013128>.
- [9] H.P. Ciolino, P.J. Daschner, G.C. Yeh, Dietary flavonols quercetin and kaempferol are ligands of the aryl hydrocarbon receptor that affect CYP1A1 transcription differentially, *Biochem. J.* 340 (1999) 715–722. <https://doi.org/10.1042/0264-6021:3400715>.
- [10] T.H. Scheuermann, D.R. Tomchick, M. Machius, Y. Guo, R.K. Bruick, K.H. Gardner, Artificial ligand binding within the HIF2 α PAS-B domain of the HIF2 transcription factor, *Proc. Natl. Acad. Sci. U. S. A.* 106 (2009) 450–455. <https://doi.org/10.1073/pnas.0808092106>.
- [11] M.B. Kumar, P. Ramadoss, R.K. Reen, J.P. Vanden Heuvel, G.H. Perdew, The Q-rich Subdomain of the Human Ah Receptor Transactivation Domain Is Required for Dioxin-mediated Transcriptional Activity, *J. Biol. Chem.* 276 (2001) 42302–42310. <https://doi.org/10.1074/jbc.M104798200>.
- [12] F.J. Quintana, A.S. Basso, A.H. Iglesias, T. Korn, M.F. Farez, E. Bettelli, M. Caccamo, M. Oukka, H.L. Weiner, Control of Treg and TH17 cell differentiation by the aryl hydrocarbon receptor, *Nature.* 453 (2008) 65–71. <https://doi.org/10.1038/nature06880>.
- [13] A.A. Soshilov, M.S. Denison, Ligand Promiscuity of Aryl Hydrocarbon Receptor Agonists and Antagonists Revealed by Site-Directed Mutagenesis, *Mol. Cell. Biol.* 34 (2014) 1707–1719. <https://doi.org/10.1128/mcb.01183-13>.
- [14] Y. Xing, M. Nukaya, K.A. Satyshur, L. Jiang, V. Stanevich, E.N. Korkmaz, L. Burdette, G.D.

- Kennedy, Q. Cui, C.A. Bradfield, Identification of the Ah-receptor structural determinants for ligand preferences, *Toxicol. Sci.* 129 (2012) 86–97. <https://doi.org/10.1093/toxsci/kfs194>.
- [15] D. Dolciemi, M. Gargaro, B. Cerra, G. Scalisi, L. Bagnoli, G. Servillo, M.A. Della Fazio, P. Puccetti, F.J. Quintana, F. Fallarino, A. Macchiarulo, Binding Mode and Structure–Activity Relationships of ITE as an Aryl Hydrocarbon Receptor (AhR) Agonist, *ChemMedChem*. 13 (2018) 270–279. <https://doi.org/10.1002/cmdc.201700669>.
- [16] K.N. Chitralla, X. Yang, P. Nagarkatti, M. Nagarkatti, Comparative analysis of interactions between aryl hydrocarbon receptor ligand binding domain with its ligands: A computational study, *BMC Struct. Biol.* 18 (2018). <https://doi.org/10.1186/s12900-018-0095-2>.
- [17] E. Goya-Jorge, T.Q. Doan, M.L. Scippo, M. Muller, R.M. Giner, S.J. Barigye, R. Gozalbes, Elucidating the aryl hydrocarbon receptor antagonism from a chemical-structural perspective, *SAR QSAR Environ. Res.* 31 (2020) 209–226. <https://doi.org/10.1080/1062936X.2019.1708460>.
- [18] J. Chen, C.A. Haller, F.E. Jernigan, S.K. Koerner, D.J. Wong, Y. Wang, J.E. Cheong, R. Kosaraju, J. Kwan, D.D. Park, B. Thomas, S. Bhasin, R.C. de la Rosa, A.M. Premji, L. Liu, E. Park, A.C. Moss, A. Emili, M. Bhasin, L. Sun, E.L. Chaikof, Modulation of lymphocyte-mediated tissue repair by rational design of heterocyclic aryl hydrocarbon receptor agonists, *Sci. Adv.* 6 (2020) 1–16. <https://doi.org/10.1126/sciadv.aay8230>.
- [19] M. Mescher, T. Haarmann-Stemmann, Modulation of CYP1A1 metabolism: From adverse health effects to chemoprevention and therapeutic options, *Pharmacol. Ther.* 187 (2018) 71–87. <https://doi.org/10.1016/j.pharmthera.2018.02.012>.
- [20] K.W. Bock, From TCDD-mediated toxicity to searches of physiologic AHR functions, *Biochem. Pharmacol.* 155 (2018) 419–424. <https://doi.org/10.1016/j.bcp.2018.07.032>.
- [21] C. Esser, B.P. Lawrence, D.H. Sherr, G.H. Perdew, A. Puga, R. Barouki, X. Coumoul, Old receptor, new tricks—The ever-expanding universe of aryl hydrocarbon receptor functions. Report from the 4th AHR meeting, 29–31 August 2018 in Paris, France, *Int. J. Mol. Sci.* 19 (2018). <https://doi.org/10.3390/ijms19113603>.
- [22] S. Zhang, P. Lei, X. Liu, X. Li, K. Walker, L. Kotha, C. Rowlands, S. Safe, The aryl hydrocarbon receptor as a target for estrogen receptor-negative breast cancer chemotherapy, *Endocr. Relat. Cancer*. 16 (2009) 835–844. <https://doi.org/10.1677/erc-09-0054>.
- [23] K.W. Bock, Human AHR functions in vascular tissue: Pro- and anti-inflammatory responses of AHR agonists in atherosclerosis, *Biochem. Pharmacol.* 159 (2019) 116–120. <https://doi.org/10.1016/j.bcp.2018.11.021>.
- [24] N. Guerrina, H. Traboulsi, D.H. Eidelman, C.J. Baglione, The aryl hydrocarbon receptor and the maintenance of lung health, *Int. J. Mol. Sci.* 19 (2018). <https://doi.org/10.3390/ijms19123882>.
- [25] C. Duval, E. Blanc, X. Coumoul, Aryl hydrocarbon receptor and liver fibrosis, *Curr. Opin. Toxicol.* 8 (2018) 8–13. <https://doi.org/10.1016/j.cotox.2017.11.010>.
- [26] M. Puccetti, G. Paolicelli, V. Oikonomou, A. De Luca, G. Renga, M. Borghi, M. Pariano, C. Stincardini, L. Scaringi, S. Giovagnoli, M. Ricci, L. Romani, T. Zelante, Towards targeting the aryl hydrocarbon receptor in cystic fibrosis, *Mediators Inflamm.* 2018 (2018).

- <https://doi.org/10.1155/2018/1601486>.
- [27] C. Dietrich, Antioxidant Functions of the Aryl Hydrocarbon Receptor, *Stem Cells Int.* 2016 (2016). <https://doi.org/10.1155/2016/7943495>.
- [28] L. Juricek, X. Coumoul, The Aryl Hydrocarbon Receptor and the Nervous System, *Int. J. Mol. Sci.* 19 (2018) 2504. <https://doi.org/10.3390/ijms19092504>.
- [29] T. Bradshaw, A. Westwell, The Development of the Antitumour Benzothiazole Prodrug, Phortress, as a Clinical Candidate, *Curr. Med. Chem.* 11 (2005) 1009–1021. <https://doi.org/10.2174/0929867043455530>.
- [30] S. Safe, Y. Cheng, U.H. Jin, The aryl hydrocarbon receptor (AhR) as a drug target for cancer chemotherapy, *Curr. Opin. Toxicol.* 1 (2017) 24–29. <https://doi.org/10.1016/j.cotox.2017.01.012>.
- [31] B. Lamas, J.M. Natividad, H. Sokol, Aryl hydrocarbon receptor and intestinal immunity review-article, *Mucosal Immunol.* 11 (2018) 1024–1038. <https://doi.org/10.1038/s41385-018-0019-2>.
- [32] J. Gao, K. Xu, H. Liu, G. Liu, M. Bai, C. Peng, T. Li, Y. Yin, Impact of the Gut Microbiota on Intestinal Immunity Mediated by Tryptophan Metabolism, *Front. Cell. Infect. Microbiol.* 8 (2018) 1–22. <https://doi.org/10.3389/fcimb.2018.00013>.
- [33] C. Esser, A. Rannug, B. Stockinger, The aryl hydrocarbon receptor in immunity, *Trends Immunol.* 30 (2009) 447–454. <https://doi.org/10.1016/j.it.2009.06.005>.
- [34] I. Marafini, D. Di Fusco, V. Dinallo, E. Franzè, C. Stolfi, G. Sica, G. Monteleone, I. Monteleone, NPD-0414-2 and NPD-0414-24, two chemical entities designed as aryl hydrocarbon receptor (AHR) ligands, inhibit gut inflammatory signals, *Front. Pharmacol.* 10 (2019) 1–9. <https://doi.org/10.3389/fphar.2019.00380>.
- [35] P. Tarnow, T. Tralau, A. Luch, Chemical activation of estrogen and aryl hydrocarbon receptor signaling pathways and their interaction in toxicology and metabolism, *Expert Opin. Drug Metab. Toxicol.* 15 (2019) 219–229. <https://doi.org/10.1080/17425255.2019.1569627>.
- [36] E.F. O'Donnell, D.C. Koch, W.H. Bisson, H.S. Jang, S.K. Kolluri, The aryl hydrocarbon receptor mediates raloxifene-induced apoptosis in estrogen receptor-negative hepatoma and breast cancer cells, *Cell Death Dis.* 5 (2014) 1–12. <https://doi.org/10.1038/cddis.2013.549>.
- [37] G. Guedes, Á. Amesty, R. Jiménez-Monzón, J. Marrero-Alonso, M. Díaz, L. Fernández-Pérez, A. Estévez-Braun, Synthesis of 4,4'-Diaminotriphenylmethanes with Potential Selective Estrogen Receptor Modulator (SERM)-like Activity, *ChemMedChem.* 10 (2015) 1403–1412. <https://doi.org/10.1002/cmdc.201500148>.
- [38] Z. Dvořák, F. Kopp, C.M. Costello, J.S. Kemp, H. Li, A. Vrzalová, M. Štěpánková, I. Bartoňková, E. Jiskrová, K. Poulíková, B. Vyhlídalová, L.U. Nordstroem, C. V Karunaratne, H.S. Ranhotra, K.S. Mun, A.P. Naren, I.A. Murray, G.H. Perdew, J. Brtko, L. Toporova, A. Schön, W.G. Wallace, W.G. Walton, M.R. Redinbo, K. Sun, A. Beck, S. Kortagere, M.C. Neary, A. Chandran, S. Vishveshwara, M.M. Cavalluzzi, G. Lentini, J.Y. Cui, H. Gu, J.C. March, S. Chatterjee, A. Matson, D. Wright, K.L. Flannigan, S.A. Hirota, R.B. Sartor, S. Mani, Targeting the pregnane X receptor using microbial metabolite mimicry, *EMBO Mol. Med.* 12 (2020) 1–19. <https://doi.org/10.15252/emmm.201911621>.
- [39] S. Mondal, G. Panda, Synthetic methodologies of achiral diarylmethanols, diaryl and

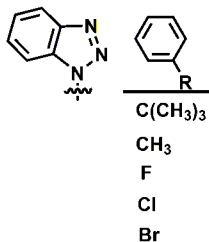
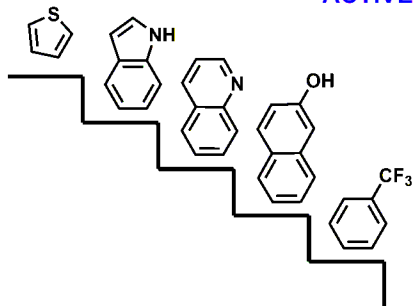
- triarylmethanes (TRAMs) and medicinal properties of diaryl and triarylmethanes-an overview, *RSC Adv.* 4 (2014) 28317–28358. <https://doi.org/10.1039/c4ra01341g>.
- [40] J.L. Douglas, M.L. Panis, E. Ho, K.-Y. Lin, S.H. Krawczyk, D.M. Grant, R. Cai, S. Swaminathan, T. Cihlar, Inhibition of Respiratory Syncytial Virus Fusion by the Small Molecule VP-14637 via Specific Interactions with F Protein, *J. Virol.* 77 (2003) 5054–5064. <https://doi.org/10.1128/jvi.77.9.5054-5064.2003>.
- [41] G. Panda, Shagufta, A.K. Srivastava, S. Sinha, Synthesis and antitubercular activity of 2-hydroxy-aminoalkyl derivatives of diaryloxy methano phenanthrenes, *Bioorganic Med. Chem. Lett.* 15 (2005) 5222–5225. <https://doi.org/10.1016/j.bmcl.2005.08.045>.
- [42] S.K. Chauthé, S.B. Bharate, S. Sabde, D. Mitra, K.K. Bhutani, I.P. Singh, Biomimetic synthesis and anti-HIV activity of dimeric phloroglucinols, *Bioorganic Med. Chem.* 18 (2010) 2029–2036. <https://doi.org/10.1016/j.bmc.2010.01.023>.
- [43] C. Ricco, F. Abdmouleh, C. Riccobono, L. Guenineche, F. Martin, E. Goya-Jorge, N. Lagarde, B. Liagre, M. Ben Ali, C. Ferroud, M. El Arbi, M.S.I. Veitía, Pegylated triarylmethanes: Synthesis, antimicrobial activity, anti-proliferative behavior and in silico studies, *Bioorg. Chem.* 96 (2020) 103591. <https://doi.org/10.1016/j.bioorg.2020.103591>.
- [44] M.S.-I. Veitia, D. Siverio Mota, V. Lerari, M. Marín, R.M. Giner, L. Vicet Muro, Y.R. Guerra, F. Dumas, C. Ferroud, P.A.M. De Witte, A.D. Crawford, V.J. Arán, Y.M. Ponce, Fishing anti-inflammatories from known drugs: In silico repurposing, design, synthesis and biological evaluation of bisacodyl analogues, *Curr. Top. Med. Chem.* 17 (2017) 2866–2887. <https://doi.org/10.2174/1568026617666170817161953>.
- [45] R.A. Al-Qawasmeh, Y. Lee, M.Y. Cao, X. Gu, A. Vassilakos, J.A. Wright, A. Young, Triaryl methane derivatives as antiproliferative agents, *Bioorganic Med. Chem. Lett.* 14 (2004) 347–350. <https://doi.org/10.1016/j.bmcl.2003.11.004>.
- [46] M. Seto, Y. Aramaki, H. Imoto, K. Aikawa, T. Oda, N. Kanzaki, Y. Iizawa, M. Baba, M. Shiraishi, Orally active CCR5 antagonists as anti-HIV-1 agents 2: Synthesis and biological activities of anilide derivatives containing a pyridine N-oxide moiety, *Chem. Pharm. Bull.* 52 (2004) 818–829. <https://doi.org/10.1248/cpb.52.818>.
- [47] F. Trécourt, G. Breton, V. Bonnet, F. Mongin, F. Marsais, G. Quéguiner, New syntheses of substituted pyridines via bromine-magnesium exchange, *Tetrahedron.* 56 (2001) 1349–1360. [https://doi.org/10.1016/S0040-4020\(00\)00027-2](https://doi.org/10.1016/S0040-4020(00)00027-2).
- [48] M. Sylla-Iyarreta Veitía, C. Rampal, C. Ferroud, An efficient access to unsymmetrical triarylmethanes by regioselective Friedel-Crafts hydroxyalkylation, *Trends Org. Chem.* 20 (2019) 1–13.
- [49] M. Görmén, M.S.I. Veitía, F. Trigui, M. El Arbi, C. Ferroud, Ferrocenyl analogues of bisacodyl: Synthesis and antimicrobial activity, *J. Organomet. Chem.* 794 (2015) 274–281. <https://doi.org/10.1016/j.jorganchem.2015.07.016>.
- [50] J.C. Stockert, R.W. Horobin, L.L. Colombo, A. Blázquez-Castro, Tetrazolium salts and formazan products in Cell Biology: Viability assessment, fluorescence imaging, and labeling perspectives, *Acta Histochem.* 120 (2018) 159–167. <https://doi.org/10.1016/j.acthis.2018.02.005>.
- [51] E. Goya-Jorge, F. Abdmouleh, L.E. Carpio, R.M. Giner, M. [Sylla-I. Veitía], Discovery of 2-aryl and 2-pyridinylbenzothiazoles endowed with antimicrobial and aryl hydrocarbon receptor agonistic activities, *Eur. J. Pharm. Sci.* 151 (2020) 105386.

- <https://doi.org/https://doi.org/10.1016/j.ejps.2020.105386>.
- [52] A. Mohammadi-Bardbori, M. Omid, M.R. Arabnezhad, Impact of CH223191-Induced Mitochondrial Dysfunction on Its Aryl Hydrocarbon Receptor Agonistic and Antagonistic Activities, *Chem. Res. Toxicol.* 32 (2019) 691–697. <https://doi.org/10.1021/acs.chemrestox.8b00371>.
- [53] OECD, Test No. 455: Performance-Based Test Guideline for Stably Transfected Transactivation In Vitro Assays to Detect Estrogen Receptor Agonists and Antagonists, 2016. <https://doi.org/https://doi.org/https://doi.org/10.1787/9789264265295-en>.
- [54] H. Kim, S. Reddy, R.F. Novak, 3-Methylcholanthrene and pyridine effects on CYP1A1 and CYP1A2 expression in rat renal tissue., *Drug Metab. Dispos.* 23 (1995) 818 LP – 824. <http://dmd.aspetjournals.org/content/23/8/818.abstract>.
- [55] P. De Medina, R. Casper, J.F. Savouret, M. Poirot, Synthesis and biological properties of new stilbene derivatives of resveratrol as new selective aryl hydrocarbon modulators, *J. Med. Chem.* 48 (2005) 287–291. <https://doi.org/10.1021/jm0498194>.
- [56] M.S. Denison, A. Pandini, S.R. Nagy, E.P. Baldwin, L. Bonati, Ligand binding and activation of the Ah receptor, *Chem. Biol. Interact.* 141 (2002) 3–24. [https://doi.org/10.1016/S0009-2797\(02\)00063-7](https://doi.org/10.1016/S0009-2797(02)00063-7).
- [57] M. Nambo, Z.T. Ariki, D. Canseco-Gonzalez, D.D. Beattie, C.M. Crudden, Arylative Desulfonation of Diarylmethyl Phenyl Sulfone with Arenes Catalyzed by Scandium Triflate, *Org. Lett.* 18 (2016) 2339–2342. <https://doi.org/10.1021/acs.orglett.6b00744>.
- [58] R. Pohjanvirta, *The AH Receptor in Biology and Toxicology*, John Wiley and Sons, 2011. <https://doi.org/10.1002/9781118140574>.
- [59] Á.C. Roman, J.M. Carvajal-Gonzalez, J.M. Merino, S. Mulero-Navarro, P.M. Fernández-Salguero, The aryl hydrocarbon receptor in the crossroad of signalling networks with therapeutic value, *Pharmacol. Ther.* 185 (2018) 50–63. <https://doi.org/10.1016/j.pharmthera.2017.12.003>.
- [60] S. Safe, M. Wormke, Inhibitory Aryl Hydrocarbon Receptor–Estrogen Receptor α Cross-Talk and Mechanisms of Action, *Chem. Res. Toxicol.* 16 (2003) 807–816. <https://doi.org/10.1021/tx034036r>.
- [61] A.J. Lucas, J.L. Sproston, P. Barton, R.J. Riley, Estimating human ADME properties, pharmacokinetic parameters and likely clinical dose in drug discovery, *Expert Opin. Drug Discov.* 14 (2019) 1313–1327. <https://doi.org/10.1080/17460441.2019.1660642>.
- [62] A. Leo, C. Hansch, D. Elkins, Partition coefficients and their uses, *Chem. Rev.* 71 (1971) 525–616. <https://doi.org/10.1021/cr60274a001>.
- [63] D. Dolciemi, M. Ballarotto, M. Gargaro, L.C. López-Cara, F. Fallarino, A. Macchiarulo, Targeting Aryl hydrocarbon receptor for next-generation immunotherapies: Selective modulators (SAhRMs) versus rapidly metabolized ligands (RMAhRLs), *Eur. J. Med. Chem.* 185 (2020). <https://doi.org/10.1016/j.ejmech.2019.111842>.
- [64] O. Trott, A. Olson, Software News and Update. AutoDock Vina Improving the Speed and Accuracy of Docking with a New Scoring Function, Efficient Optimization, and Multithreading, *J. Comput. Chem.* 31 (2009) 455–461. <https://doi.org/10.1002/jcc.21334>.
- [65] E. Krieger, G. Vriend, YASARA View - molecular graphics for all devices - from smartphones to workstations, *Bioinformatics.* 30 (2014) 2981–2982. <https://doi.org/10.1093/bioinformatics/btu426>.

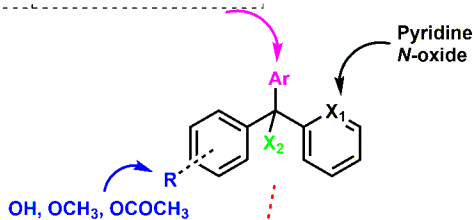
- [66] S. Giani Tagliabue, S.C. Faber, S. Motta, M.S. Denison, L. Bonati, Modeling the binding of diverse ligands within the Ah receptor ligand binding domain, *Sci. Rep.* 9 (2019) 1–14. <https://doi.org/10.1038/s41598-019-47138-z>.
- [67] L. Bonati, D. Corrada, S. Giani Tagliabue, S. Motta, Molecular modeling of the AhR structure and interactions can shed light on ligand-dependent activation and transformation mechanisms, *Curr. Opin. Toxicol.* 1 (2017) 42–49. <https://doi.org/10.1016/j.cotox.2017.01.011>.
- [68] S. Salentin, S. Schreiber, V.J. Haupt, M.F. Adasme, M. Schroeder, PLIP: Fully automated protein-ligand interaction profiler, *Nucleic Acids Res.* 43 (2015) W443–W447. <https://doi.org/10.1093/nar/gkv315>.
- [69] E.F. Pettersen, T.D. Goddard, C.C. Huang, G.S. Couch, D.M. Greenblatt, E.C. Meng, T.E. Ferrin, UCSF Chimera—A visualization system for exploratory research and analysis, *J. Comput. Chem.* 25 (2004) 1605–1612. <https://doi.org/10.1002/jcc.20084>.

ACTIVE

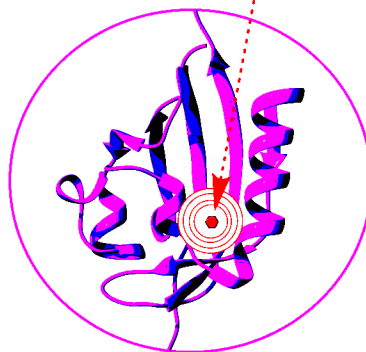
INACTIVE



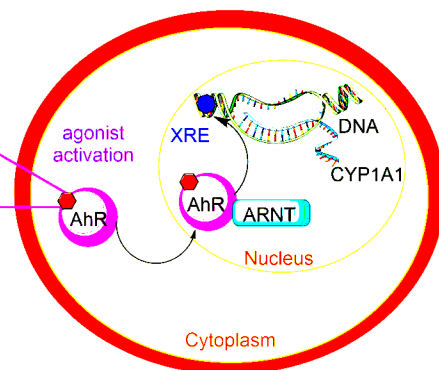
Triaryl methane compounds



Aryl hydrocarbon receptor



AhR Ligand Binding Domain



AhR canonical signaling pathway